

1979

# Optimization of separation in continuous particle electrophoresis

Tina Jean Vital  
*Lehigh University*

Follow this and additional works at: <https://preserve.lehigh.edu/etd>



Part of the [Chemical Engineering Commons](#)

---

## Recommended Citation

Vital, Tina Jean, "Optimization of separation in continuous particle electrophoresis" (1979). *Theses and Dissertations*. 5138.  
<https://preserve.lehigh.edu/etd/5138>

This Thesis is brought to you for free and open access by Lehigh Preserve. It has been accepted for inclusion in Theses and Dissertations by an authorized administrator of Lehigh Preserve. For more information, please contact [preserve@lehigh.edu](mailto:preserve@lehigh.edu).

9174  
2

OPTIMIZATION OF SEPARATION IN CONTINUOUS  
PARTICLE ELECTROPHORESIS

By

Tina Jean Vital

A Research Report  
Presented to the Graduate Committee  
of Lehigh University  
in Candidacy for the Degree of  
Master of Science  
in  
Chemical Engineering

Lehigh University

1979

CERTIFICATE OF APPROVAL

This research report is accepted and approved in partial fulfillment of the requirements for the degree of Master of Science in Chemical Engineering.

12/12/79

(date)

Professor in Charge

F. J. Micale

Dr. F. J. Micale

Head of Department

L. A. Wenzel

Dr. L. A. Wenzel

9174  
2

OPTIMIZATION OF SEPARATION IN CONTINUOUS  
PARTICLE ELECTROPHORESIS

By

Tina Jean Vital

A Research Report  
Presented to the Graduate Committee  
of Lehigh University  
in Candidacy for the Degree of  
Master of Science  
in  
Chemical Engineering

Lehigh University

1979

CERTIFICATE OF APPROVAL

This research report is accepted and approved in partial fulfillment of the requirements for the degree of Master of Science in Chemical Engineering.

12/12/79

(date)

Professor in Charge

F. J. Micale

Dr. F. J. Micale

Head of Department

L. A. Wenzel

Dr. L. A. Wenzel

## ACKNOWLEDGEMENTS

I would like to express my sincere appreciation to:

Dr. F. J. Micale for his patient and continued support and advice throughout this study.

Drs. M. El-Aasser, J. W. Vanderhoff and L. A. Wenzel for their interest and encouragement.

Paul Krumrine for his patience and advice.

Olga Shaffer for her technical assistance.

Gloria Gibson for typing this manuscript.

Ahmed Kamel for teaching me conductometric titration.

Joe Hojsak for his mechanical assistance.

Xenophon Verykios, Hans Kast, Babu Patrose, Nopporn Pramojaney and David Sudol for their friendship, and helpful advice and suggestion during my research and course study.

The Emulsion Polymers Institute for their financial support during my research assistantship.

TO MY MOTHER.

## TABLE OF CONTENTS

	<u>Page</u>
Abstract	1
I. Introduction	3
II. Development of a Coating with Controlled Electro- kinetic Properties	5
A. Background and Previous Work	5
B. Experimental Results and Discussion	14
III. Particle-Particle Interactions Affecting the Separation of Colloid Particles	26
A. Background and Apparatus	26
B. Applications of Continuous Particle Electro- phoresis	36
C. Experimental Results and Discussion	40
IV. Experimental Verification of a Computer Model and Evaluation of Operational Parameters	62
A. Background and Previous Work	62
B. Experimental Results	64
C. Conclusions	78
V. Surface Charge Density and Electrophoretic Mobility	80
A. Experimental Results and Conclusions	80
VI. Conclusions	84



	<u>Page</u>
Appendices	88
Bibliography	112
Vita	117

# LIST OF TABLES

<u>Table</u>		<u>Page</u>
1	Electrokinetic mobility results of coated glass capillaries in distilled-deionized water	20
2	Electrokinetic mobility results of coated glass capillaries in R-1 buffer	21
3	Effect of dynamic rinsing upon the electrokinetic mobility results of coated glass capillaries in distilled-deionized water	23
4	Effect of dynamic rinsing upon the electrokinetic mobility results of coated glass capillaries in R-1 buffer	24
5	Comparison of electrophoretic mobility results of polystyrene latexes, buffer-exchanged in $1 \times 10^{-4}$ BSB, obtained by microcapillary and continuous particle electrophoresis	41
6	The effect of various degrees of cleaning upon the electrophoretic mobilities of polystyrene latexes	81
7	Comparison of surface charge to the electrophoretic mobility and the zeta potential (H <sup>+</sup> counterion)	82
A-1	Composition and properties of R-1 buffer <sup>(69)</sup>	89

# LIST OF FIGURES

<u>Figure</u>		<u>Page</u>
1	Schematic diagram of microcapillary electrophoresis apparatus	7
2	Photograph of Rank Brothers Microcapillary Electrophoresis Apparatus, voltmeter-ammeter-timer unit and microscope illuminators (visible light source and Neon laser)	8
3	Electrokinetic mobilities for 0.794 $\mu$ m. polystyrene latex in $1 \times 10^{-4}$ I.S. barbital sodium barbital buffer as a function of their position in the cylindrical electrophoresis cell	11
4	Graphical determinations of the electrophoretic and electroosmotic mobilities using a method of linearization for 0.794 $\mu$ m. polystyrene latex in $1 \times 10^{-4}$ I.S. barbital sodium barbital buffer and measured in the standard cell	12
5	Electrophoresis cell with removable capillary cell (12)	17
6	Schematic diagram of the Beckman CPE separation chamber	30
7	Photograph of modified Beckman continuous particle electrophoresis apparatus with scanning UV light source (1), syringe-variable speed motor injection system (2), Houston Instruments	31

<u>Figure</u>		<u>Page</u>
	X-Y recorder (3), and refrigeration unit (4)	
8	Laminar flow through the CPE separation chamber, where: $2d = 0.15$ cm., $H = 30.0$ cm, $W = 4.5$ cm.	33
9	Collision of a larger particle against two smaller particles of equal size	39
10	Peak-to-peak distance versus particle concentration for $1.10$ $\mu$ m. and $0.109$ $\mu$ m. polystyrene latexes	43
11	The effect of particle size and concentration on the absolute migration distance of $1.10$ $\mu$ m. and $0.109$ $\mu$ m. PS, buffer-exchanged in $1 \times 10^{-4}$ BSB	44
12	The effect of particle size and number on the absolute migration distance of $1.10$ $\mu$ m. and $0.109$ $\mu$ m. PS, buffer-exchanged in $1 \times 10^{-4}$ BSB	45
13	Peak-to-peak separation distance versus particle concentration for $1.10$ $\mu$ m. and $0.234$ $\mu$ m. poly- styrene latexes	47
14	The effect of particle size and concentration on the absolute migration distance of $1.10$ $\mu$ m. and $0.234$ $\mu$ m. PS, buffer-exchanged in $1 \times 10^{-4}$ BSB	48
15	The effect of particle size and number on the absolute migration distance of $1.10$ $\mu$ m. and $0.234$ $\mu$ m. PS, buffer-exchanged in $1 \times 10^{-4}$ BSB	49

<u>Figure</u>		<u>Page</u>
16	Peak-to-peak separation distance versus particle concentration for 1.10 $\mu\text{m}$ . and 0.357 $\mu\text{m}$ . polystyrene latexes	50
17	The effect of particle size and concentration on the absolute migration distance of 1.10 $\mu\text{m}$ . and 0.357 $\mu\text{m}$ . PS, buffer-exchanged in $1 \times 10^{-4}$ BSB	51
18	The effect of particle size and number on the absolute migration distance of 1.10 $\mu\text{m}$ . and 0.357 $\mu\text{m}$ . PS, buffer-exchanged in $1 \times 10^{-4}$ BSB	52
19	Peak-to-peak separation distance versus particle concentration for 0.357 $\mu\text{m}$ . and 0.109 $\mu\text{m}$ . polystyrene latexes	53
20	The effect of particle size and concentration on the absolute migration distance of 0.357 $\mu\text{m}$ . and 0.109 $\mu\text{m}$ . PS, buffer-exchanged in $1 \times 10^{-4}$ BSB	54
21	The effect of particle size and number on the absolute migration distance of 0.357 $\mu\text{m}$ . and 0.109 $\mu\text{m}$ . PS, buffer-exchanged in $1 \times 10^{-4}$ BSB	55
22	Peak-to-peak separation distance versus particle concentration for 0.234 $\mu\text{m}$ . and 0.109 $\mu\text{m}$ . polystyrene latexes	56
23	The effect of particle size and concentration on the absolute migration distance of 0.234 $\mu\text{m}$ . and 0.109 $\mu\text{m}$ . PS, buffer-exchanged in $1 \times 10^{-4}$ BSB	57

<u>Figure</u>		<u>Page</u>
24	The effect of particle size and number on the absolute migration distance of 0.234 $\mu\text{m}$ . and 0.109 $\mu\text{m}$ . PS, buffer-exchanged in $1 \times 10^{-4}$ BSB	58
25	The effect of particle size and concentration on the absolute migration distance of 0.357 $\mu\text{m}$ . and 0.234 $\mu\text{m}$ . PS, buffer-exchanged in $1 \times 10^{-4}$ BSB	59
26	The effect of particle size and number on the absolute migration distance of 0.357 $\mu\text{m}$ . and 0.234 $\mu\text{m}$ . PS, buffer-exchanged in $1 \times 10^{-4}$ BSB	60
27	Comparison of the theoretical and experimental separations of two latexes, 0.357 and 0.234 $\mu\text{m}$ . in size, 26 cc/min.	65
28	Comparison of the theoretical and experimental separations of two latexes, 1.1 and 0.234 $\mu\text{m}$ . in size, 26 cc/min.	66
29	Comparison of the theoretical and experimental separations of four latexes, 1.1, 0.357, 0.234 and 0.109 $\mu\text{m}$ . in size, 26 cc/min.	67
30	Hypothetical separation at three stages of a mixture of two latexes, 1.1 and 0.234 $\mu\text{m}$ ., under real conditions	69
31	Computed particle displacement showing the effect of off-center injection on band separation with $U_{os} = -21.37 \text{ cm/volt sec.}$ , and $R = 0.2$ ; A. Centered, B. Off-Center	70

Figure

Page

- 32 Computed particle displacement showing the effect of electroosmosis with  $R = 0.2$ ; A.  $U_{os} = -21.37$   $\mu\text{m. cm/volt sec.}$ , at 15, 35 and 45 volts/cm.; B.  $U_{os} = -11.37$   $\mu\text{m. cm/volt sec.}$ , at 15, 35 and 45 volts/cm.; C.  $U_{os} = -31.37$   $\mu\text{m. cm/volt sec.}$ , at 15, 35 and 45 volts/cm. 71
- 33 Computed particle displacement showing the effect of different values of  $U_{os}$  for the front and rear walls with  $R = 0.2$  and average  $U_{os} = -21.37$   $\mu\text{m. cm/volt sec.}$ ; A.  $U_{osf} = U_{osr} = -21.37$   $\mu\text{m. cm/volt sec.}$ , B.  $U_{osf} = -31.37$   $\mu\text{m. cm/volt sec.}$ ,  $U_{osr} = -11.37$   $\mu\text{m. cm/volt sec.}$ , C.  $U_{osf} = -11.37$   $\mu\text{m. cm/volt sec.}$ ,  $U_{osr} = -31.37$   $\mu\text{m. cm/volt sec.}$  73
- 34 Computed particle displacement showing the effect of increasing the injection radius with  $U_{os} = -21.37$   $\mu\text{m. cm/volt sec.}$ ; A.  $R = 0.2$ , B.  $R = 0.4$ , and C.  $R = 0.6$  74
- 35 Computed particle displacement showing the effect of increasing band volume in the  $R$  or  $\theta$  direction with  $U_{os} = -21.37$   $\mu\text{m. cm/volt sec.}$ ; A.  $R = 0.2$ ,  $\theta = 0.4$ , D.  $R = 0.6$ ,  $\theta = 0.2$ , and E.  $R = 0.2$ ,  $\theta = 0.6$  76
- 36 Computed particle displacement showing the effect of increasing band volume in the  $R$  or  $\theta$  direction 77

Figure

Page

- with  $U_{os} = -11.37 \text{ um. cm/volt sec.}$ ; A.  $R = 0.2$ ,  $\theta = 0.2$ , B.  $R = 0.4$ ,  $\theta = 0.2$ , C.  $R = 0.2$ ,  $\theta = 0.4$ , D.  $R = 0.6$ ,  $\theta = 0.2$ , and E.  $R = 0.2$ ,  $\theta = 0.6$
- B-1 Comparison of electrokinetic mobilities versus the square of the distance for coated capillaries using distilled-deionized water as the solvent. A. Uncoated, B. Acrysol coated, C. XX210 coated, and D. Locron-P coated capillaries 91
- B-2 Comparison of controlled electrokinetic mobilities versus the square of the distance for coated capillaries using distilled-deionized water as the solvent. A. Acrysol coated, B. XX210 coated, C. 50/50 by weight XX210/Acrysol coated, and D. 75/25 by weight XX210/Acrysol coated capillaries 92
- B-3 Comparison of electrokinetic mobilities versus the square of the distance for coated capillaries using R-1 buffer as the solvent. A. Uncoated, B. Acrysol coated, C. Locron-P coated, D. Polystyrene in toluene, and E. XX210 coated capillaries 93
- B-4 Comparison of controlled electrokinetic mobilities versus the square of the distance for coated capillaries using R-1 buffer as the solvent. A. Acrysol coated, B. XX210 coated, C. 75/25 by weight XX210/Acrysol coated, and D. 50/50 by weight XX210/Acrysol coated capillaries 94



<u>Figure</u>		<u>Page</u>
B-5	Effect of dynamic rinsing upon the electrokinetic mobility results of coated glass capillaries in distilled-deionized water	95
B-6	Effect of dynamic rinsing upon the electrokinetic mobility results of coated glass capillaries in distilled-deionized water	96
B-7	Effect of dynamic rinsing upon the electrokinetic mobility results of coated glass capillaries in distilled-deionized water	97
B-8	Effect of dynamic rinsing upon the electrokinetic mobility results of coated glass capillaries in distilled-deionized water	98
B-9	Effect of dynamic rinsing upon the electrokinetic mobility results of coated glass capillaries in R-1 buffer	99
B-10	Effect of dynamic rinsing upon the electrokinetic mobility results of coated glass capillaries in R-1 buffer	100
B-11	Effect of dynamic rinsing upon the electrokinetic mobility results of coated glass capillaries in R-1 buffer	101
B-12	Effect of dynamic rinsing upon the electrokinetic mobility results of coated glass capillaries in R-1 buffer	102

<u>Figure</u>		<u>Page</u>
D-1	Conductometric titration of 0.109 $\mu\text{m}$ . PS latex after cleaning three times using the ion-exchange technique	108
D-2	Conductometric titration of 0.109 $\mu\text{m}$ . PS latex after cleaning four times using the ion-exchange technique	109
D-3	Conductometric titration of 1.10 $\mu\text{m}$ . PS latex after cleaning three times using the ion-exchange technique	110
D-4	Conductometric titration of 1.10 $\mu\text{m}$ . PS latex after cleaning four times using the ion-exchange technique	111

# ABSTRACT

The objective of this investigation was to maximize the electrophoretic separation of particles using the Continuous Particle Electrophoresis (CPE) Apparatus. Theoretically in order to obtain optimum resolution of separation in the CPE the electroosmotic flow must be equal to the mean electrophoretic mobility of the particles to be separated. Electroosmosis may be controlled by the development of a stable coating with controlled electrokinetic properties. Several stable continuous coatings were evaluated using the idea that a combination of at least two different latexes, where at least one of the latexes is a film-former, will result in a coating with electrokinetic properties inbetween the electrokinetic properties of the two latexes. Such a coating was developed using XX210 (polyvinyl acetate) and Acrysol (acrylic copolymer). Combinations of XX210 and Acrysol showed electroosmotic mobility values as a function of their respective concentrations. The coatings appeared stable after a 48-hour dynamic rinse.

The resolution of separation in the CPE may be reduced by particle-particle interactions and/or the influence of electroosmosis. The affect of particle-particle interactions as a function of particle size and concentration upon the separation of latex particles was investigated and found to be a problem of the separated system at high particle concentrations or low electrolyte concentrations. The influence of electroosmosis was evaluated using a computer model previously developed by Krumrine. This computer model was experimentally

verified for separations where particle-particle interactions and sedimentation effects were negligible.

In addition, the surface charge densities of monodisperse polystyrene latexes were determined as a function of their sulfate endgroups. These values were compared to the electrophoretic mobilities and the zeta potentials of the latexes. No direct relationship could be drawn between the number of sulfate endgroups determined by conductometric titration and the zeta potential or the electrophoretic mobility of these latexes.

## CHAPTER I

### INTRODUCTION

Electrophoresis is defined as the migration of particles through a solution under the influence of an electric field<sup>(1)</sup>. Electrophoretic techniques have been developed primarily as a tool for the separation and characterization of biological macromolecules, e.g. cells, proteins.

Continuous Particle Electrophoresis (CPE) is uniquely characterized by a free flow system designed for preparative use, but modified for analytical use, of charged colloid particles. Interest in the CPE has centered around the evaluation of parameters involved in separation using monodisperse polystyrene (PS) latexes as model colloids. Previously, Krumrine<sup>(2)</sup> initiated this work by the development of a computer model to simulate the separation process of particles in the CPE. This present study will continue this work to verify Krumrine's computer model against experimental data and will evaluate the parameters that influence separation against those present in the computer model. Then this model will be used to illustrate how resolution can be affected by electroosmosis and can be optimized by proper selection of operational parameters.

The main problem in obtaining maximum resolution in continuous electrophoresis is the control of electroosmosis. This is a design problem arising from the charges present along the walls of the separation chamber of the CPE. According to theory<sup>(3,4)</sup>, maximum separation occurs when electroosmosis is matched to the mean electro-

phoretic mobility of the particles to be separated<sup>(6,12)</sup>. Therefore, if a coating with controlled electrokinetic properties could be developed, then the electroosmotic mobility could be selected for any particular separation system. This study has evaluated several coatings on the premise that a combination of at least two different latexes, where at least one of the latexes is a film-former, will result in a coating with electrokinetic properties inbetween the electrokinetic properties of the two latexes.

The resolution of separation in the CPE can also be reduced by particle-particle interactions between the colloid particles undergoing separation. This is a problem of the separated system and depends upon the particle concentration, particle size and medium of suspension. These interactions will be evaluated in order that they might be minimized for a given separation system.

Also, the surface charge densities of the latexes of interest in this investigation were determined as a function of their sulfate end groups. These values were compared to the electrophoretic mobilities and the zeta potentials of the latexes.

## CHAPTER II

### Development of a Coating with Controlled Electrokinetic Properties

#### A. Background and Previous Work

Microcapillary electrophoresis (MCE) utilizes the classical microscope method of visually observing the migration of particles under the influence of an electric field. The particles are suspended in solution and placed in either a cylindrical or flat (rectangular) cell and an electric current applied through the cell. The velocity of a particle can be determined by measuring the time for a particle to transverse a given distance using a micrometer eyepiece and an electromagnetic timer. The electric field strength can be calculated from the cell constant and the applied voltage. The migration of a particle is then expressed in terms of mobility, or velocity per unit field strength ( $\mu\text{m cm/volt sec.}$ ).

(5,6,7,8) Microcapillary electrophoresis has been used to study the electrophoretic mobility of cells<sup>(9)</sup>, albumin<sup>(10)</sup>, latexes<sup>(11)</sup>, viruses<sup>(5)</sup>, carbon<sup>(5)</sup>, detergents<sup>(5)</sup>, and many more.

There are several advantages to MCE over other electrophoretic techniques<sup>(5,12,10)</sup>:

1. only small concentrations of suspended particles (0.001% solids) are required for observation, therefore particle-particle interactions are avoided,
2. the shape, size and orientation of the particles can be observed during the measurement,
3. the mobilities can be measured at very low ionic strengths,
4. the environment in which the particles are migrating is the same

for all the particles and is constant,

5. differences in relative mobilities can be observed by comparing various particles simultaneously,
6. isoelectric points of submicroscopic particles insoluble at their isoelectric points can be determined from the mobility of the resulting microscopic aggregates,
7. high magnification can be used for greater sensitivity,
8. the observations can be made fast, and
9. the apparatus is affordable and easy to maintain.

Disadvantages to this method over other electrophoretic techniques are: (5,10)

1. the concentrations required for observation are too low, and
2. observations are limited to microscopic sized particles.

A schematic diagram of the MCE is shown in Figure 1. The apparatus consists of a standard quartz cell, two blacked platinum electrodes, a water reservoir and an optical microscope. A photograph of the Rank Brothers apparatus in our laboratory is shown in Figure 2. The figure also shows the electromagnetic timer attached to an ammeter-voltmeter-timer unit and microscope illuminators.

Factors of considerable importance on MCE measurements are: (5,6,13)

1. electroosmotic flow,
2. convection generated by Joule heating,



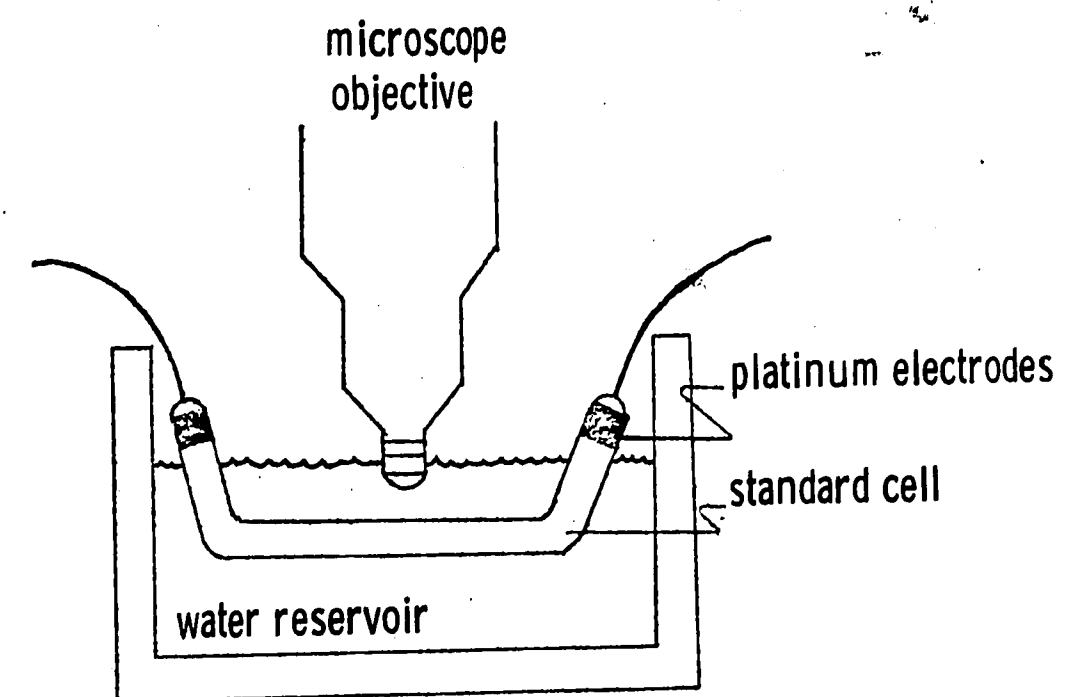


Figure 1. Schematic diagram of Microcapillary Electrophoresis Apparatus.

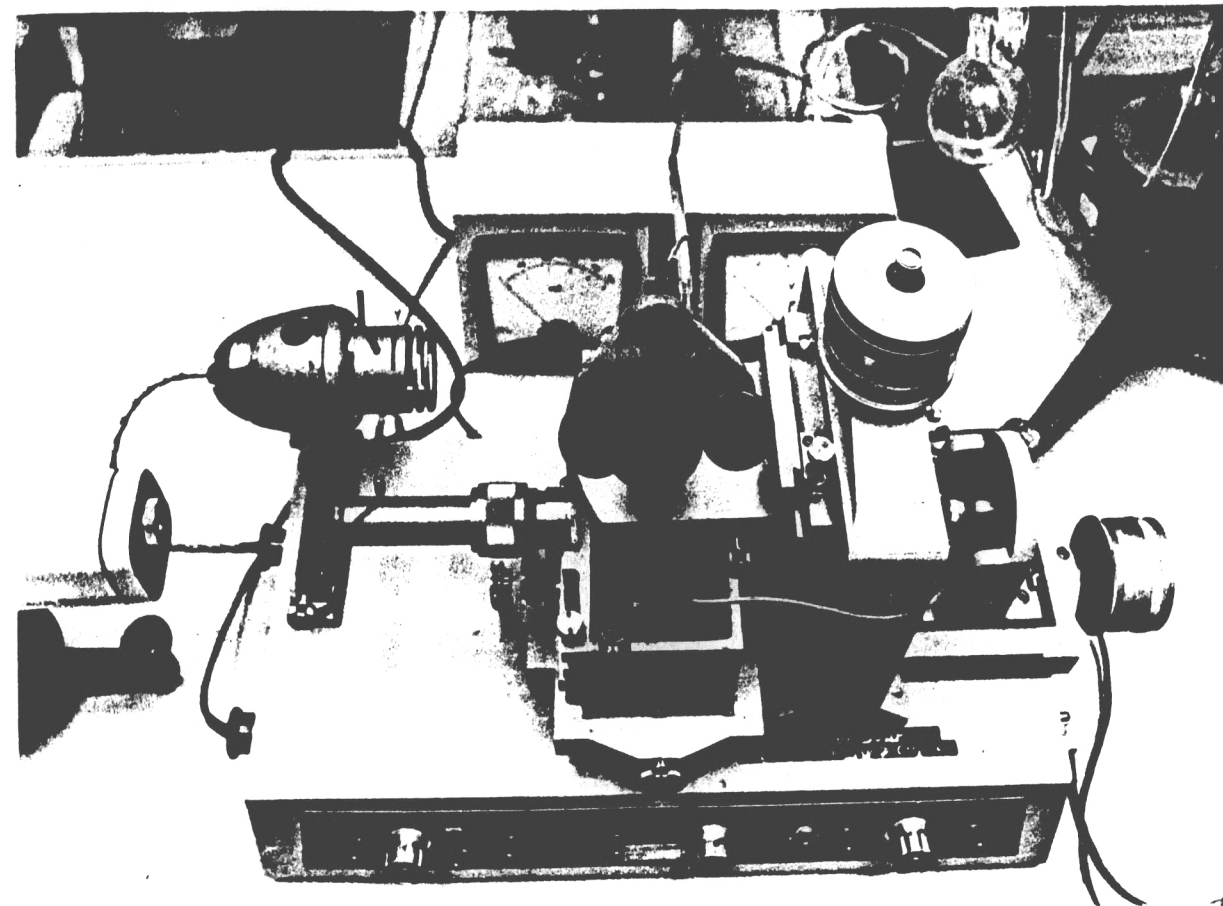


Figure 2. Photograph of Rank Brothers Microcapillary Electrophoresis Apparatus, voltmeter-ammeter-timer unit and microscope illuminators (visible light source and Neon laser).

3. inaccurate determination of the stationary level\*, or zero solvent flow level,
4. sedimentation due to gravity,
5. impurities within the cell which changes the surface characteristics of the cell wall,
6. gassing at the electrodes,
7. air bubbles introduced during filling of the cell, and
8. pressure differences caused by poor sealing at the electrode-cell interface.

Gassing at the electrodes, air bubbles introduced during filling of the cell and pressure differences caused by poor sealing at the electrode-cell interface can be avoided by careful use. Impurities within the cell were removed by a cleaning procedure which will be discussed later. Convection and sedimentation can be avoided by operating electrophoresis in the gravity-free environment of space<sup>(16,9,17,13)</sup>. Lerche, Brinton and Lauffer<sup>(5,6,14)</sup> have studied errors involved in MCE and found that overall reproducibility of duplicate mobility measurements on homogeneous samples on the same day was 2% and on different days was 5%.

Microcapillary electrophoresis measurements involve numerous observations of particle migration at different depths of focus within the

\* Stationary level, or zero solvent flow level-position in the cell where the particle mobility is unaffected by the effects of electroosmosis; at this position electroosmotic flow and backflow in the cell exactly cancel.

electrophoresis cell. Electrophoretic mobilities\* are superimposed on electroosmotic mobilities\*\* which must be corrected to give accurate values for mobility. Each observed migration is a function of its position in the cell and a parabolic profile results due to the superposition of the electroosmotic and electrophoretic flows<sup>(9,12,15)</sup>, Figure 3. These values may be linearized by plotting the electrokinetic mobility versus the square of the distance from the center of the cell<sup>(18,11,12)</sup>, as shown in Figure 4. The true electrophoretic mobility (at the zero solvent flow position) can be observed at a distance of 29.3% of the cell radius from the wall of a cylindrical cell<sup>(7,6)</sup>. However, the true electrophoretic mobility is positioned along a steep slope of the parabola and interpolation between the data points may lead to some error in determining the electrophoretic mobility. This problem can be solved if the electroosmotic flow is reduced or maintained at a constant value throughout the cell. Van Oss has obtained this result using agrose gel coatings to increase the viscosity near the wall, thus simplifying MCE<sup>(7)</sup>.

Two limiting and serious problems inherent in the electrophoresis of particles are convection and sedimentation. A temperature gradient in an electrophoresis cell occurs due to the transfer of heat generated by the electric field across the resistance of the electrolyte. In the presence of gravity, this temperature gradient will result in

\* electrophoretic mobility-migration of a particle relative to the continuous phase which surrounds it<sup>(15)</sup>.

\*\* electroosmotic mobility-solution phase which moves relative to the stationary walls<sup>(15)</sup>.

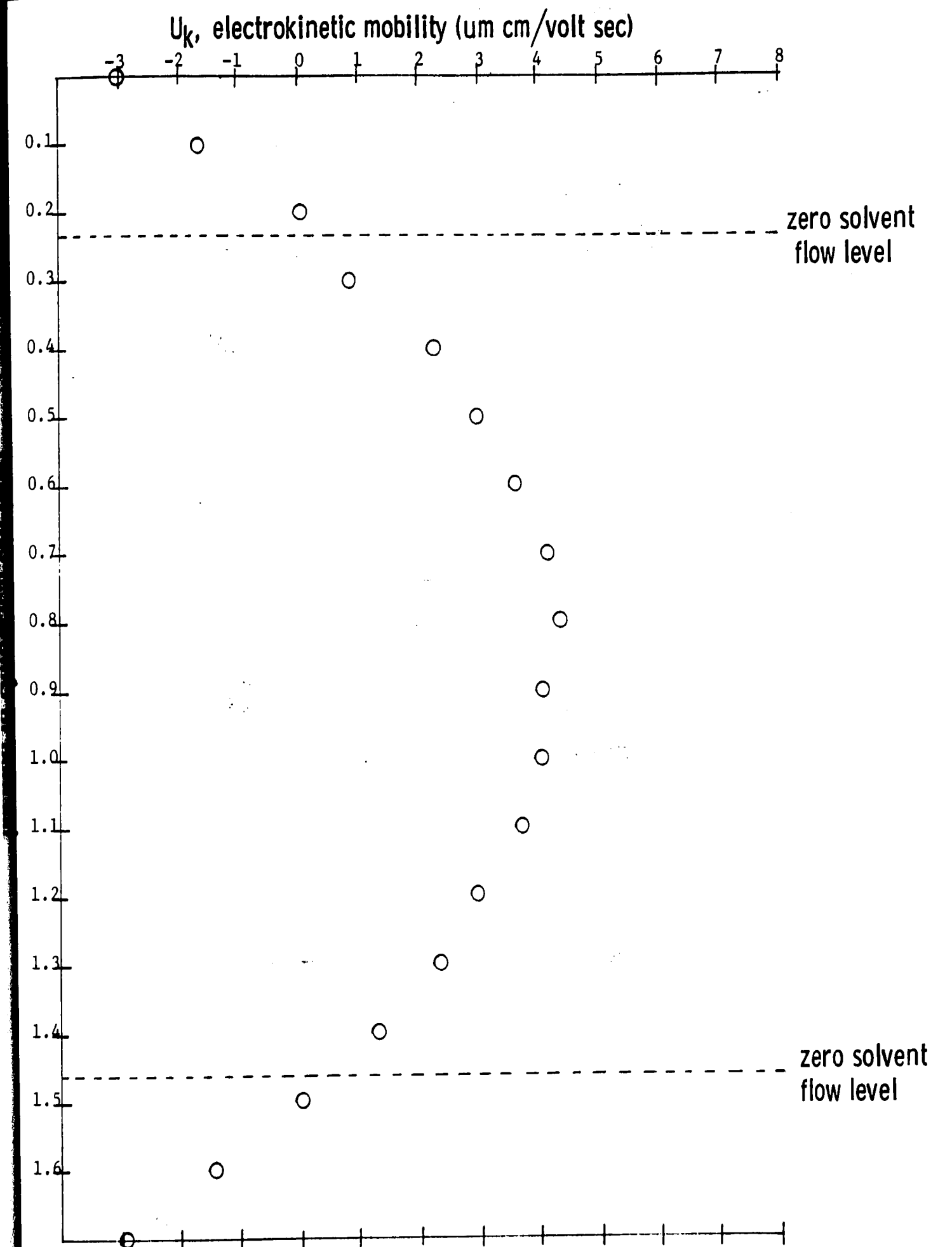


Figure 3. Electrokinetic mobilities for 0.794 um. PS latex in  $1 \times 10^{-4}$  BSB as a function of their position in the cylindrical electrophoresis cell.

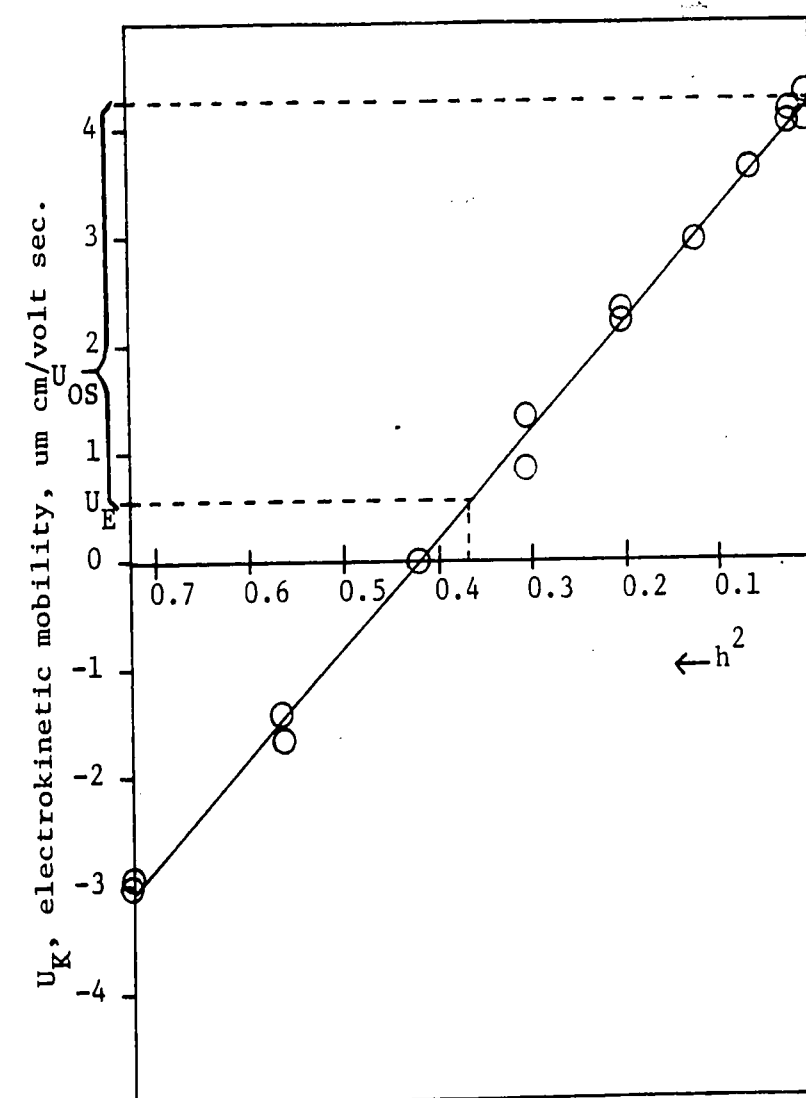


Figure 4. Graphical determinations of the electrophoretic and electroosmotic mobilities using a method of linearization for 0.794  $\mu$ m. PS latex in  $1 \times 10^{-4}$  BSB and measured in the standard cell.

thermal convection that will remix separated particles. Also the sedimentation of particles will either complicate the interpretation of the results or prevent continued observations once the particles reach the bottom of the electrophoresis cell<sup>(19)</sup>. Therefore, it would be advantageous to perform electrophoresis in space, to avoid convection and sedimentation effects.

Our laboratory has been active in the operation of electrophoresis in space since it was first performed on the return trip from the moon aboard Apollo 14. The separation involved that of red and blue dyes, and of hemoglobin and DNA in a closed cylindrical system which will be referred to as "free-fluid electrophoresis" (FFE). Later, aboard Apollo 16, another FFE experiment was carried out using monodisperse polystyrene latexes<sup>(17,9,11,20)</sup>. Photographs of the performed experiments in space and on earth indicated that future separations would be impossible without the reduction of electroosmotic backflow<sup>(16,11,18)</sup>. Hence, work was undertaken to develop coatings to reduce the zeta potential at the cell wall-liquid interface to near zero, since the zeta potential is the driving force responsible for electroosmosis in the presence of an applied potential<sup>(18,11)</sup>.

Five methods are known to reduce electroosmosis which arises from the charge on the cell wall: <sup>(7,9,21)</sup>

1. construct the cell from a solid material with no surface charge,
2. coat the cell wall with a highly viscous solution,
3. coat the cell wall with a hydrophobic, uncharged material, or
4. coat the cell wall with a hydrophilic, uncharged material, or

5. apply counterflow of liquid to exactly cancel electroosmotic reflow.

It is not desirable to construct a cell from a solid material with no surface charge because it limits the materials of construction. The second method of coating the cell wall with a highly viscous solution does not yield a permanent coating and is not desirable. Hjerten<sup>(11,21)</sup> tried the third, fourth and fifth methods with limited success. The third and fourth methods, of surface treatment to reduce the surface potential, did not appear to adhere to the cell wall efficiently. Later, Krumrine<sup>(18,17,12,22)</sup> investigated the third and fourth methods of reducing the electroosmotic flow. He found that methyl cellulose reduced electroosmosis most efficiently when coated on glass, polymethylmethacrylate (Plexiglas) or polycarbonate cells and appeared stable. However, he found that methyl cellulose can desorb and adsorb onto the surfaces of the particles in the dispersion. Therefore, it was important that the methyl cellulose was strongly bound ("chemically bound") and that looser bound ("physically bound") material was removed by dynamic rinsing.

#### B. Experimental Results and Discussion:

Previously our laboratory has been interested in the operation of free fluid electrophoresis. Analysis of collected data in space and on earth indicated that desired separations were prevented by the presence of electroosmosis. Work was undertaken in this laboratory to reduce electroosmosis by the surface treatment of the cell wall with various polymer coatings. These coatings were successful in reducing electroosmosis and appeared stable after a 48-hour dynamic rinse.



The objective of the present work is to try a different approach to the problem of electroosmosis in continuous electrophoresis for use in space and on earth. Theoretically maximum separation should occur when electroosmosis is matched to the mean electrophoretic mobility of the particles to be separated <sup>(4,3)</sup>. Therefore, if a coating with controlled electrokinetic properties could be developed, then the electroosmotic mobility could be selected for any particular separated system. Such coatings would be based on the concept that a combination of at least two different latexes, where at least one of the latexes is a film-former, will result in a coating with electrokinetic properties inbetween the electrokinetic properties of the two latexes. This investigation was directed towards the development of a stable continuous coating with controlled electrokinetic properties for the optimization of separation in continuous electrophoresis.

Coatings for the separation chamber of the continuous particle electrophoresis (CPE) apparatus must have the physical properties of good adhesion and durability under flow conditions for long periods of time <sup>(12)</sup>. These coatings must be effective on different types of surfaces, e.g. glass, plastic, ceramic alumina, which are now being used in the electrophoresis channel of the CPE. Also, these coatings must be uniform, transparent, stable and only a few layers of molecules thick.

Several coatings were evaluated for their electrokinetic properties using 0.80  $\mu\text{m}$ . in diameter monodisperse polystyrene (PS) latex in two different solvents, distilled-deionized (DDI) water and R-1 buffer (see Appendix A). These coatings were applied to glass capillary

tubes that could be easily placed and removed from an electrophoresis cell holder, Figure 5<sup>(12)</sup>. The electroosmotic mobilities were evaluated using the Rank Brothers microelectrophoresis apparatus. Film-forming latexes, such as XX210 (polyvinyl acetate; Air Products and Chemicals Company) and Acrysol (acrylic copolymer; Rohm and Haas Company) were evaluated along with Locron-P (Hoechst Corporation) and high molecular weight polystyrene in toluene solution.

The procedure used for coating the glass capillary tubes consisted of two main parts:

1. cleaning the glass capillary tubes

- a. put the capillary tube in a test tube with a screw top,
- b. fill the test tube with potassium dichromate-sulfuric acid solution<sup>(23)</sup> and let set for one day,
- c. remove the dichromate solution and rinse well with DDI,
- d. fill the test tube with tetrahydrofuran (THF) and let set for one hour,
- e. remove the THF and rinse well with acetone,
- f. allow the test tubes to dry in the oven overnight (avoid touching the capillaries with your fingers; this leaves an oily residue).

2. coating the glass capillary tubes

- a. dip the cleaned capillary tube into a 5-10% solids suspension for 30 minutes,
- b. remove the capillary carefully from the test tube and blot the tip with a kimwipe,

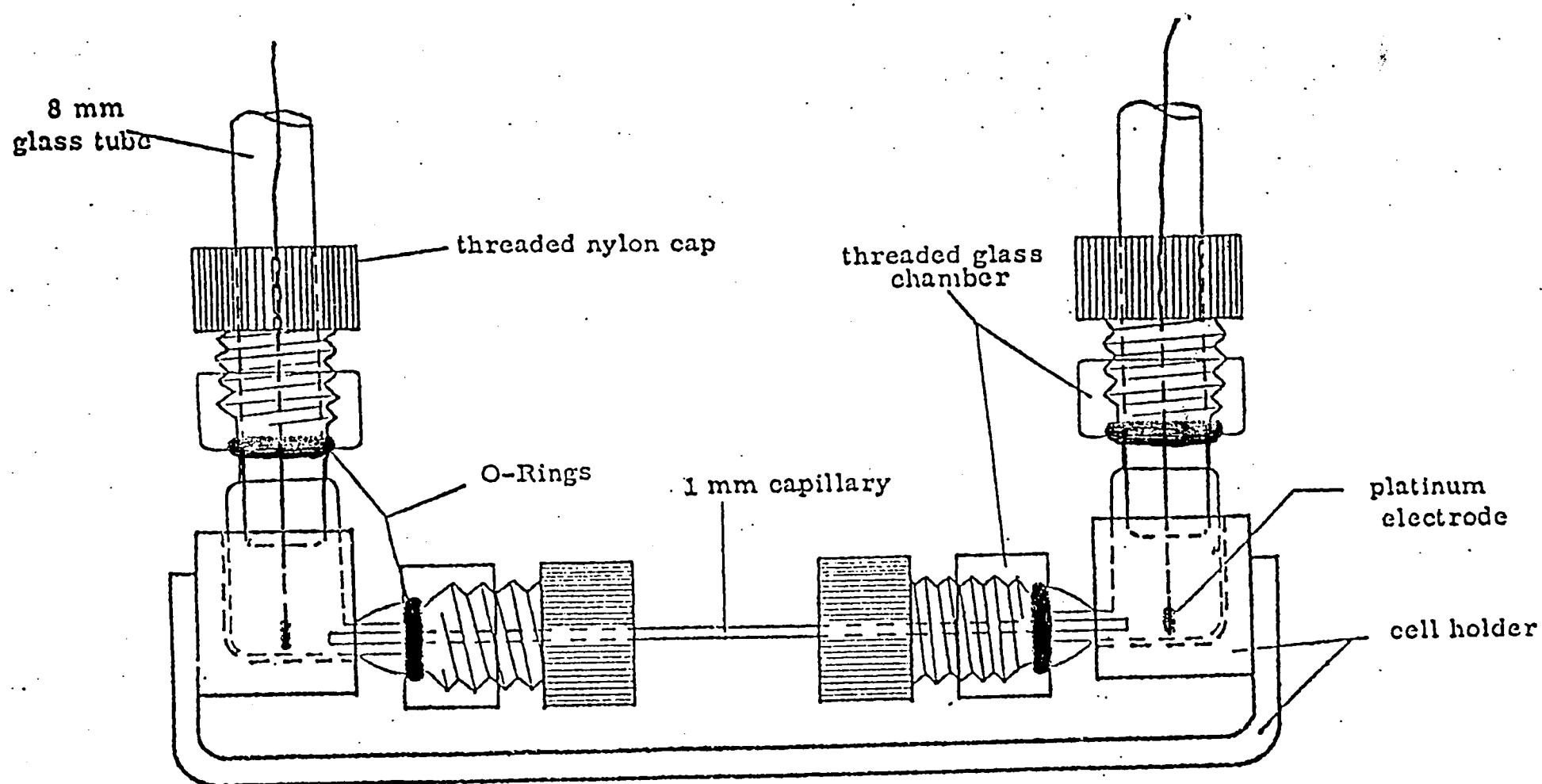


Figure 5. Electrophoresis cell with removable capillary cell (12).

- c. hydrolyze the coating by placing the capillary in the oven for at least 24 hours,
- d. previous and present work suggest that a dynamic rinse for at least 48-hours will remove any physically adsorbed material,

To ensure proper working conditions, two methods of cleaning the MCE cells were used:

1. for measurements in aqueous solutions
  - a. fill the cell with sulfuric acid-dichromate solution<sup>(23)</sup> and let set for 5 minutes,
  - b. rinse well with DDI,
  - c. fill the cell with sodium bicarbonate and let set for 5 minutes,
  - d. rinse well with DDI.
2. for measurements in organic solvents
  - a. fill the cell with aqua-regia and let set for 10 minutes,
  - b. rinse well with DDI,
  - c. dry overnight in the oven at approximately 80°C.

The experimental results are summarized in Tables 1 through 4 and plotted versus the square of the distance in Appendix B. Tables 1 and 2 show the effect of the various coatings on the electroosmotic mobility results for the 0.80  $\mu$ m. latex in DDI and R-1 buffer, respectively. It can be observed that the Acrysol coating has a large negative electroosmotic mobility, therefore a high surface charge density and a high zeta potential. Some discontinuities could be observed on the Acrysol coating. The XX210 coating appears to have a small negative surface charge density in DDI and R-1 buffer; the polystyrene in

toluene coating showed a small negative surface charge in R-1 buffer; and the Locron-P coating showed a small positive surface charge density in DDI and a small negative surface charge density in R-1 buffer. Further experimental work is needed before an explanation can be given for this change in surface charge density of the Locron-P coating in the different mediums. The results show that the Locron-P coating gave a positive electroosmotic mobility value in deionized water. Until now no coating has been found which would give a positive electroosmotic mobility. Such a coating would be instrumental<sup>(12)</sup> in obtaining optimum resolution of separation in the CPE when the problem of Joule heating necessitates maintaining the wall temperature of the separation chamber lower than the temperature at the center of the chamber.

The data summarized in Tables 1 and 2 provided the basis for attempting to control the electrokinetic properties of a stable coating using at least two latexes, where one of the latexes has a high zeta potential, such as Acrysol, and one of the latexes has a low zeta potential, such as XX210. Also, at least one of the latexes must be a film-former, but in this study both Acrysol and XX210 are film-formers. The coating resulting from this mixture should have a zeta potential intermediate between the Acrysol and the XX210 latexes. From Tables 1 and 2, it is shown that 50/50 by volume percent mixtures of XX210 and Acrysol give electrokinetic results inbetween the XX210 and Acrysol latexes independently. Further, the 50/50 and 75/25 by weight percent solids mixtures of XX210 and Acrysol gave electrokinetic results that indicated their electrokinetic properties are a function of their respective concentrations.

TABLE 1

Electrokinetic mobility results of coated glass capillaries in  
distilled-deionized water

Coating	U <sub>os</sub>	Ratio $\frac{U_{os} \text{ Coated}}{U_{os} \text{ Uncoated}}$	U <sub>E</sub>
*cleaned, uncoated	-9.16	--	+1.943
Locron-P	+0.546	-0.062	+1.720
XX210	-2.900	+0.330	+1.305
Acrysol	-8.910	+1.013	+2.120
50/50 by vol. XX210/Acrysol	-4.920	+0.560	+1.500
50/50 by wt. XX210/Acrysol	-6.205	+0.705	+1.150
75/25 by wt. XX210/Acrysol	-3.050	+0.347	+1.080

\* Determined by Krumrine<sup>(8)</sup>

(refer to Figures B-1 and B-2)

TABLE 2

Electrokinetic mobility results of coated glass

capillaries in R-1 buffer

Coating	U <sub>os</sub>	Ratio $\frac{U_{os} \text{ Coated}}{U_{os} \text{ Uncoated}}$	U <sub>E</sub>
*cleaned, uncoated	-5.76	--	+3.974
HMW, PS in toluene	-1.58	+0.425	+1.620
Locron-P	-2.45	+0.657	+2.660
XX210	-0.725	+0.195	+1.400
Acrysol	-7.97	+2.142	+2.690
50/50 by vol. XX210/Acrysol	-2.382	+0.640	+0.468
50/50 by wt. XX210/Acrysol	-1.496	+0.402	+0.834
75/25 by wt. XX210/Acrysol	-2.023	+0.544	+1.182

\* Determined by Krumrine<sup>(8)</sup>.

(refer to Figures B-3 and B-4)

A coating for the Beckman CPE separation chamber must be durable under fluid flow conditions for long periods of time. In order to test the XX210/Acrysol coating for good adhesion and durability, a dynamic rinse was performed at a rate of 0.5 liters per hour. This rinse would remove any physically adsorbed XX210 or Acrysol latex which may have caused erratic results. The data which shows the effect of dynamic rinsing upon the electroosmotic mobility results are summarized in Tables 3 and 4 for the 0.80  $\mu$ m. latex in DDI and R-1 buffer, respectively.

The XX210 coated capillary in DDI and R-1 buffer appears very stable after a 48-hour rinse. The observed electrokinetic mobilities have essentially remained unchanged and any variations in mobilities may be attributed to scatter in the experimental data points. The electroosmotic mobility appears to have decreased in magnitude in the R-1 buffer system; this may be due to an affinity of the R-1 buffer ions to the XX210 coating along its surface.

The Acrysol coated capillary in DDI appears to decrease in magnitude in electroosmotic mobility after a 48-hour rinse. This high zeta potential observed using this coating may be partially contributed by the physically adsorbed Acrysol and the chemically adsorbed Acrysol may exhibit a lower zeta potential than expected. Also, these results may be due to some ageing effects upon rinsing. In the R-1 buffer system, the electroosmotic mobility has decreased in magnitude and the electrophoretic mobility has increased. This decrease in electroosmotic mobility has been discussed above and the increase in electrophoretic mobility may be due to the increased ionic medium of the R-1 buffer.



TABLE 3

Effect of dynamic rinsing upon the electrokinetic mobility  
results of coated glass capillaries in distilled-deionized water

Coating	U <sub>os</sub>			U <sub>E</sub>		
	0 hours	48 hours	96 hours	0 hours	48 hours	96 hours
*cleaned, uncoated	-9.160	--	--	+1.943	---	--
XX210	-2.900	-1.510	--	+1.305	+1.440	--
Acrysol	-8.910	-1.580	--	+2.120	+2.540	--
50/50 by wt. XX210/Acrysol	-6.205	-4.600	-0.780	+1.150	+1.398	+1.920
75/25 by wt. XX210/Acrysol	-3.050	-1.520	--	+1.080	+1.640	--

\* Determined by Krumrine<sup>(8)</sup>.

(refer to Figures B-5, B-6, B-7 and B-8)

TABLE 4

Effect of dynamic rinsing upon the electrokinetic mobility  
results of coated glass capillaries in R-1 buffer

Coating	Uos			UE		
	0 hours	48 hours	96 hours	0 hours	48 hours	96 hours
*cleaned, uncoated	-5.760	--	--	+3.974	--	--
XX210	-0.725	-0.876	--	+1.400	+1.280	--
Acrysol	-7.970	-1.340	--	+2.690	+4.040	--
50/50 by wt. XX210/Acrysol	-1.496	-1.250	--	+0.834	+1.900	--
75/25 by wt. XX210/Acrysol	-2.023	-0.804	--	+1.182	+2.960	--

\* Determined by Krumrine <sup>(8)</sup>.

(refer to Figures B-9, B-10, B-11, and B-12).

The 50/50 by weight percent solids XX210/Acrysol coating appears stable after a 48-hour rinse in DDI and R-1 buffer. Again, the electrophoretic mobility of the particles have increased in the R-1 buffer, and the magnitude of the electroosmotic mobility is greater in the R-1 buffer than in DDI. Possible explanations for this behavior have been given above. Essentially the electroosmotic mobility has remained unchanged upon rinsing and any variation may be attributed to scatter in the data points. The coating appears to break-down after a 96-hour rinse, perhaps due to the partial removal of one or both of the components of the coating.

Similarly, the 75/25 by weight percent solids XX210/Acrysol coating appears stable after a 48-hour rinse in DDI and R-1 buffer, and the electroosmotic mobilities have decreased and the electrophoretic mobilities have increased in the R-1 buffer system. Variations in electroosmotic mobility upon rinsing may be due to scatter in the data points and the removal of physically adsorbed material.

In summary, detailed examination of the data collected was limited because these results need to be confirmed by repeated experimentation. However, an attempt was made to develop a coating with controlled electrokinetic properties and these results are encouraging, and the coating appears stable under flow conditions for extended periods of time.

### CHAPTER III

#### Particle-Particle Interactions Affecting the Separation of Colloid Particles

##### A. Background and Apparatus

Electrophoresis is defined as the migration of particles through a solution under the influence of an electric field. Electrophoretic methods are a powerful means of fractionating the components of a mixture<sup>(1)</sup>. This technique is the most effective known for the separation and isolation of biological macromolecules. Although both apparatus and procedure has been well-developed for analytical purposes, e.g. Tiselius and disc gel electrophoresis, no preparative method was available for about fifty years. Initially Philipot<sup>(24)</sup> was interested in continuous electrophoresis, but he reported difficulties in achieving free-boundary flow and level stability. Therefore, later designs made use of a stabilized media or electroconvection. Some of these designs were based on the electrode-cantation principle of Pauli<sup>(25)</sup>. Here charged colloids were separated by an electric field, but as they migrate to one of the electrodes they are layered along a semi-permeable membrane which lies inbetween the electrodes. This layer of particles eventually settles and can be withdrawn from the rest of the suspension. This principle was adopted by Kirkwood<sup>(26)</sup> in the electrophoresis-convection method using the Clusius column and later by Bier<sup>(26)</sup> in his continuous free-boundary flow-electrophoresis method. Also, electrochromatographic techniques were developed by Grassmann<sup>(27,28)</sup>, Hannig<sup>(27,29,30)</sup>, Duarum<sup>(31)</sup>, Svensson<sup>(27)</sup>, Brattsten<sup>(27)</sup>,

Strain<sup>(31)</sup> and Karler<sup>(31)</sup>. These techniques used a stabilized medium, e.g. filter paper, packed bed, down which a fluid medium or background electrolyte is continuously fed and across which a continuous direct current is applied.

Dobry and Finn<sup>(32)</sup> reported a different approach to continuous electrophoresis using a vertically positioned apparatus, upward fluid flow thickened by a high viscosity polymer to suppress thermal convection, and electrodes separated from the separation chamber by a thermoplastic resin. This work appears to have inspired Mel<sup>(24,3)</sup> to construct a horizontally positioned apparatus, which was essentially a continuous gradient zone electrophoresis, with electrodes separated from the separation chamber by a semi-permeable membrane. This density gradient method was later referred to as stable-flow free-boundary electrophoresis (STAFLO). Finally, Kolin<sup>(27)</sup> was able to obtain continuous electrophoretic fractionation without the use of a porous media or concentration gradients previously required for stabilization against thermal convection. This was very desirable because measured migration velocities could be used directly to calculate the zeta potentials without effects due to density gradients or chromatography. Kolin used an electromagnetic force field and rotation of the fluid to overcome thermal convection. The resulting separation was fast, sharp and stable to 100 volts/cm., however only minute quantities could be separated. Later, Kolin proposed alternative methods for stabilization against thermal convection, such as; using a vertically positioned serpentine column with an electric current applied at right angles to the

upward flowing fluid<sup>(33,34)</sup>, and a fluid endless belt electrophoresis apparatus<sup>(19)</sup>.

A continuous free-film electrophoresis apparatus was developed by Barrolier in 1958<sup>(35)</sup> and improved upon by Hannig<sup>(29,30)</sup> for the separation of dissolved components. Hannig<sup>(36,37,38,39)</sup> further developed this technique for the fractionation of small particles.

In 1965, Strickler<sup>(40)</sup> developed an apparatus for the separation and fractionation of particles in a free-flowing fluid, at Beckman Instruments, Inc. This apparatus became known as continuous particle electrophoresis (CPE). This system was different from other traditional systems of electrophoresis in several respects. The sample was injected as a capillary stream into a thin flowing curtain of buffer, across which a lateral direct current is applied, Figure 6. Continuous collection of particles resulted from this migration under the influence of an electric field, and their electrophoretic migration can be observed and recorded. In 1967, Huebner<sup>(41,42)</sup>, also at Beckman Instruments, improved and simplified the operation of Strickler's design of the CPE. The Beckman CPE<sup>(43,44,45)</sup> consists of a 0.15 cm. thick rectangular separation chamber positioned vertically with platinum electrodes on opposite sides along this chamber. Electrolyte curtain fluid is pumped by a peristaltic pump into the top of the channel and empties out the bottom through forty-eight tubes set edge-to-edge. The electrodes are separated from the electrophoresis channel by semi-permeable membranes, and a separate centrifugal pump circulates a countercurrent flow of the same electrolyte up through the electrode compartments to remove any products

of electrolysis. The sample enters the top of the separation chamber about one-third of the way from the left-hand of the way from the left-hand edge. This sample stream descends vertically in the absence of a voltage gradient, the sample stream fans out according to the respective particle mobilities.

The Beckman CPE used in our laboratory is based upon Huebner's modified design of the CPE. Our laboratory has further modified the CPE's sample injection and detection systems and a refrigeration unit was added. The sample to be analyzed was now injected using a microsyringe attached to a variable speed motor for greater reproducibility. The detection of particle streams in the CPE was modified by the addition of a small scanning UV light source (on loan from Dow Chemical) attached to the face plate of the CPE. The light was received by a photomultiplier tube in the rear of the apparatus and the signal amplified and drawn on a Houston Instruments X-Y recorder. This system allowed detection of separated particle bands to 0.15 mobility units, which could not be observed visually or collected in fractions because of a limiting number of fractions available. The magnification from the separation chamber to the X-Y recorder is about 18.2X. It has been possible to separate particles from 0.04 to 100  $\mu$ m. in diameter, and up to 30 weight percent solids using this system. Figure 7 shows a photograph of the modified Beckman CPE apparatus in our laboratory, on loan from the U. S. Government.

The principle of flow in the CPE has been described by Strickler<sup>(46)</sup> and Hannig<sup>(36)</sup>. A schematic representation of the electro-

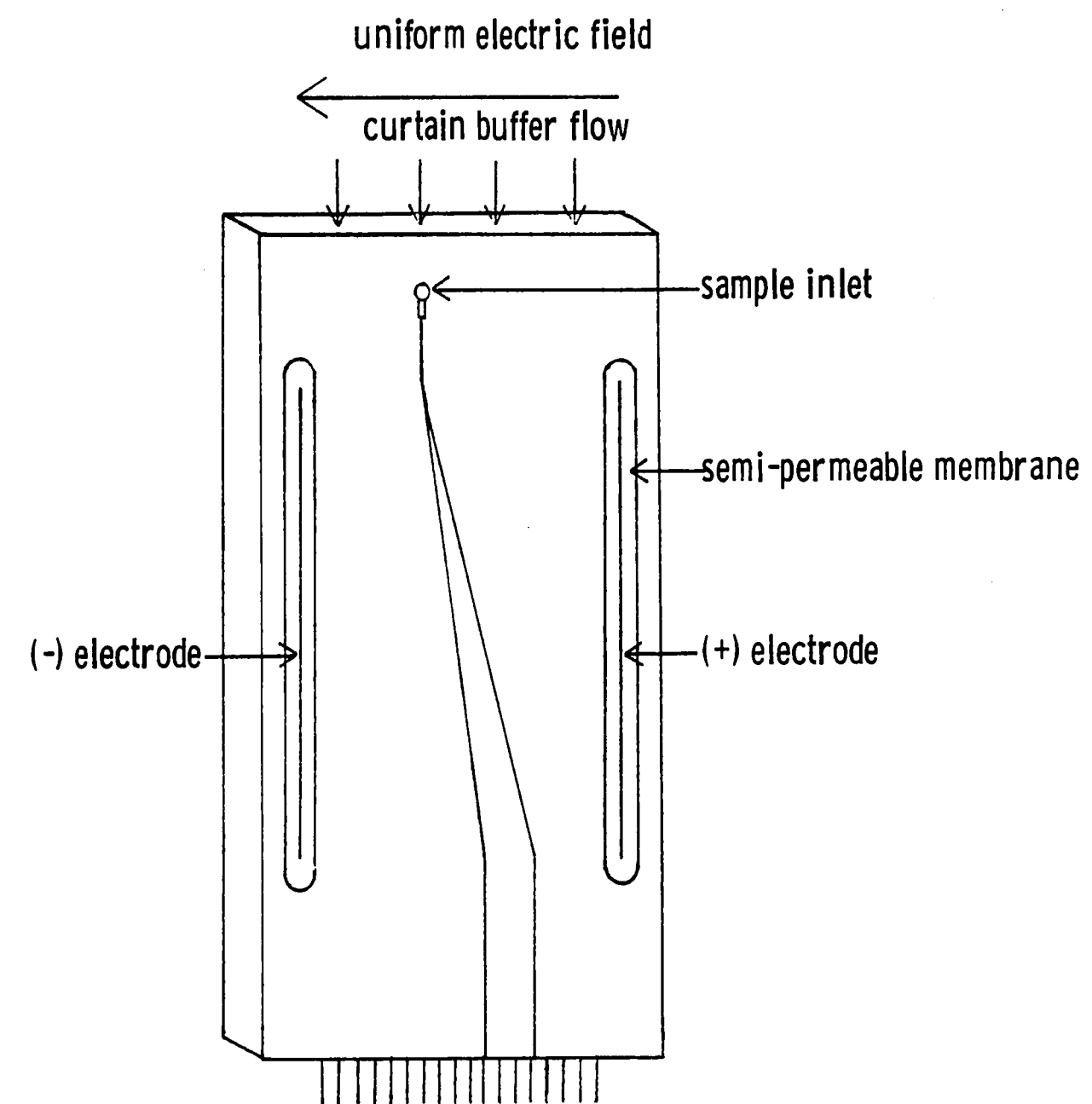


Figure 6. Schematic diagram of the Beckman CPE separation chamber.



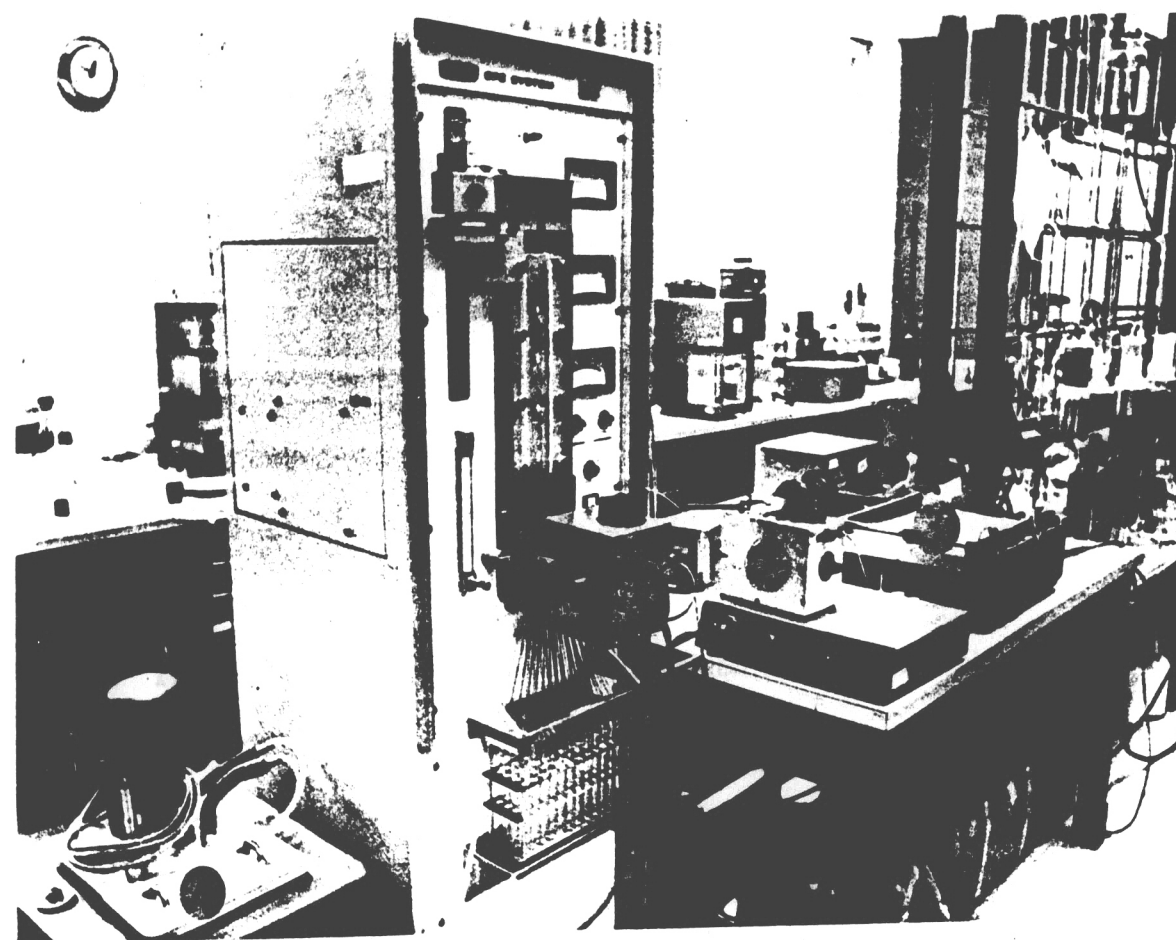


Figure 7. Photograph of the modified Beckman CPE apparatus with scanning UV light source (1), syringe-variable speed motor injection system (2), Houston Instruments X-Y recorder (3), and refrigeration unit (4).

osmotic and laminar flow of the curtain is shown in Figure 8. The electroosmotic flow is in the X-Z plane and is either positive or negative in the X-direction. The curve results from the superposition of the Poiseville and the Couette flows in this plane. The laminar Poiseville flow is in the Y-Z plane and is always positive in the Y-direction. The sample is injected in the center of the stream in a cylindrical configuration and moves with a constant electrophoretic velocity in the X-direction in the presence of an applied potential. The migration of the particles is affected by two factors, both of which are a function of their position in the Z-direction:

1. The electroosmosis of the electrolyte medium which affects the net parabolic velocity, and
2. The laminar parabolic flow profile which affects the velocity of the particle in the Y-direction and hence the time of exposure of the particle to the electric field.

Both factors ultimately affect the migration distance of the particle and the configuration of the sample stream.

In principle, it is possible to match the electroosmotic flow to the induced flow so that any band-broadening disappears<sup>(46)</sup>. Under these conditions, the displacement of the sample will be controlled by the particles in the center of the curtain, where the velocity in the Y-direction and the particle velocity of buffer in the X-direction are both at a maximum.

The principle equation which describes the displacement of a particle in the flow fields was derived by Strickler in 1973<sup>(46,47)</sup>.

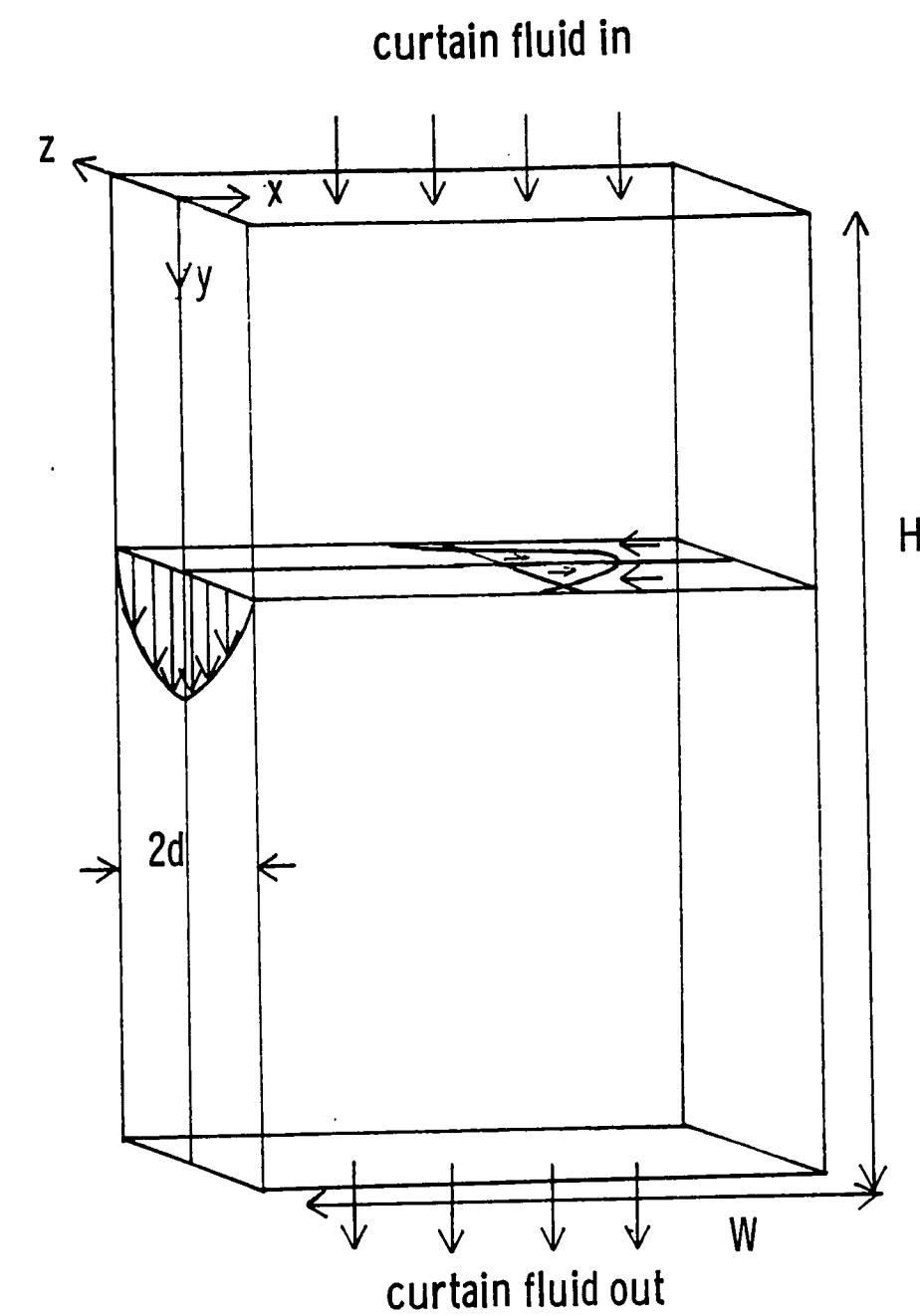


Figure 8. Laminar flow through the separation chamber of the CPE,

where:

$$2d = 0.15 \text{ cm.}$$

$$H = 30.00 \text{ cm.}$$

$$W = 4.50 \text{ cm.}$$

For example, consider anionic particles undergoing separation in continuous electrophoresis. Assume:

1. electroosmosis at both walls are the same,
2. the effect of temperature is small, and
3. changes in viscosity and dielectric constant of the fluid medium are negligible.

Therefore, the following mathematical model can be developed.

$$X = \frac{HE}{v_o} \left( \frac{U_{os} + U_E}{1 - z^2/d^2} - \frac{3}{2} U_{os} \right) \quad \text{Equation (1)}$$

where:

- X = horizontal displacement distance (um.)
- H = electric field length through which the particles travel vertically (cm.)
- E = applied potential (volt/cm)
- $v_o$  = maximum fluid velocity at the midplane (cm./sec.)
- $U_{os}$  = electroosmotic mobility of the particles (um. cm./volt sec.)
- d = curtain half-thickness (cm.)
- Z = particle depth from the curtain midplane (cm.)
- $U_E$  = electrophoretic mobility of the particles (um. cm./volt sec.)

Equation 1 was derived from the classical hydrodynamic equation for viscous flow, assuming Hagen-Poiseville flow through a narrow slit (except the wall mobility is  $U_{os}$  instead of zero), and using the Helmholtz-Smoluchowski equation and the electrical focusing principle for continuous electrophoresis. Thus, we have an expression for the

crescent-shaped sample stream as it migrates through the CPE. The migration distance is directly proportional to the electric field length and applied voltage, and inversely proportional to the curtain flow rate. Changing any of these parameters will change the particle migration.

Equation 1 assumes the electroosmotic mobility is the same for both walls and the effect of temperature is small. This may not always be true. If the electroosmotic mobilities of the front and rear walls are not equal, then:

Equation (2)

$$X = \frac{HE}{v_0} \left( \frac{1}{2} \left( \frac{U_{osr}}{1-z/d} + \frac{U_{osf}}{1+z/d} \right) - \frac{3}{4} (U_{osr} + U_{osf}) + \frac{U_E}{1-z^2/d^2} \right)$$

where:

$U_{osr}$  = electroosmotic mobility along rear wall

$U_{osf}$  = electroosmotic mobility along front wall

If the effect of temperature is also considered, then:

Equation (3)

$$X = \frac{HE}{v_0} \left( \frac{1}{2} R_W \left( \frac{U_{osr}}{1-z/d} + \frac{U_{osf}}{1+z/d} \right) - \frac{3}{4} R_W (U_{osr} + U_{osf}) + \frac{U_E R_Z}{1-z^2/d^2} \right)$$

where:

$$R_W = \frac{\epsilon_W \eta_{298}}{\eta_W \epsilon_{298}} \quad \text{and} \quad R_Z = \frac{\epsilon_Z \eta_{298}}{\eta_Z \epsilon_{298}}$$

$T = 298 \text{ K}$

$\epsilon = \text{dielectric constant}$

$\eta = \text{Viscosity}$

W = wall position

Z = particle position

The ratios  $R_W$  and  $R_Z$  correct the electroosmotic mobility values to the temperature at the walls where the driving force is located and the electrophoretic mobility values to the temperature at the particle position. This procedure allows the temperature gradient to be superimposed on the particle migration. This temperature increases to a maximum as the particles pass through the electric field and this was taken into account in these equations.

#### B. Applications of the CPE:

The CPE apparatus offers several advantages over other electrophoretic techniques<sup>(48,2)</sup>:

1. large particles at high concentrations may be separated,
2. the separation may be achieved continuously and fast,
3. the separation conditions are controlled and may be varied and reproduced,
4. low temperatures may be used,
5. acidic or basic solvents may be used, and
6. the system uses fluid flow between Lexon plates, therefore no contamination results from substances extracted from a support media.

Continuous particle electrophoresis has been used successfully for the separation of various colloids. For example, reported separations of viruses<sup>(49,50,51)</sup>, proteins<sup>(52,48,53,54)</sup>, cells<sup>(55,39,22,13,43,36,51,38,56,53)</sup>, clay and minerals<sup>(57)</sup>, bacteria<sup>(24,51)</sup>, latexes<sup>(43,44,22,12,</sup>

<sup>2)</sup>, phytoplankton<sup>(58)</sup>, hormones<sup>(59)</sup>, isoenzymes<sup>(60,61)</sup>, lipoproteins<sup>(62)</sup>, ribosomes<sup>(37)</sup> and nucleotides<sup>(63)</sup> have been achieved. The possibility of separating latex and carbon particles with different adsorbed substances using the CPE offers extensive possibilities in particle surface phenomena and structure. These might include adsorption and desorption, ionization, ion-exchange, and surface chemical reactions which would be of interest in the areas of water pollution, soil stability, manufacture of ceramics, paints, inks, adhesives and pharmaceuticals<sup>(64)</sup>.

In 1973, McCann and Vanderhoff<sup>(43)</sup> at Dow Chemical explored the possible application of the CPE for the determination of latex particle size distributions. It was found that generally the electrophoretic migration of the Dow monodisperse latexes increased with particle size, but these values could only yield relative electrophoretic mobilities.

Over the past several years, our laboratory has been interested in the CPE as an analytical tool to provide information about particle mobilities, interactions and surfactant addition<sup>(2)</sup>. This information can be obtained from recorded scans of separated fractions of particles. Using the modified Beckman CPE apparatus in our laboratory, Krumrine<sup>(44,2)</sup> was able to develop a method to measure the absolute electrophoretic mobilities of colloid particles. The value obtained were in good agreement with those obtained by microcapillary electrophoresis (MCE). However, it was found that at high particle concentrations and at very low electrolyte concentrations, i.e. electrical double layer extensions greater than 10% of the particle radius, that sometimes the separated bands did not agree well with MCE results. This conditional

disruptancy was attributed to particle-particle interaction between the electrical double layers of the separated particles.

Krumrine<sup>(2)</sup> studied these interactions theoretically and experimentally at an ionic concentration of  $1 \times 10^{-3}$  barbital sodium barbital (BSB). Consider the separation of one particle from another particle of different size under the influence of an applied potential in the CPE, as shown in Figure 9. As the particles traverse each other, their electrical double layers interact, and by particle dynamics, the slower moving particles will be accelerated by the faster moving particles depending on their respective sizes and electrolyte concentration of the media. Hence a smaller particle will exert less force on a larger particle than vice versa.

These interactions were investigated at an ionic concentration of  $1 \times 10^{-3}$  barbital sodium barbital (BSB) as a function of the number of collisions between particles which could be directly related to the distance between separated bands of latex particles. It was concluded that larger particles accelerated the migration of smaller particles and that this effect was more pronounced as the particle concentration, or number of collisions, increased. At high particle concentrations, particle-particle interaction appeared sensitive to particle concentration; and at low particle concentration, particle-particle interaction appeared to be a less defined function of particle concentration. The effect of particle concentration was not found to influence the migration distance of single particle species. Also, it was found that these latexes should undergo serum replacement to exchange the initial serum with a buffer



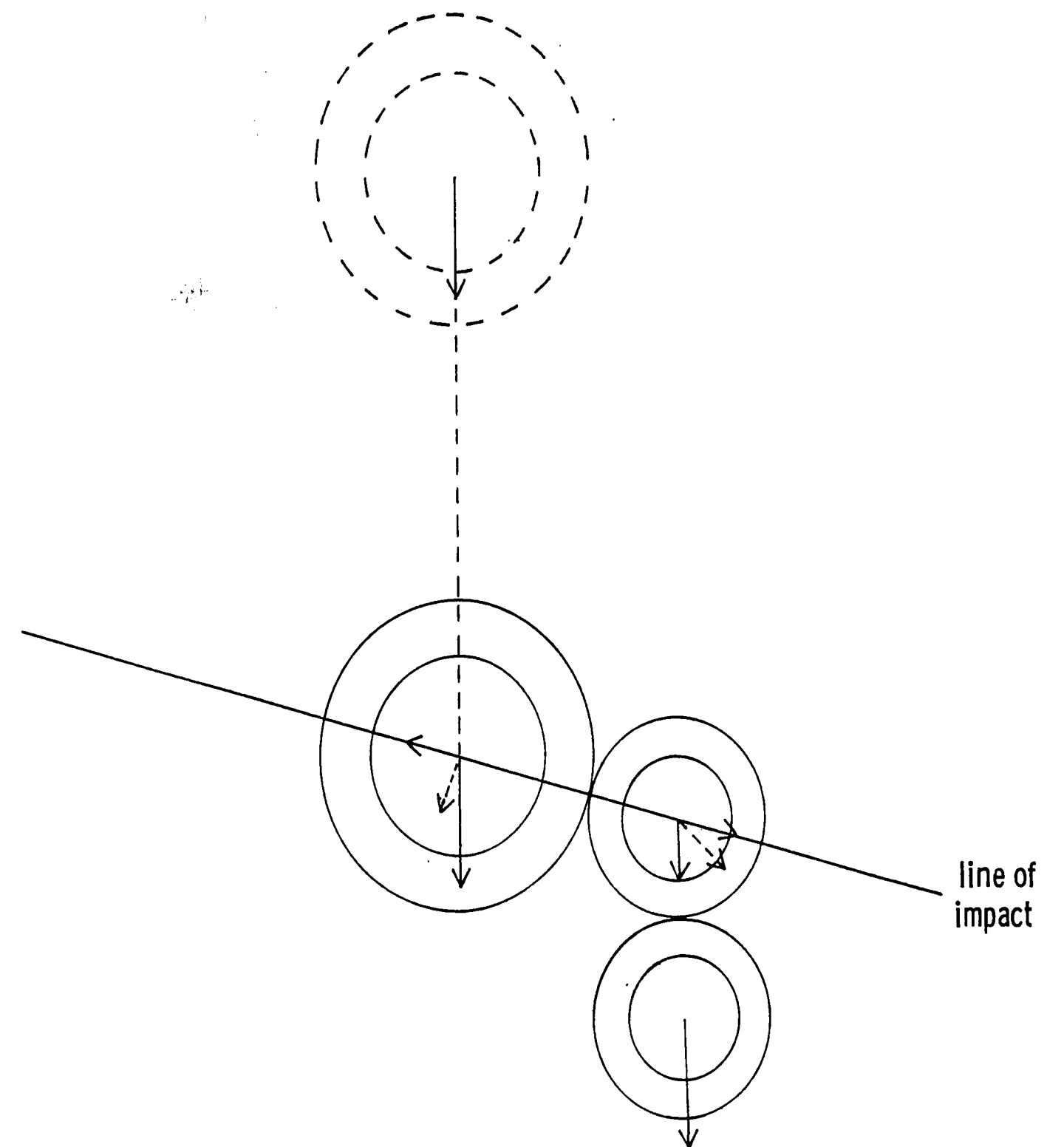


Figure 9. Collision of a larger particle against two smaller particles of equal size.

identical to that of the curtain buffer used in the CPE. This increased control over the experimental conditions since the amount of surfactant and composition of the initial serum was unknown.

### C. Experimental Results and Conclusions:

The present work is an extensive of Krumrine's study of particle-particle interactions in order to better understand the effect of particle size, concentration and electrolyte concentration on the separation of colloid particles. Krumrine used three monodisperse latexes of different mobility at an ionic concentration of  $1 \times 10^{-3}$  BSB. This study will use four monodisperse latexes of similar and different mobility at an ionic concentration of  $1 \times 10^{-4}$  BSB. This decrease in ionic concentration of the buffer should extend the electrical double layers of the particles to be separated and magnify their affect on particle-particle interaction. These interactions will be a function of the number of collisions between particles and will be reflected in the distance between separated bands of latex particles. This phenomena can be observed from recordings of optical density scans of the separated particle bands, where the distance between the recorded peaks, i.e. the peak-to-peak distance, decreases as the number of particles, i.e. particles collisions, increases.

Initially four monodisperse latexes were sought with specific particle size and mobility characteristics. Finally, four monodisperse latexes of diameter 1.10, 0.357, 0.234 and 0.109  $\mu\text{m}$ . PS were chosen because the 1.10 and 0.109  $\mu\text{m}$ . PS were easily separated and differed in size by a factor of ten, and the 0.234 and 0.357  $\mu\text{m}$ . PS were of

similar size and mobility. All of these latexes were serum-replaced to exchange the initial serum with  $1 \times 10^{-4}$  BSB. No surfactant was added. to this system and the particles appeared stable.

The polystyrene latex particles were characterized by the CPE and the MCE, as shown in Table 5. The particles were separated in the CPE against the 1.10  $\mu$ m. PS at an overall solids content of 2 percent.

TABLE 5

Comparison of electrophoretic mobility results of PS latex, buffer-exchanged in  $1 \times 10^{-4}$  BSB, obtained by microcapillary and continuous particle electrophoresis

PS Latex Size, $\mu$ m.	Electrophoretic Mobility (UE)		
	CPE	MCE	( $\mu$ m. cm./volt sec.) MCE-CPE
0.109	3.06	2.33	-0.75
0.234	2.64	2.64	0.00
0.357	2.55	2.80	+0.25
1.100	---	3.52	---

where the CPE electrophoretic mobilities were calculated using the peak-to-peak migration distance and Strickler's equation as previously discussed by Krumrine<sup>(2)</sup>.

From Table 5 it can be seen that the MCE electrophoretic mobilities increase with particle size. There is good agreement between MCE and CPE results except for the 0.109  $\mu$ m. PS. This deviation is probably due to particle-particle interaction of the extended double layers of the 1.10 and 0.109  $\mu$ m. PS, which would result in the accelerated migration

of the 0.109  $\mu\text{m}$ . PS. The 0.234 and 0.357  $\mu\text{m}$ . PS appear large enough in size to overcome any interaction affects of this particle concentration.

Data was collected as a function of the weight percent solids and the number of particles of each latex. The total solids content was varied between 0.048 and 25.0 percent. These results were normalized to an applied potential of 25 volts/cm. from five applied potentials of 15, 25, 35, 45 and 50 volts/cm. and plotted versus the particle number or concentration. The experimental results are summarized in Figures 10 through 26. Figures 10, 13, 16, 19 and 22 give the difference in migration distance between two peaks, i.e. the peak-to-peak distance, and Figures 11, 12, 14, 15, 17, 18, 20, 21, 23, 24, 25 and 26 show the absolute migration distance of each particle species undergoing separation.

The effect of particle interaction on the separation of the 1.10 and 0.109  $\mu\text{m}$ . PS can be seen in Figures 10, 11, and 12. When the 1.10  $\mu\text{m}$ . PS is held at a high concentration and the 0.109  $\mu\text{m}$ . PS is varied there appears an initial increase followed by a decrease in the peak-to-peak separation distance. This indicates that the 1.10  $\mu\text{m}$ . PS pulls the 0.109  $\mu\text{m}$ . PS along until the 0.109  $\mu\text{m}$ . PS concentration increases to the point where the overall number of collisions is great enough that the particle-particle interaction is essentially a linear function of the particle concentration. When the 0.109  $\mu\text{m}$ . PS is held at a low concentration and the 1.10  $\mu\text{m}$ . PS is varied, there appears a similar but less defined result. At low concentrations of 0.109  $\mu\text{m}$ . PS, the migration of the 1.10  $\mu\text{m}$ . PS is essentially unaffected. However, the

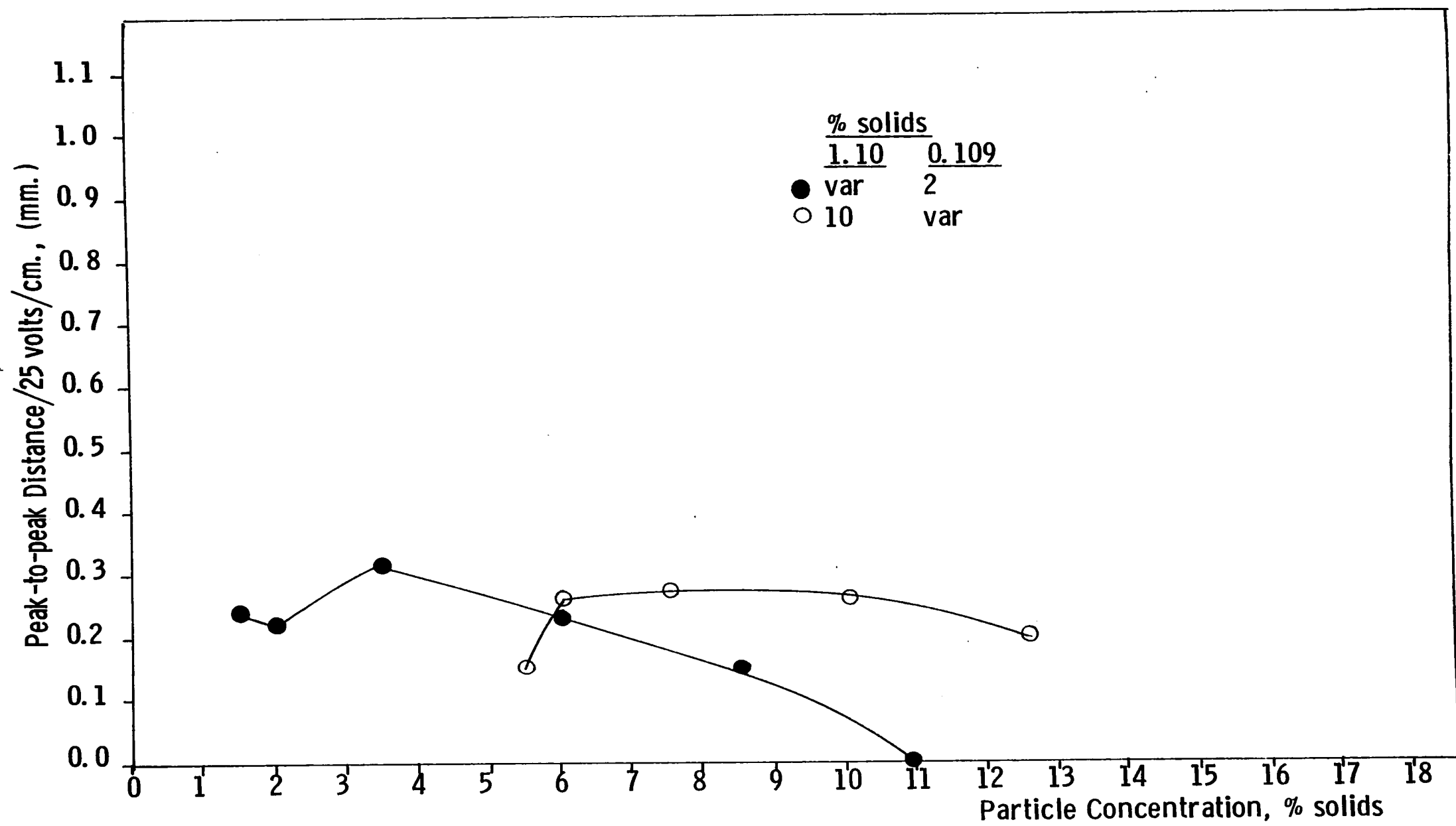


Figure 10. Peak-to-peak separation distance versus particle concentration for 1.10 um. and 0.109 um. polystyrene latexes.

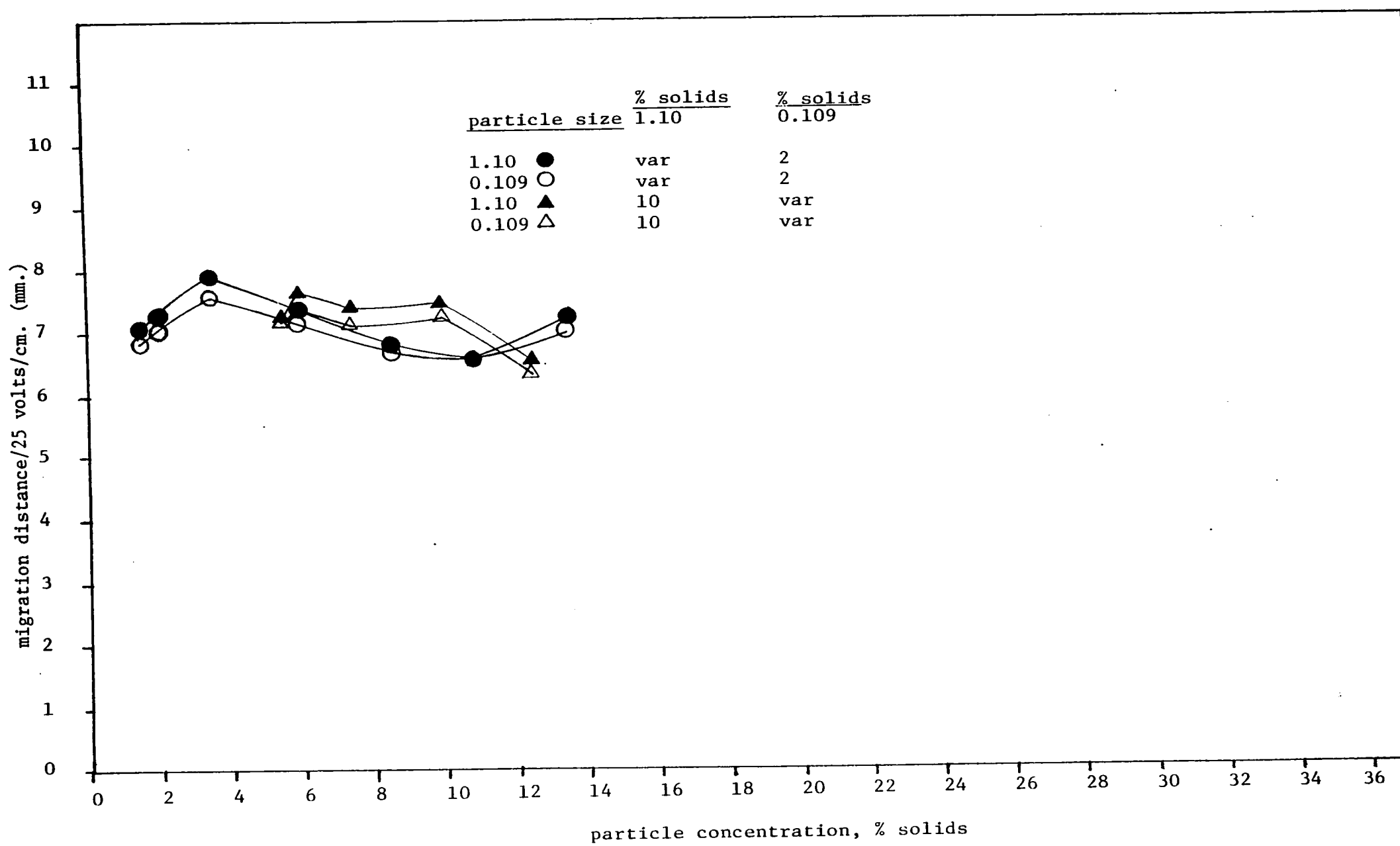


Figure 11. The effect of particle size and concentration on the absolute migration distance of 1.10 um. and 0.109 um. PS, buffer-exchanged in  $1 \times 10^{-4}$  BSB.

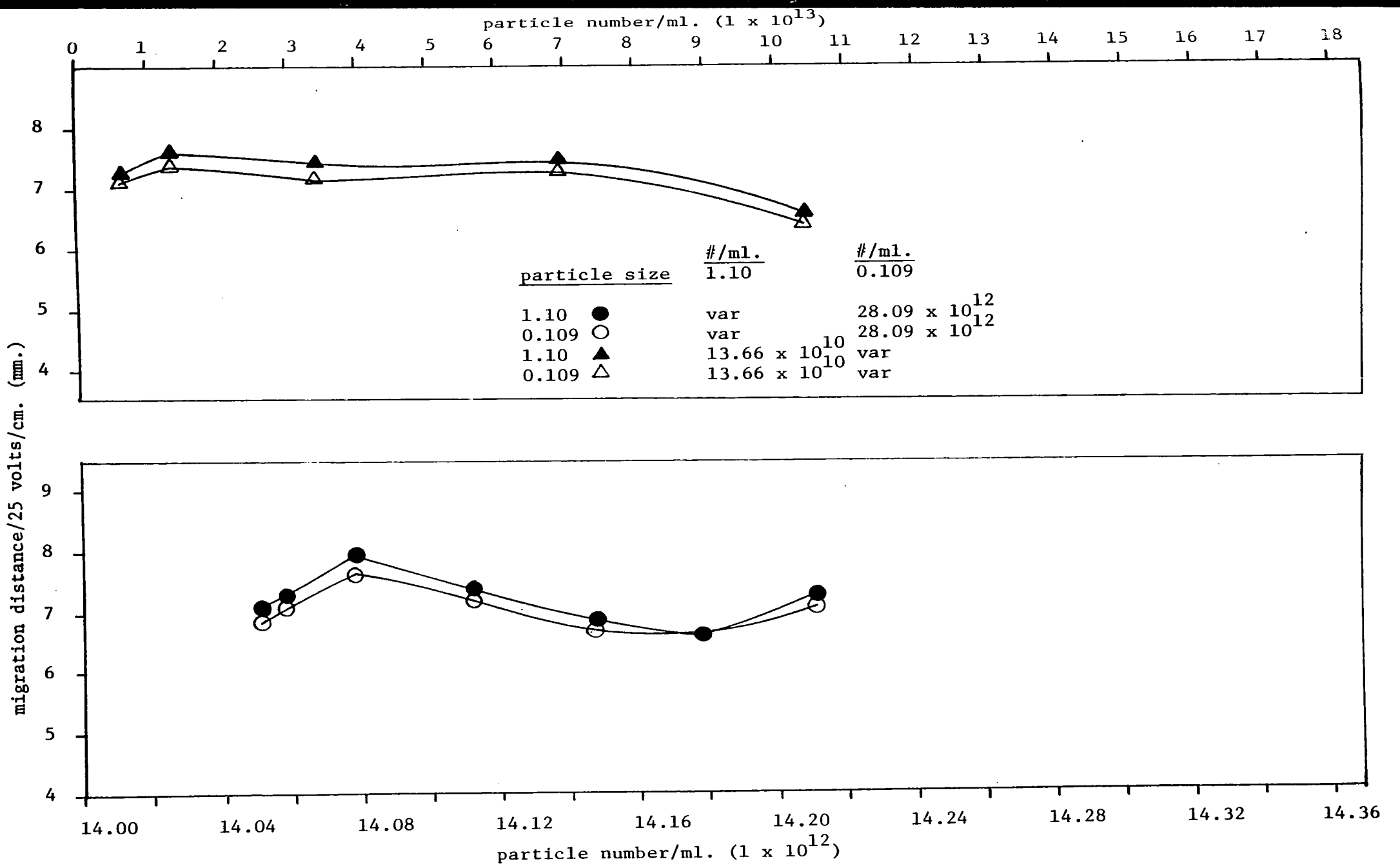


Figure 12. The effect of particle size and number on the absolute migration distance of 1.10  $\mu\text{m}$ . and 0.109  $\mu\text{m}$ . PS, buffer-exchanged in  $1 \times 10^{-4}$  BSB.

peak-to-peak separation distance decreases due to the overwhelming size effect of the 1.10  $\mu\text{m}$ . PS on the 10X smaller 0.109  $\mu\text{m}$ . PS.

Figures 13, 14 and 15 give the effect of particle size and concentration on the separation of 1.10 and 0.234  $\mu\text{m}$ . PS. No affect could be observed if the 1.10  $\mu\text{m}$ . PS is held at a high concentration and the 0.234  $\mu\text{m}$ . PS varied. Also if the 0.234  $\mu\text{m}$ . PS was held at a low concentration and the 1.10  $\mu\text{m}$ . PS varied the results obtained were erratic. This anomaly may be due to experimental limitations in determining the peak-to-peak separation distance at high solids content of one particle and at low solids content of a second particle. The light source-particle detection system may not be able to distinguish between the closely separated bands.

Figures 16, 17 and 18 show a similar effect on the separation of the 1.10 and 0.357  $\mu\text{m}$ . PS. If the 1.10  $\mu\text{m}$ . PS is at a high concentration and the 0.357  $\mu\text{m}$ . PS is varied, the separation distance decreases with the number of collisions. If the 0.357  $\mu\text{m}$ . PS is held constant at various low concentrations and the 1.10  $\mu\text{m}$ . PS is varied, the system is unaffected. Therefore the effect of particle-particle interaction is not observed where size effects do not play an important role and at low particle number concentrations.

No interpretation of the affects of particle size or concentration could be made for the separated systems of 0.357 and 0.109  $\mu\text{m}$ . PS, or 0.234 and 0.109  $\mu\text{m}$ . PS, as shown on Figures 19, 20, 21, 22, 23 and 24. The differences in size between the 0.109  $\mu\text{m}$ . PS, and the 0.234 and 0.357  $\mu\text{m}$ . PS may not be great enough to have a significant effect on their separation. Also experimental limitations in determining the



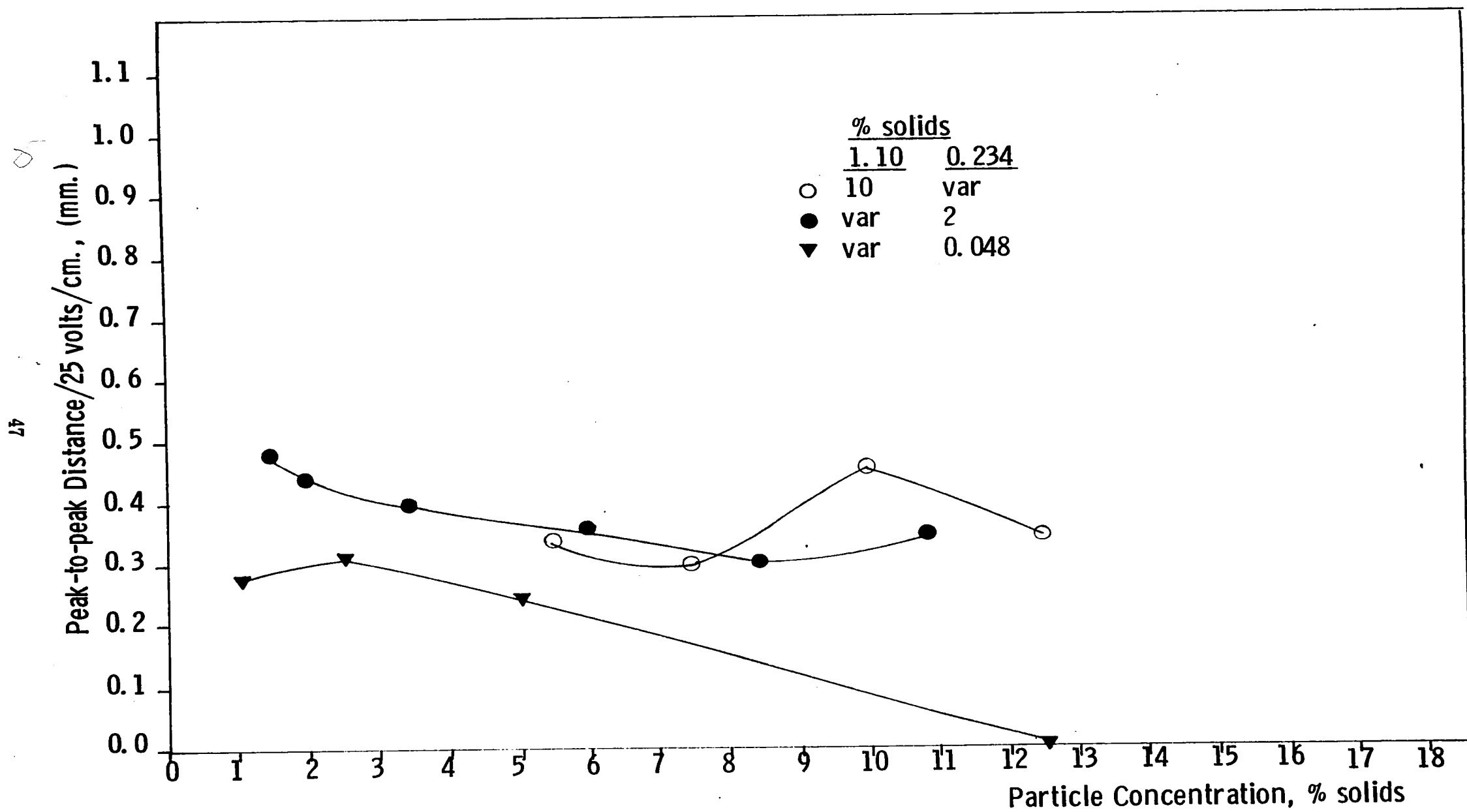


Figure 13. Peak-to-peak separation distance versus particle concentration for 1.10  $\mu\text{m}$ . and 0.234  $\mu\text{m}$ . polystyrene latexes.

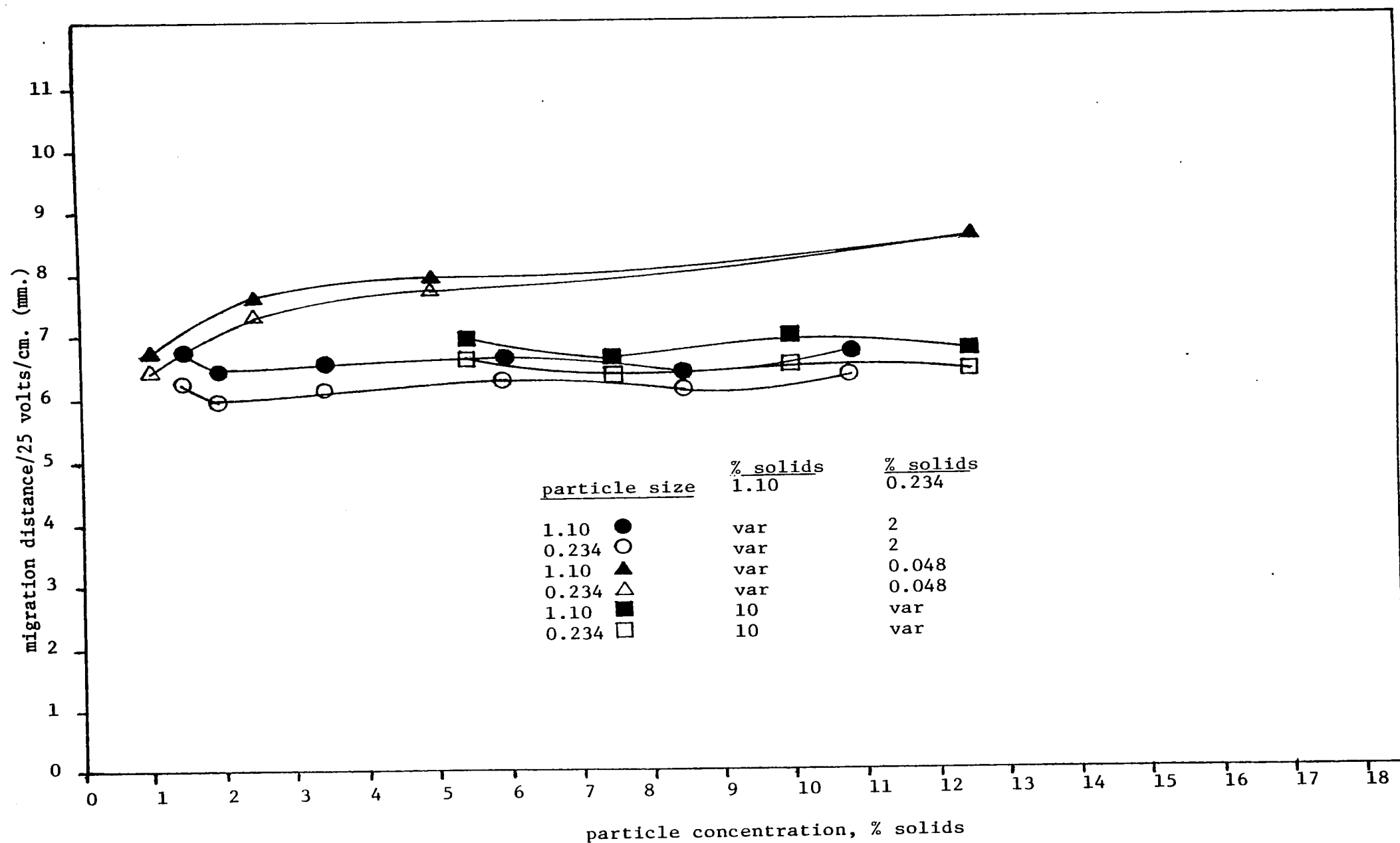


Figure 14. The effect of particle size and concentration on the absolute migration distance of 1.10 um. and 0.234 um. PS, buffer-exchanged in  $1 \times 10^{-4}$  BSB.

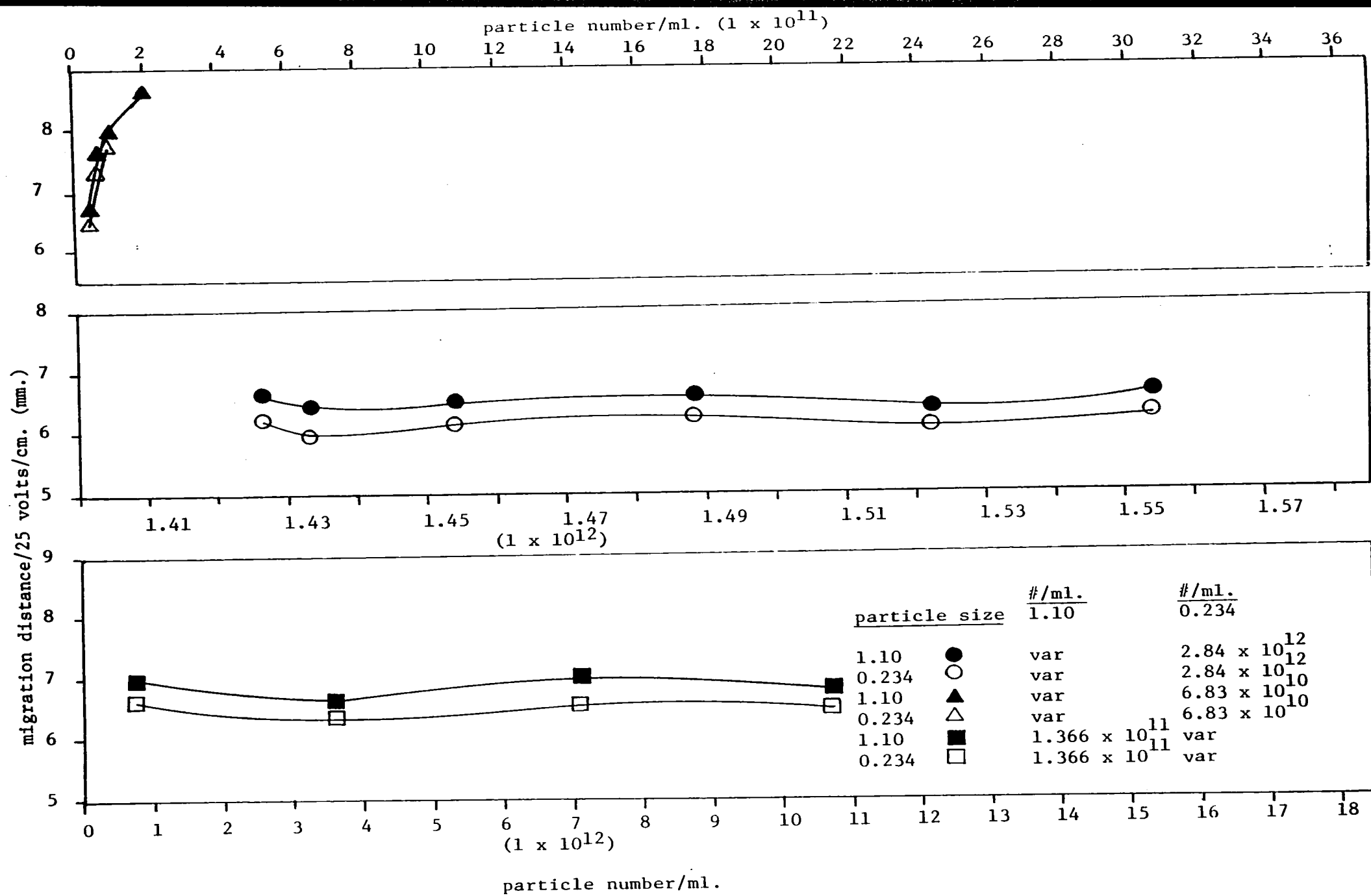


Figure 15. The effect of particle size and number on the absolute migration distance of 1.10  $\mu\text{m}$ . and 0.234  $\mu\text{m}$ . PS, buffer-exchanged in  $1 \times 10^{-4}$  BSB.

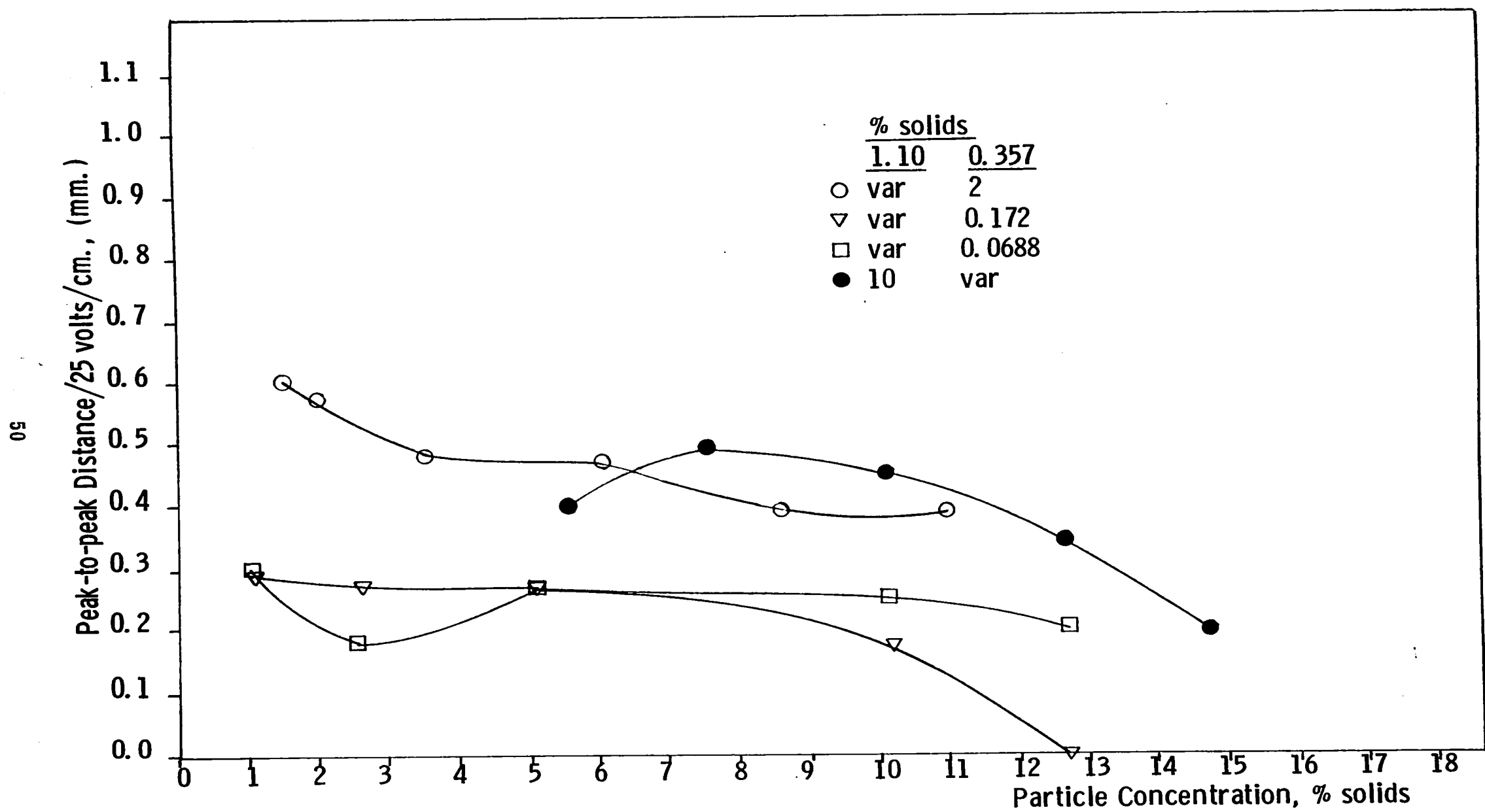


Figure 16. Peak-to-peak separation distance versus particle concentration for 1.10  $\mu\text{m}$ . and 0.357  $\mu\text{m}$ . polystyrene latexes.

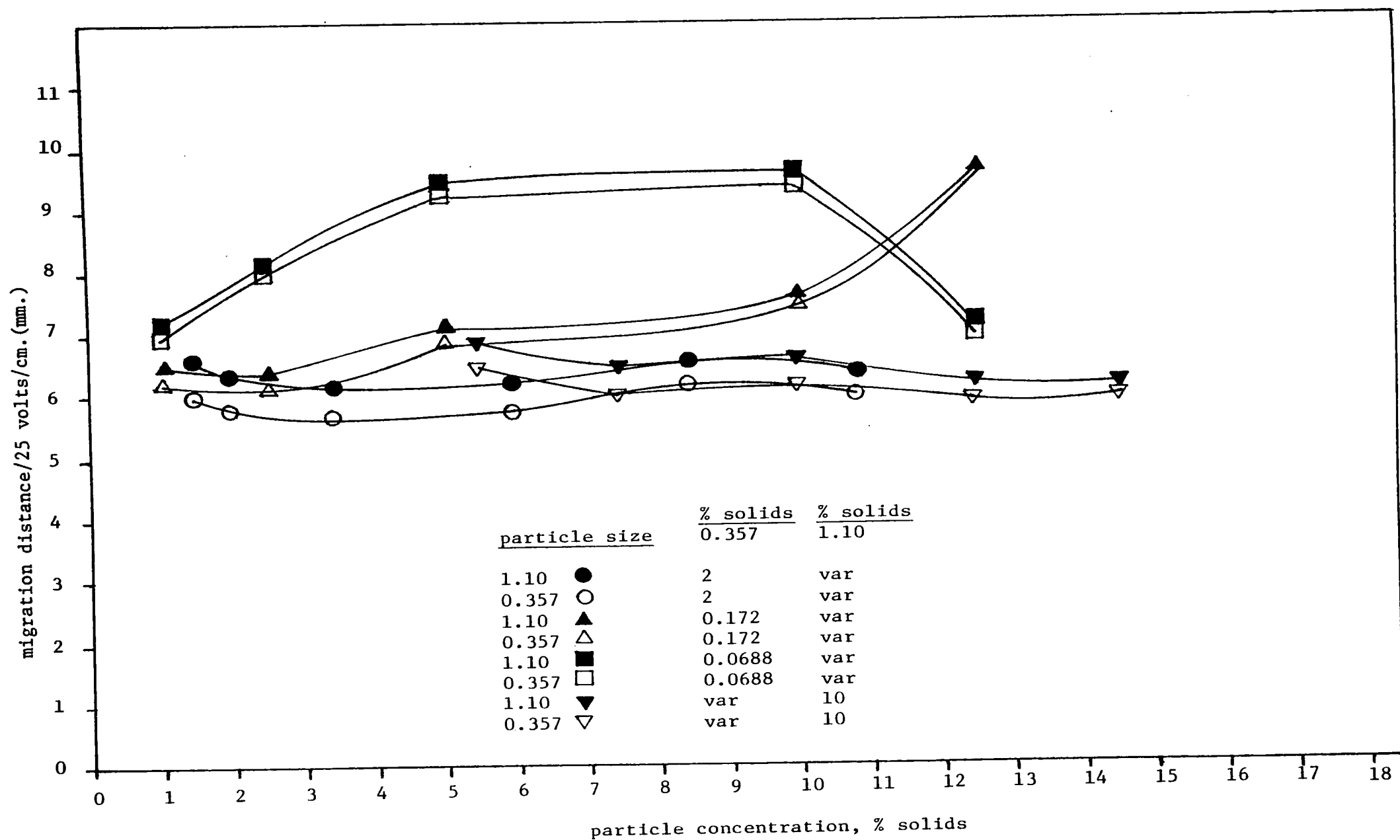


Figure 17. The effect of particle size and concentration on the absolute migration distance of 1.10 um. and 0.357 um. PS, buffer-exchanged in  $1 \times 10^{-4}$  BSB.

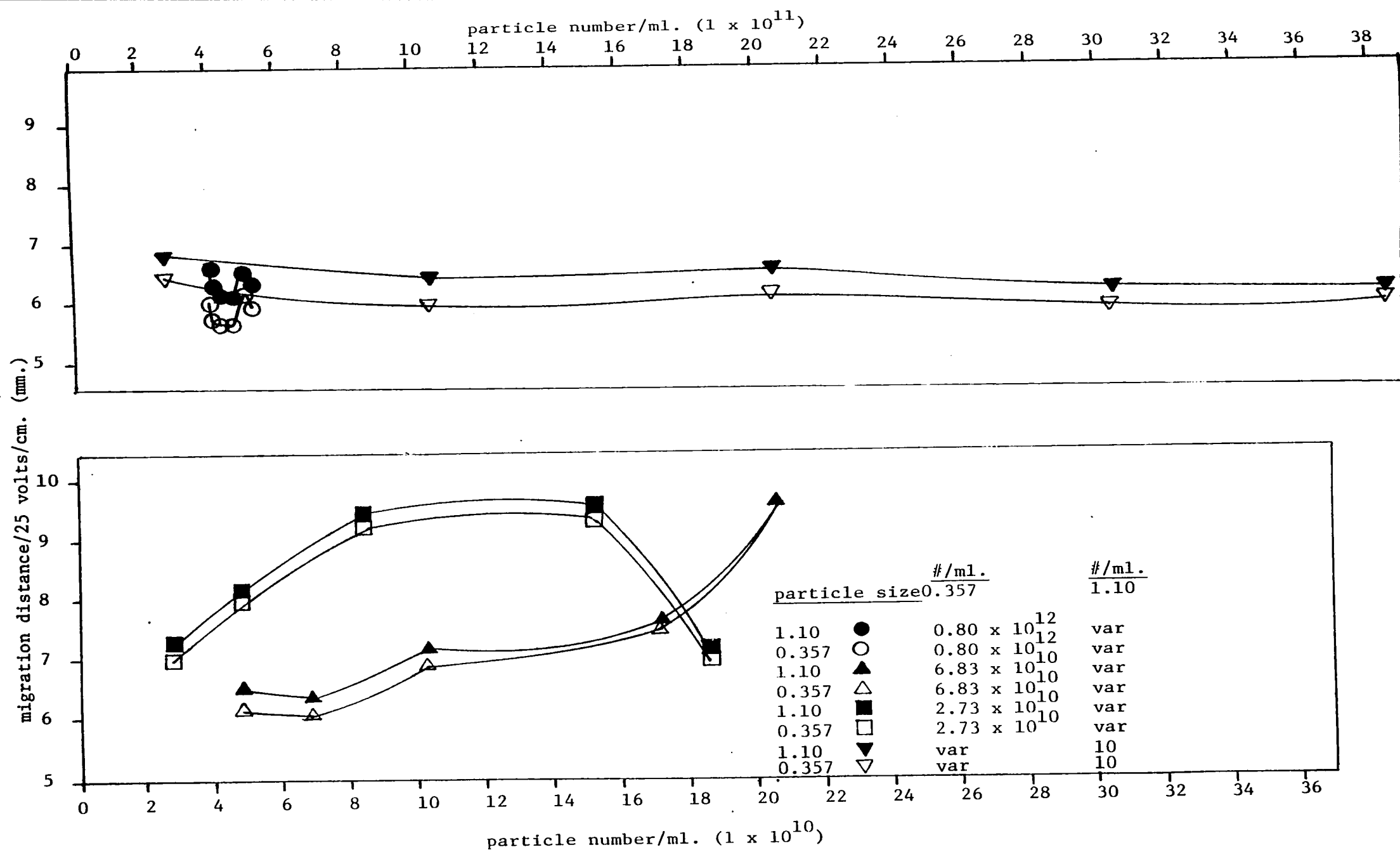


Figure 18. The effect of particle size and number on the absolute migration distance of 1.10 um. and 0.357 um. PS, buffer-exchanged in  $1 \times 10^{-4}$  BSB.

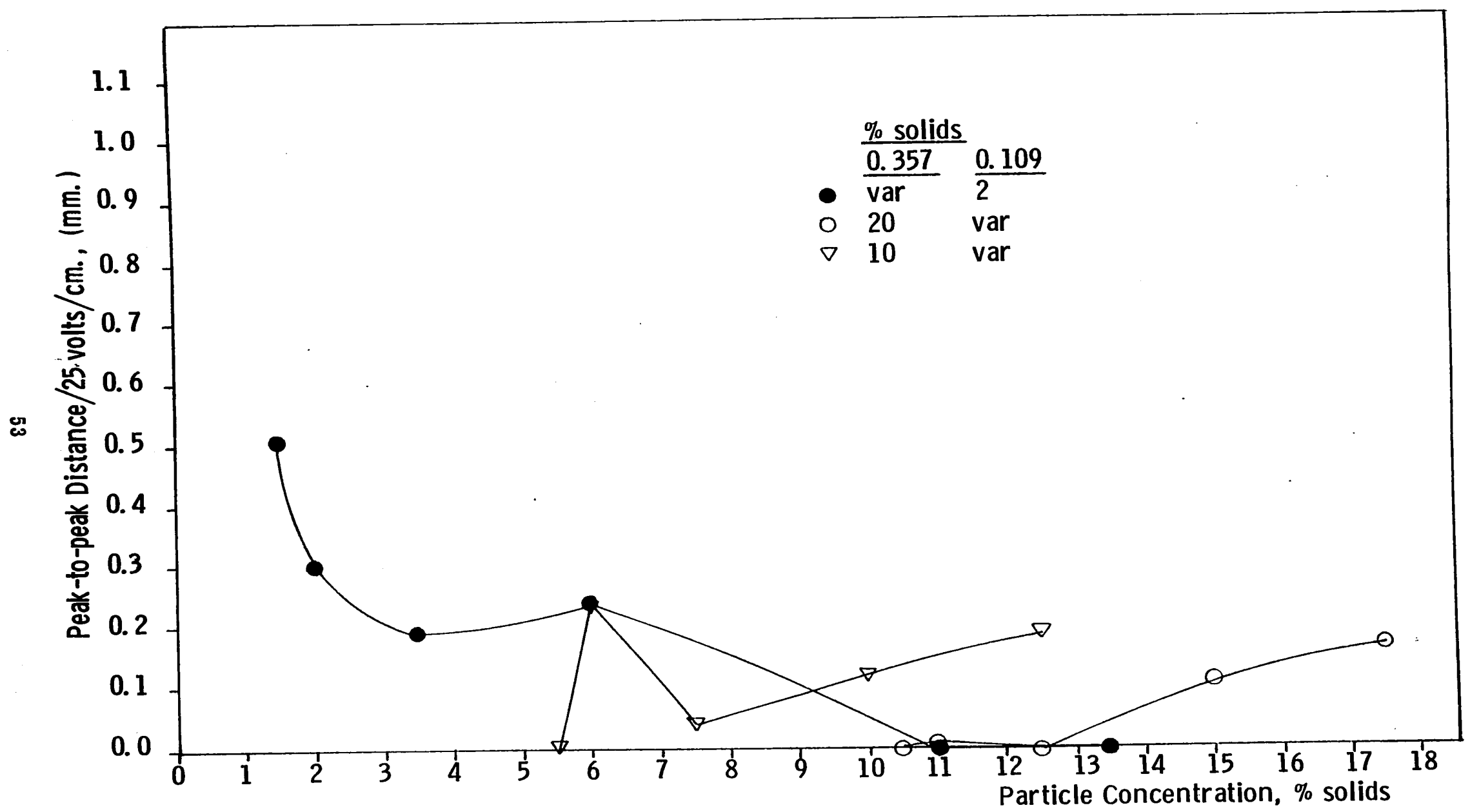


Figure 19. Peak-to-peak separation distance versus particle concentration for 0.357 um. and 0.109 um. polystyrene latexes.

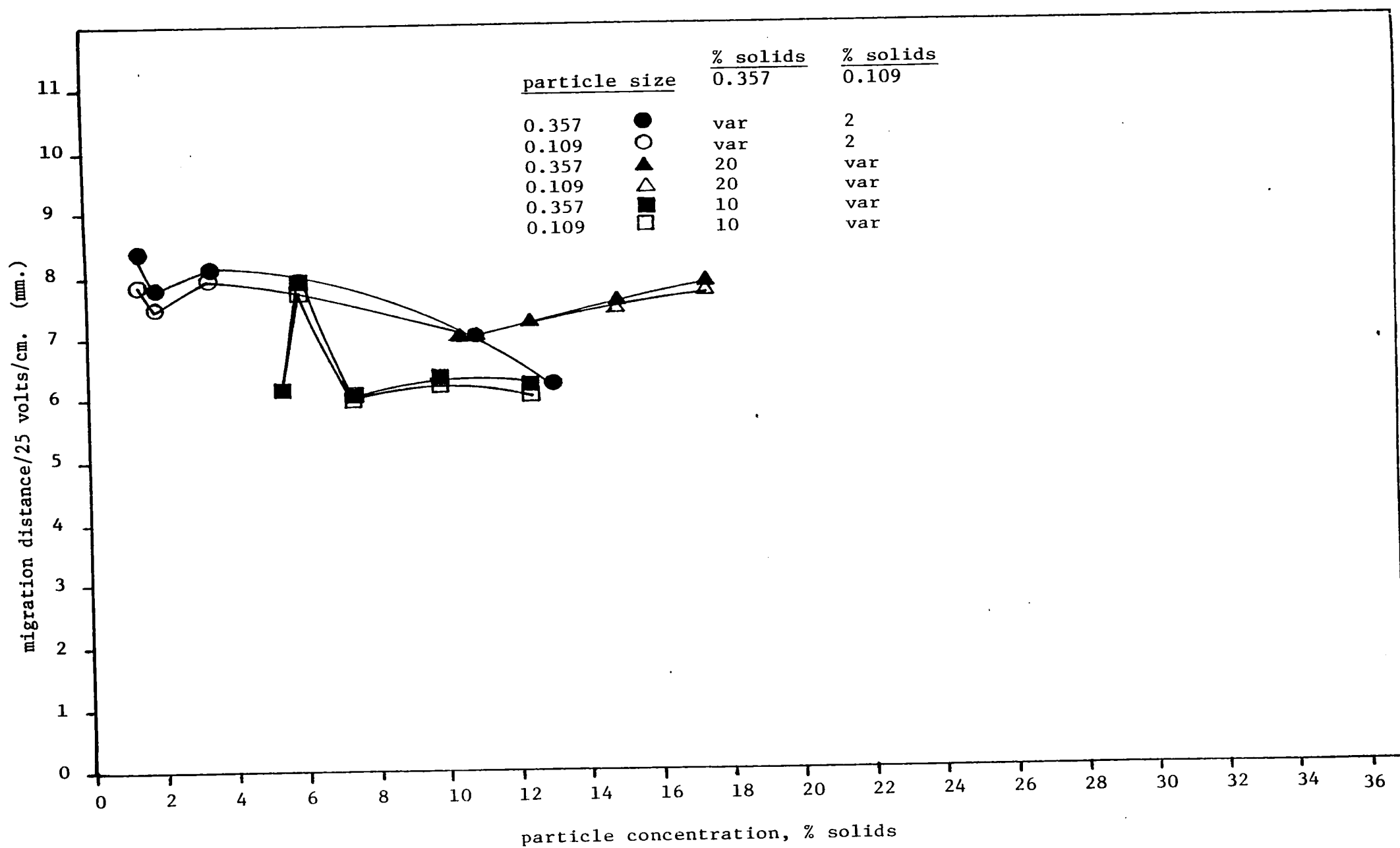


Figure 20. The effect of particle size and concentration on the absolute migration distance of 0.357 um. and 0.109 um. PS, buffer-exchanged in  $1 \times 10^{-4}$  BSB.



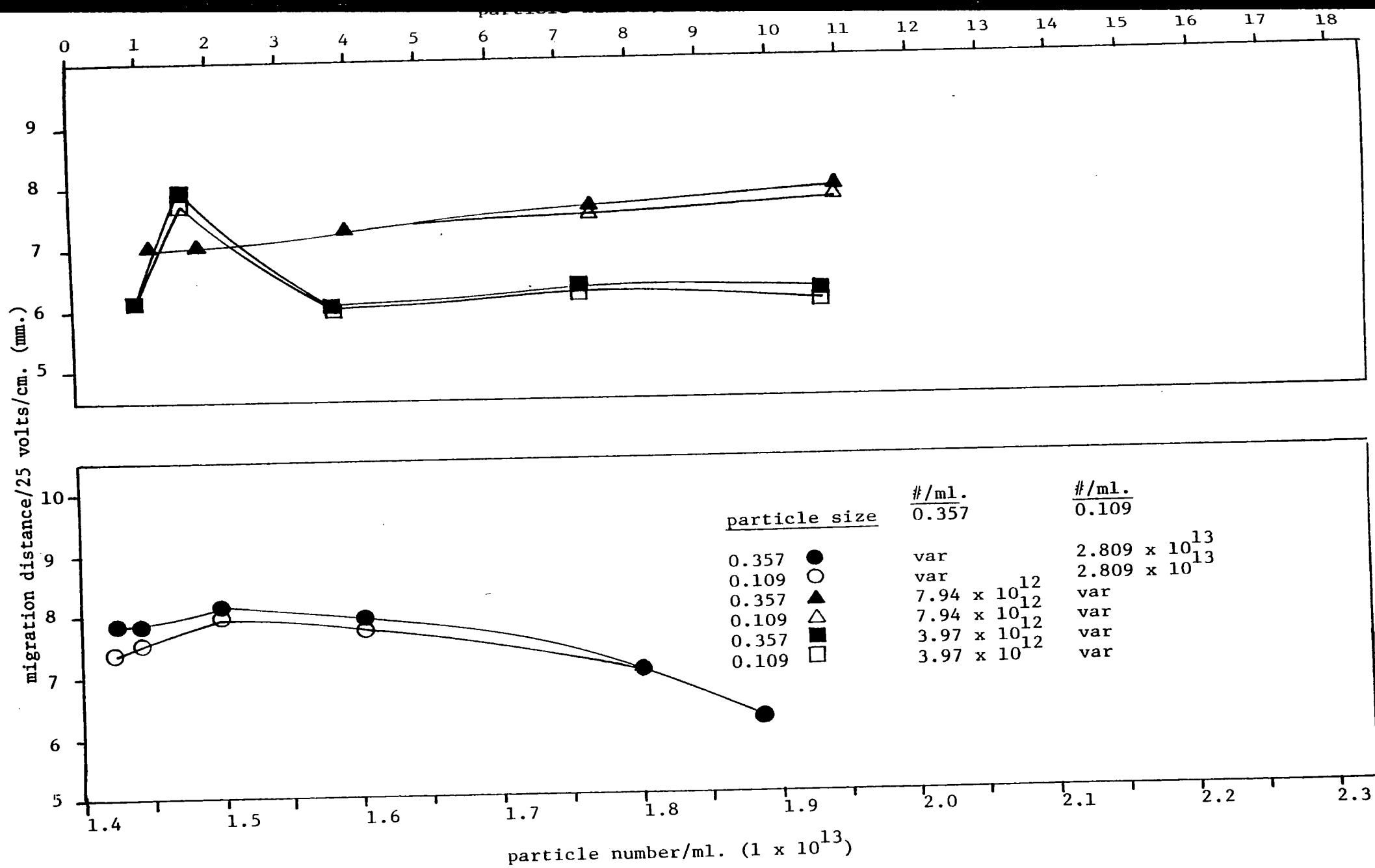


Figure 21. The effect of particle size and number on the absolute migration distance of 0.357 um. and 0.109 um. PS, buffer-exchanged in 1 x 10<sup>-4</sup> BSB.

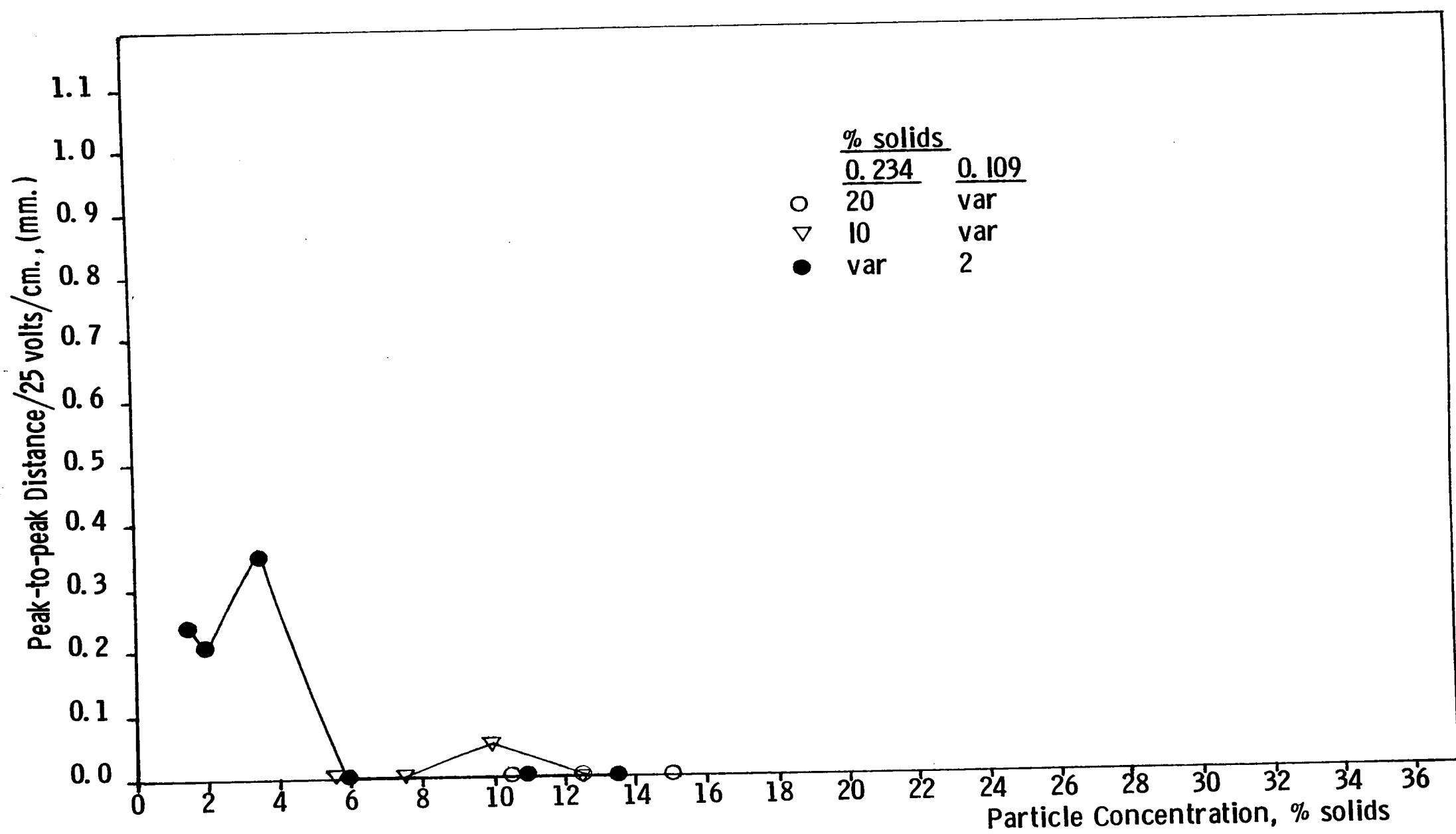


Figure 22. Peak-to-peak separation distance versus particle concentration for 0.234  $\mu\text{m}$ . and 0.109  $\mu\text{m}$  polystyrene latexes.

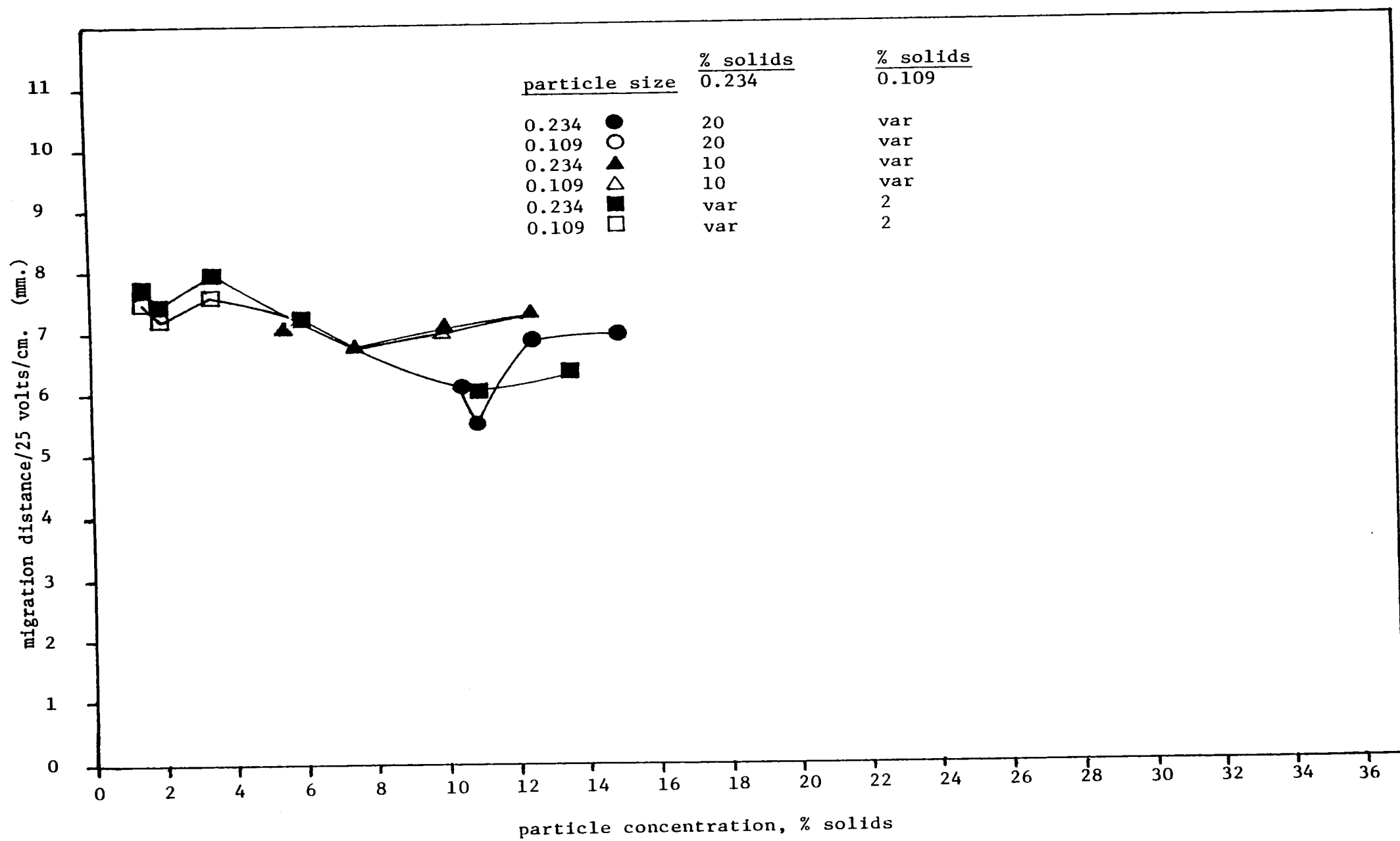


Figure 23. The effect of particle size and concentration on the absolute migration distance of 0.234 um. 0.109 um. PS, buffer-exchanged in  $1 \times 10^{-4}$  BSB.

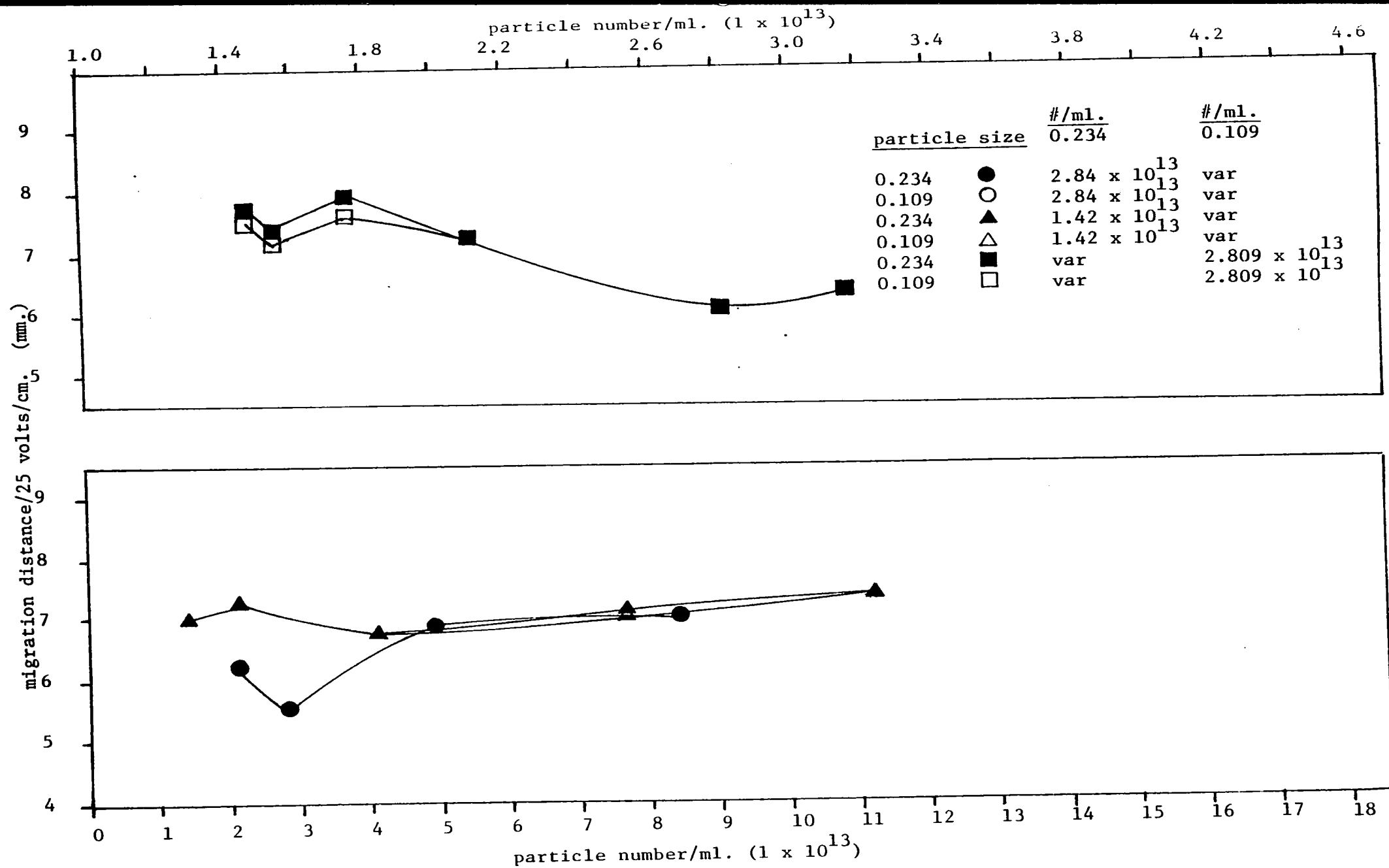


Figure 24. The effect of particle size and number on the absolute migration distance of 0.234  $\mu\text{m}$ . and 0.109  $\mu\text{m}$ . PS, buffer-exchanged in  $1 \times 10^{-4}$  BSB.

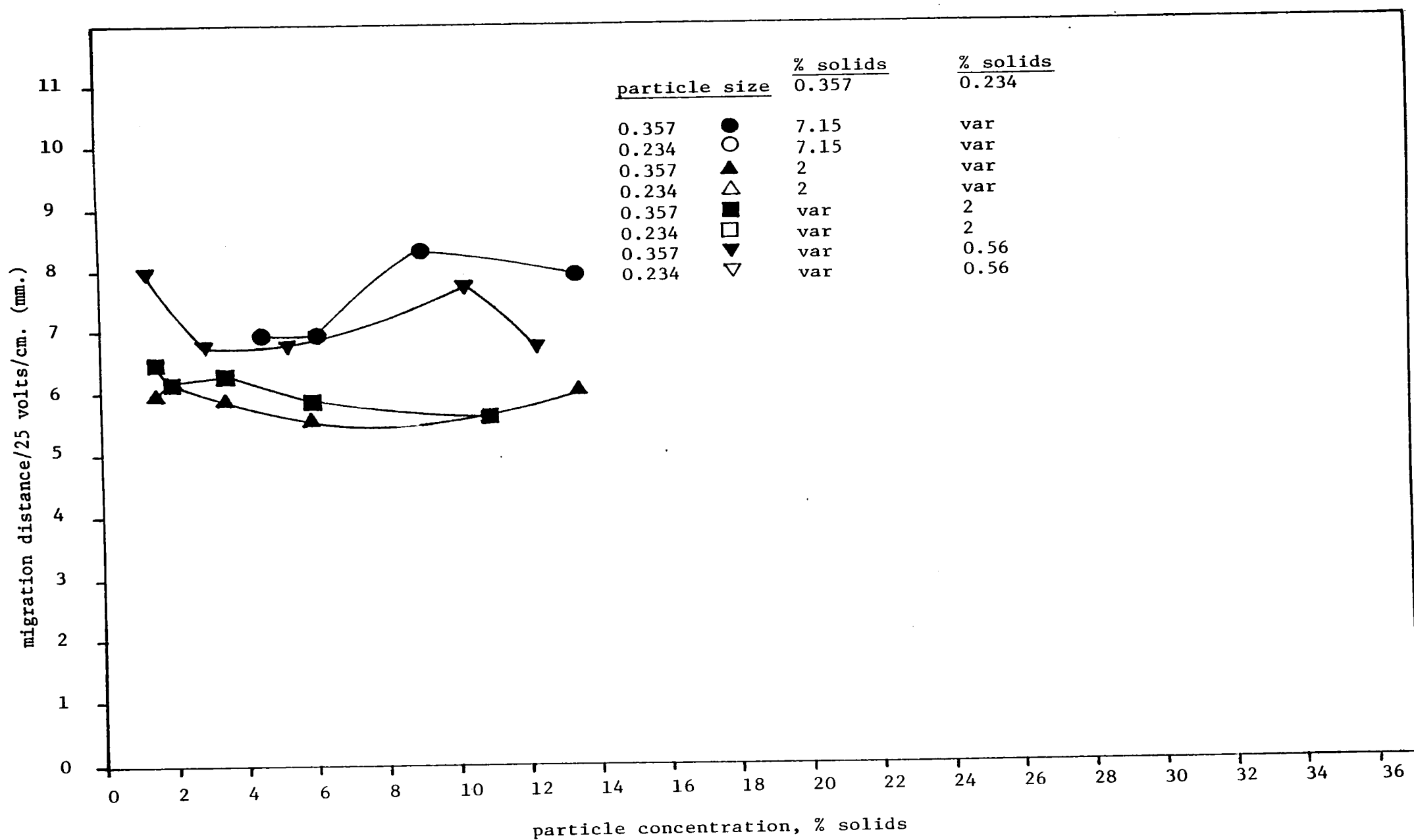


Figure 25. The effect of particle size and concentration on the absolute migration distance of 0.357  $\mu\text{m}$ . and 0.234  $\mu\text{m}$ . PS, buffer-exchanged in  $1 \times 10^{-4}$  BSB.

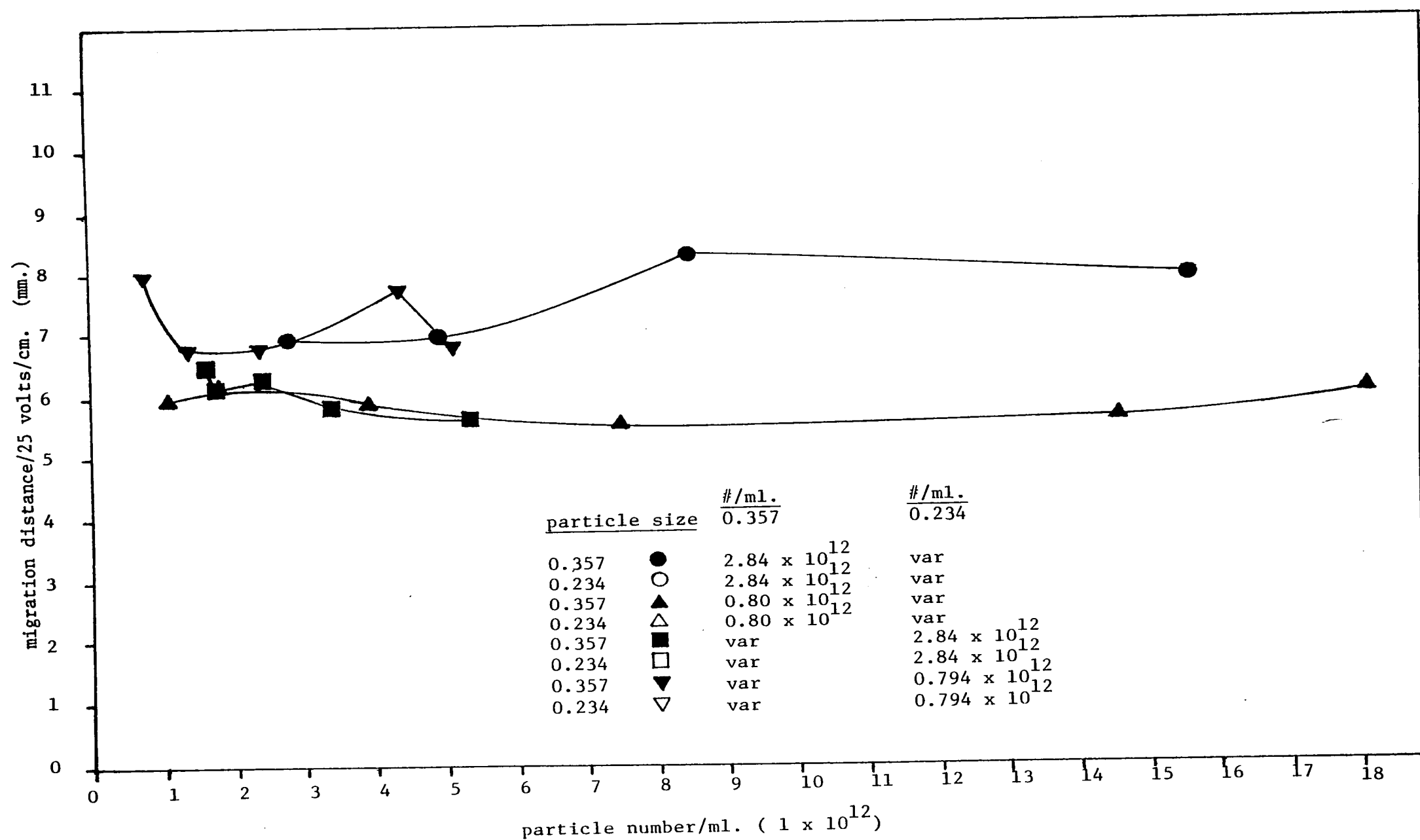


Figure 26. The effect of particle size and number on the absolute migration distance of 0.357  $\mu\text{m.}$  and 0.234  $\mu\text{m.}$  PS, buffer-exchanged in  $1 \times 10^{-4}$  BSB.

peak-to-peak separation distance at high solids content, or a concentration overloading of the light detection system may have resulted in this scatter of results.

No peak-to-peak separation distance was observed for variations in particle concentration of the 0.357 and 0.234  $\mu\text{m}$ . PS, as shown in Figures 25 and 26.

Evaluation of particle-particle interaction using this system was limited by the available light source detection system and the presence of band-broadening effects. Band broadening effects may be reduced to a minimum if the zeta potential of the chamber walls is identical to that of the particles to be separated.

## CHAPTER 4

### Experimental Verification of a Computer Model and Evaluation of Operational Parameters

#### A. Background and Previous Work

The Beckman CPE can be used to measure the absolute electrophoretic mobilities of particles as demonstrated by Krumrine<sup>(2,27)</sup>. Krumrine measured the electrophoretic mobilities of seven different monodisperse latexes in  $10^{-2}$  to  $10^{-4}$  M sodium barbital buffer by MCE and by CPE. The 1.10  $\mu$ m. PS latex was used as the standard to calculate the electrophoretic mobilities using the CPE, of all the other latexes at the different sodium barbital concentrations. These results were based on Strickler's equations<sup>(4)</sup>, see Chapter 3, as a function of the peak-to-peak distance, the migration distance, and data of the MCE. The agreement between MCE and CPE was good and demonstrated that the CPE can be used to measure the electrophoretic mobility of particles. However, the values of the electroosmotic mobility calculated from these experiments are greater than expected. These large values may result from a flow in the direction of the separation which is not entirely due to the electroosmosis along the wall. The equations used above do not involve the source of the flow and only assume that this flow is proportional to the applied potential. This proportionality has been established experimentally, hence it may be assumed that the additional flow is electroosmosis across the semi-permeable membranes which separates the electrodes from the channel.



The experimental parameters involved in the separation of hypothetical particles in the CPE were analyzed by Krumrine<sup>(45,2)</sup> and a computer model developed to illustrate how the various parameters interact to produce a desired separation. In this manner theoretical conditions can be chosen to maximize resolution and throughput. Also, comparisons may be made between theoretical and experimental results. Good agreement between theory and experiment was found for the separation of seven different latexes, indicating this CPE system is sensitive to particle size differences down to  $210 \text{ \AA}$ .

Particles undergoing separation in the CPE have a distribution of electrophoretic mobilities. Krumrine<sup>(2)</sup> modeled this distribution by segmenting the cross-sectional area and expressing the displacement as a function of position. Then the total cross-sectional distribution of particles was obtained by summing all the segments together. To further characterize the mobility distribution, the particle concentration and the breadth of the bands were specified. Also, four mobility distribution shapes, triangular, rectangular and parabolic, plus a N-th order polynomial computer--fitted to any random shape may be uniquely selected. Upon defining the distribution shape of a band, the segments can be quickly summed using the computer, where the degree of accuracy will depend upon the number of cross-sectional divisions. Hence, a concentration profile can be calculated as a function of the parameters that affect the migration distance and a cross-sectional image plotted.

## B. Experimental Results

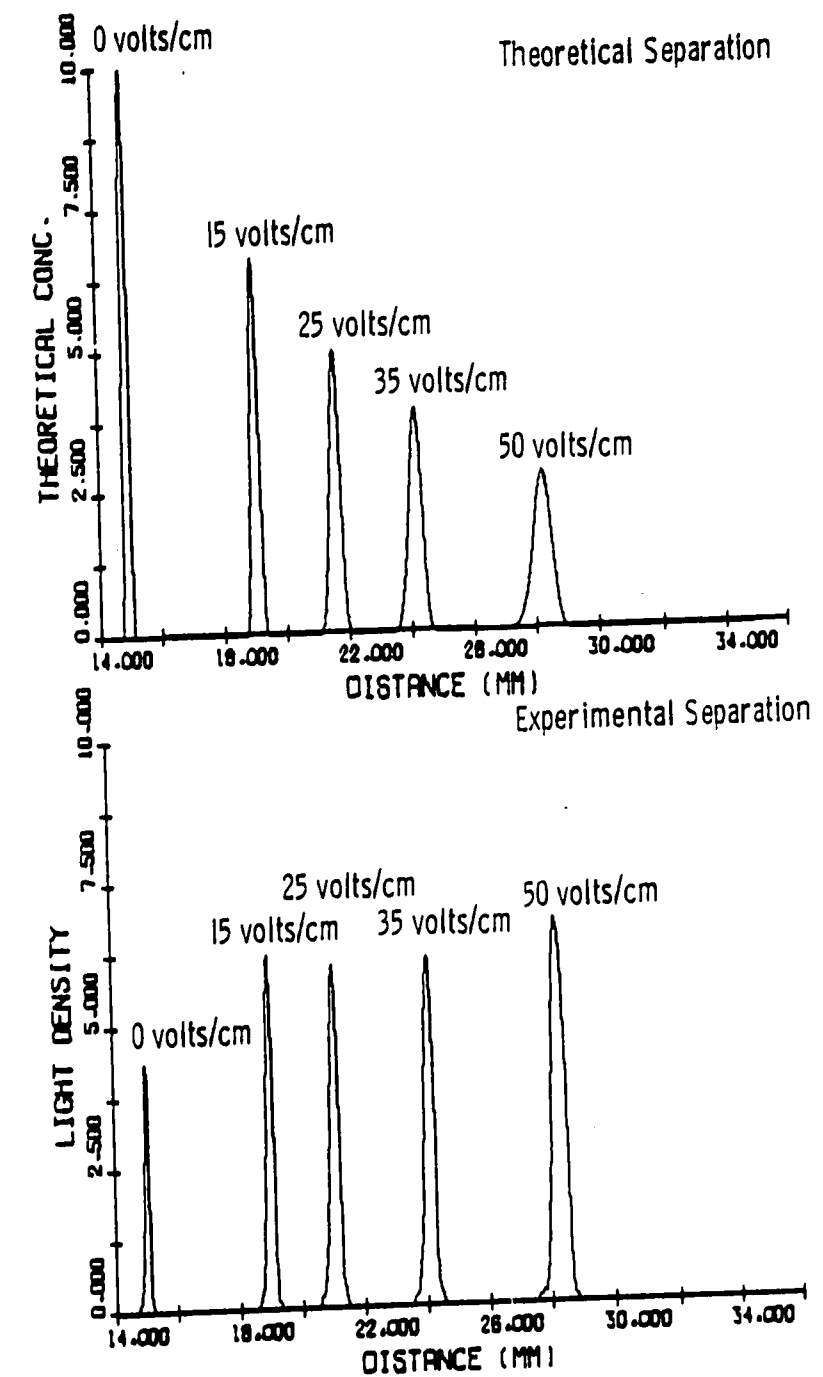
In the present work the computer model, developed by Krumrine (2), was used to compare theoretical predictions to experimental results obtained from the separation of different latexes suspended in  $1 \times 10^{-4}$  BSB. In addition, the computer program was applied to predict the influence of changes in operational parameters on the particle separation. These operational parameters include the effect of electroosmosis, and the geometry and position of the sample injection system.

### Comparison of Experimental and Theoretical Results

Figures 27, 28 and 29 show a comparison of the theoretical and experimental separations of latexes using different combinations of four monodisperse latexes. All the peak displacements are proportional to particle size. However the area under the peaks cannot be correlated to the particle concentration due to the configuration of the light source detection system. Krumrine's model does not take into account the effect of particle-particle interaction on the effect of sedimentation. Therefore the separations obtained in Figures 27, 28 and 29 are in good agreement with theoretical predictions and indicate that conditions may be found for a particular separated system where particle-particle interactions and the effect of sedimentation are kept at a minimum.

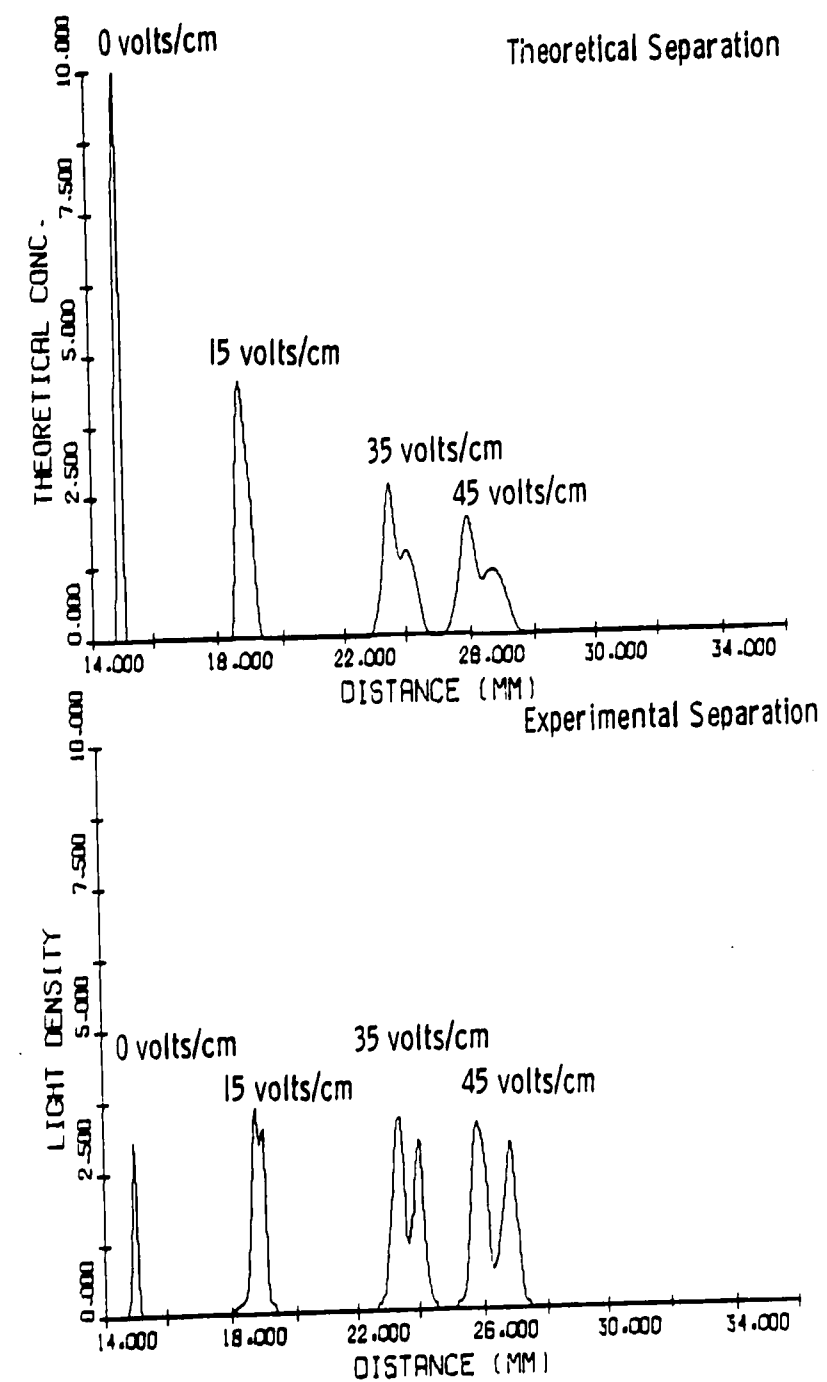
### Variation of Operational Parameters

The experimental parameters involved in the separation of particles in the CPE, e.g. electroosmosis, and geometry and position of the sample injection system, were analyzed using a real system containing two particles of diameter 1.10 and 0.234  $\mu\text{m}$ ., at 2 percent solids. The experimentally determined electrophoretic mobilities for the 1.10 and



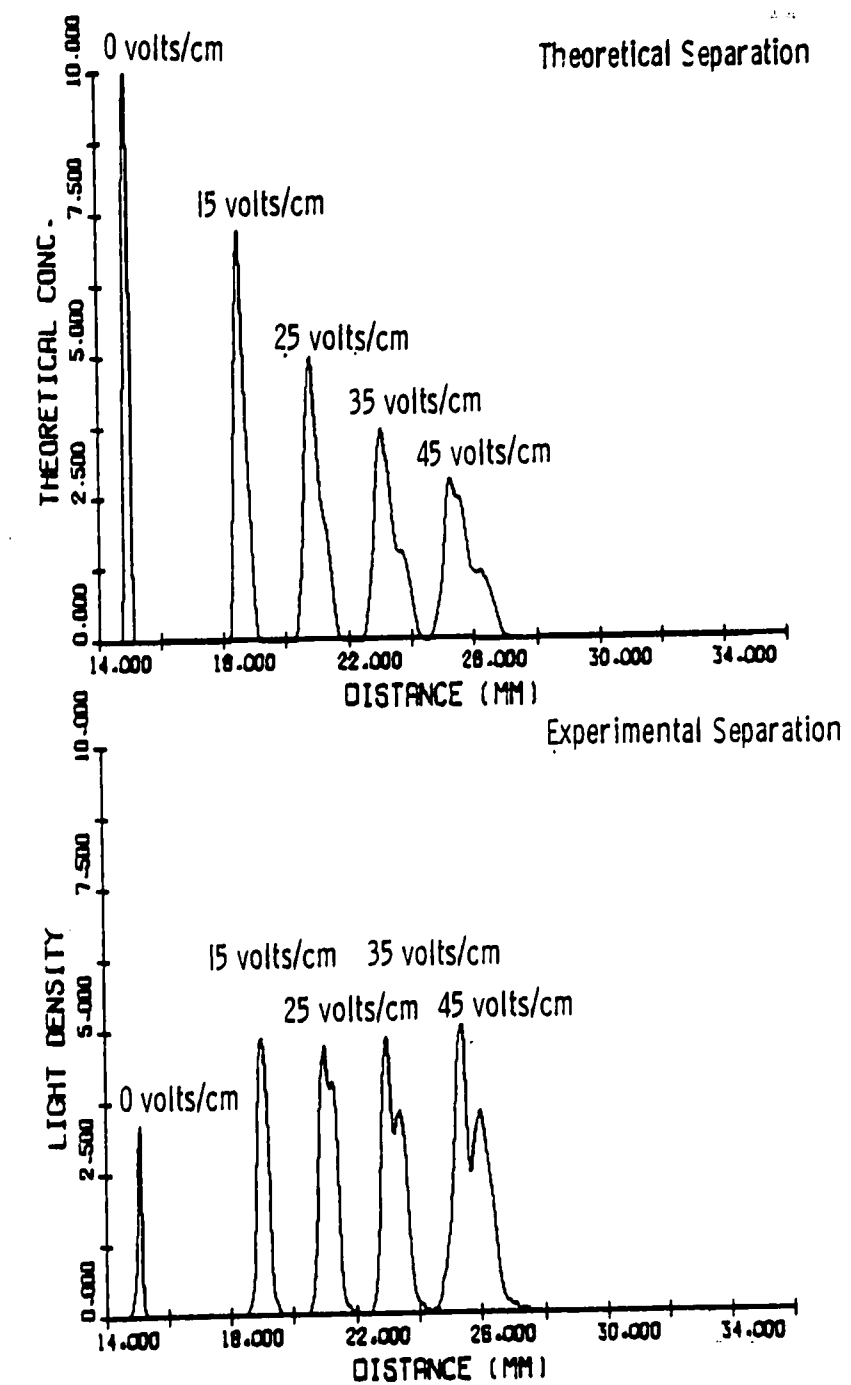
LIGHT DENSITY SCAN AND THEORETICAL DISPLACEMENT ON CPE

Figure 27. Comparison of the Theoretical and Experimental Separations of Two Latexes, 0.357 and 0.234  $\mu$ m in Size, 26 cc/min.



LIGHT DENSITY SCAN AND THEORETICAL DISPLACEMENT ON CPE

Figure 28. Comparison of the Theoretical and Experimental Separations of Two Latexes, 1.1 and 0.234  $\mu$ m in Size, 26 cc/min.



LIGHT DENSITY SCAN AND THEORETICAL DISPLACEMENT ON CPE

Figure 29. Comparison of the Theoretical and Experimental Separations of Four Latexes, 1.1, 0.357, 0.234 and 0.109  $\mu\text{m}$  in Size, 26 cc/min.

0.234  $\mu\text{m}$ . latexes are 3.52 and 2.64  $\mu\text{m}$ .  $\text{cm.}/\text{volt sec.}$ , respectively. These latexes were buffer-exchanged in  $1 \times 10^{-4}$  M barbital sodium barbital buffer to place the latexes in the same electrolyte as the curtain fluid, and to remove surfactant and other chemical species. The migration scale runs from 14.0 to 36.0 mm and the sample is injected at 15.0 mm. The separations are shown in Figure 30 for three stages 15, 35 and 45 volts/cm., where the electric field length is 30.0 cm. and the volumetric flow rate is 26 cc/min. A 3K temperature gradient was assumed from a trial and error procedure using comparative results of the experimental and theoretical separations. Experimental limitations did not allow sensitive measurement of this gradient. The migration distance is proportional to the applied electric field, hence there appears little particle-particle interaction between the 0.234 and 1.10  $\mu\text{m}$ . latex at these conditions.

#### Effect of Off-Center Injection

The effect of off-center injection on band separation is shown in Figure 31. The further off-center the bands are injected, the poorer the resolution. This is because the electroosmotic flow is greater near the walls and the bands become distorted as they are positioned closer to the walls.

#### Effect of Electroosmosis

Figure 32 shows the effect of electroosmotic mobility upon this system at a sample width to cell thickness ratio (R) of 0.2 in the Z-direction. Electroosmosis is a horizontal movement of fluid in the curtain and is additive to the particle velocity. Therefore, as the electroosmosis

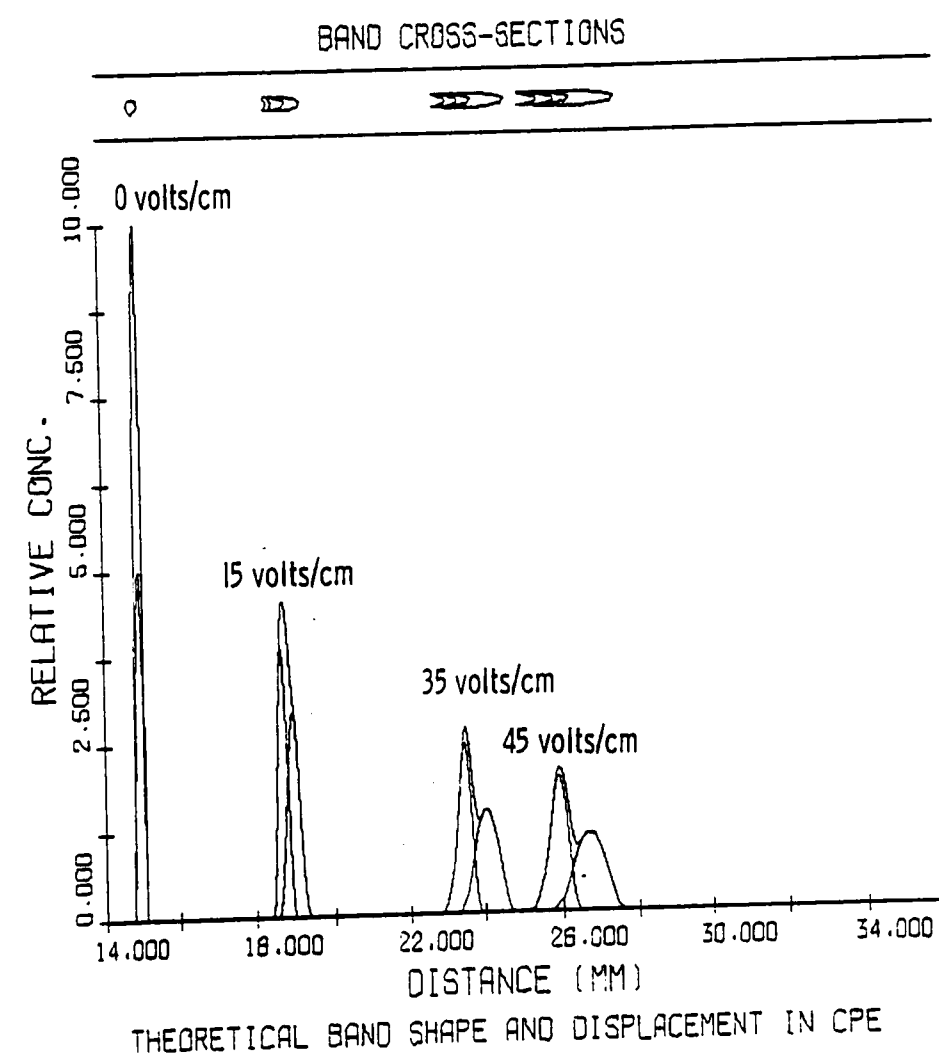


Figure 30. Hypothetical Separation at Three Stages of a Mixture of Two Latexes, 1.1 and 0.234  $\mu$ m, Under Real Conditions.

# THEORETICAL BAND SHAPE AND DISPLACEMENT IN CPE

## BAND CROSS-SECTIONS

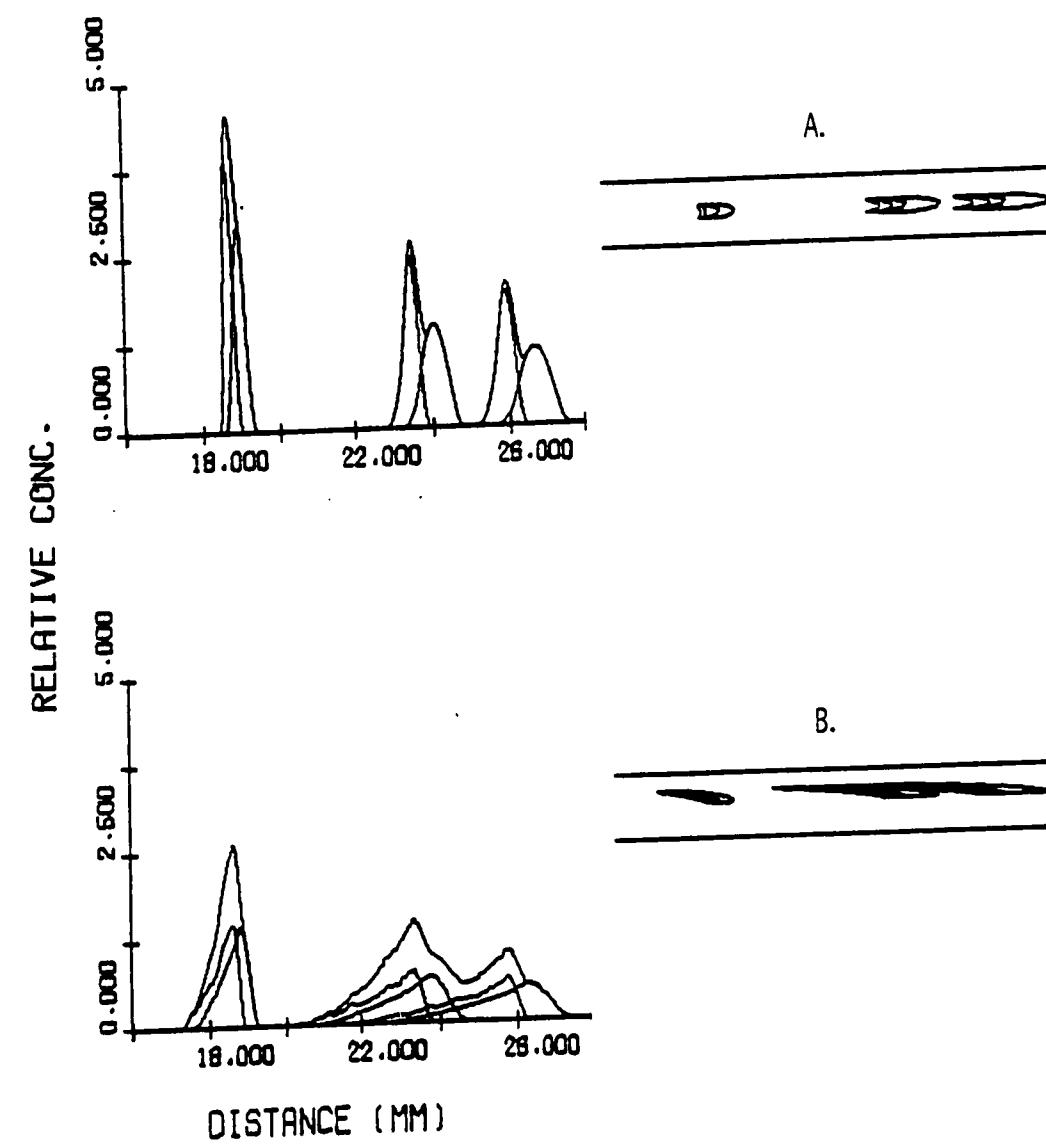


Figure 31. Computed Particle Displacement Showing the Effect of Off-Center Injection on Band Separation with  $U_{os} = -21.37 \text{ } \mu\text{m cm/volt sec.}$ , and  $R = 0.2$ ; A. Centered, B. 0.25 Off-Center.



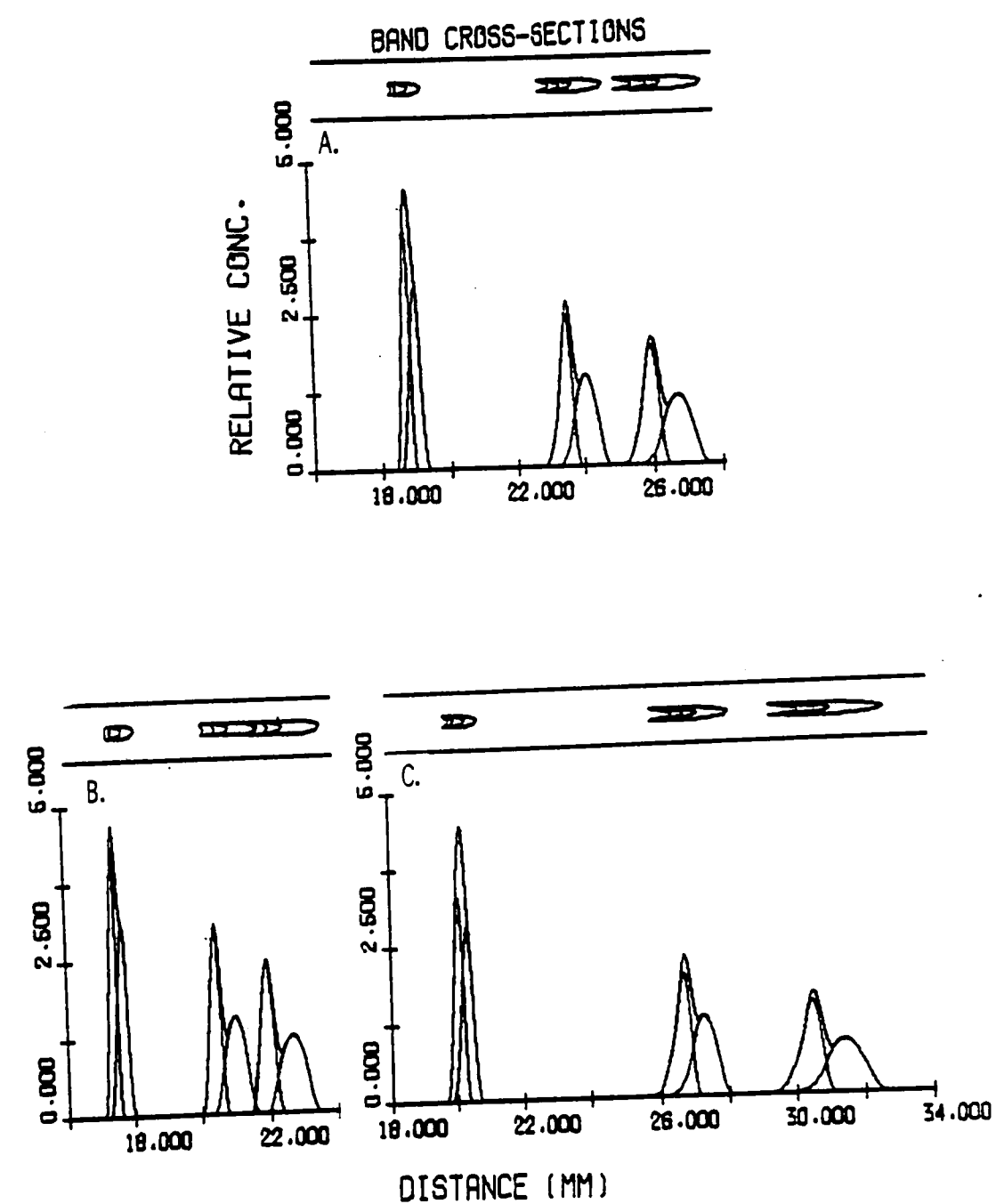


Figure 32. Computed Particle Displacement Showing the Effect of Electro-osmosis with  $R = 0.2$ ; A.  $U_{os} = -21.37 \text{ } \mu\text{m cm/volt sec}$ , at 15, 35 and 45 volts/cm; B.  $U_{os} = -11.37 \text{ } \mu\text{m cm/volt sec}$ , at 15, 35 and 45 volts/cm; C.  $U_{os} = -31.37 \text{ } \mu\text{m cm/volt sec}$ , at 15, 35 and 45 volts/cm.

decreases from C to A to B, the migration distance decreases and the crescent effect is convex towards the anode. But as the value of electroosmosis is increased, the distance increases and the crescent effect is convex towards the cathode. Strickler<sup>(47, 4)</sup> has also investigated the effect of electroosmosis on the crescent phenomena and has formulated similar results for real systems.

Figure 33 shows the effect of using different values of electroosmotic mobility for the front and rear walls of the separation chamber. The greater the difference in electroosmotic mobility values between the walls, the more distorted the sample bands become. The migration distance remains the same in all cases because the average electroosmotic mobility value for both walls is the same.

#### Effect of Size and Configuration of Injection Band Radius

Sometimes it is important to have a preparative rather than an analytical system. According to Kolin<sup>(3)</sup> and Strickler<sup>(4)</sup>, crescent curvature disappears when the electrophoretic mobility of the particle is equal to the electroosmotic mobility at the wall. This permits higher sample throughput without significant loss in resolution since distortion due to overlapping parabolic sample bands is minimized.

Figure 34 demonstrates the trade-off in resolution by increasing the injection band radius. This effect is similar to the effect of off-center injection and results from the increasing influence of electroosmotic flow upon the sample bands as the injection radius is increased. Resolution in separation techniques demands that the sample volume remain small and the migration distance be increased as far as possible. Hence, increasing the sample volume decreases the resolution of

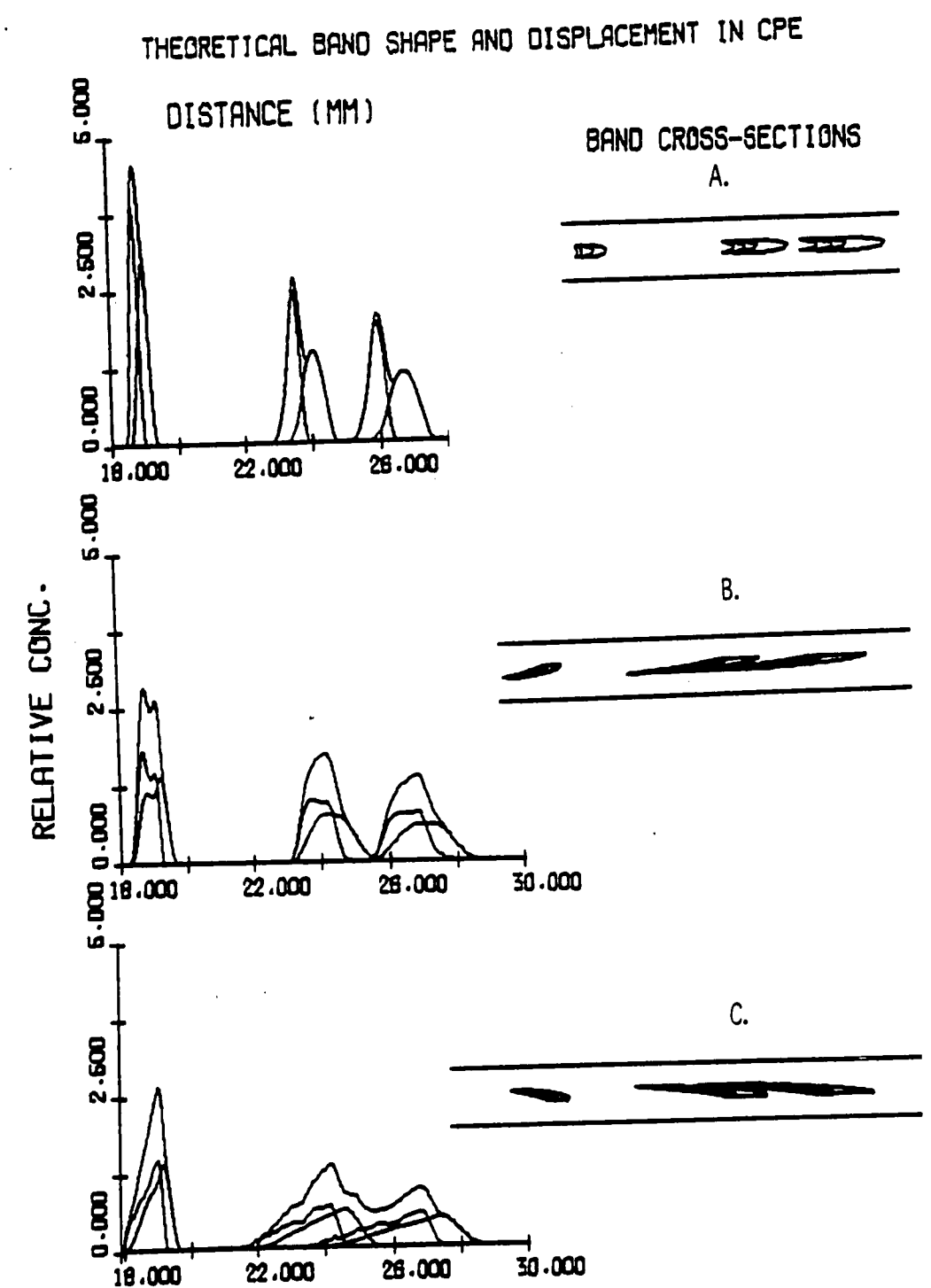


Figure 33. Computed Particle Displacement Showing the Effect of Different Values of  $U_{os}$  for the Front and Rear Walls with  $R = 0.2$  and Average  $U_{os} = -21.37 \text{ } \mu\text{m cm/volt sec.}$ ; A.  $U_{osf} = U_{osr} = -21.37 \text{ } \mu\text{m cm/volt sec.}$ , B.  $U_{osf} = -31.37 \text{ } \mu\text{m cm/volt sec.}$ ,  $U_{osr} = -11.37 \text{ } \mu\text{m cm/volt sec.}$ , C.  $U_{osf} = -11.37 \text{ } \mu\text{m cm/volt sec.}$ ,  $U_{osr} = -31.37 \text{ } \mu\text{m cm/volt sec.}$

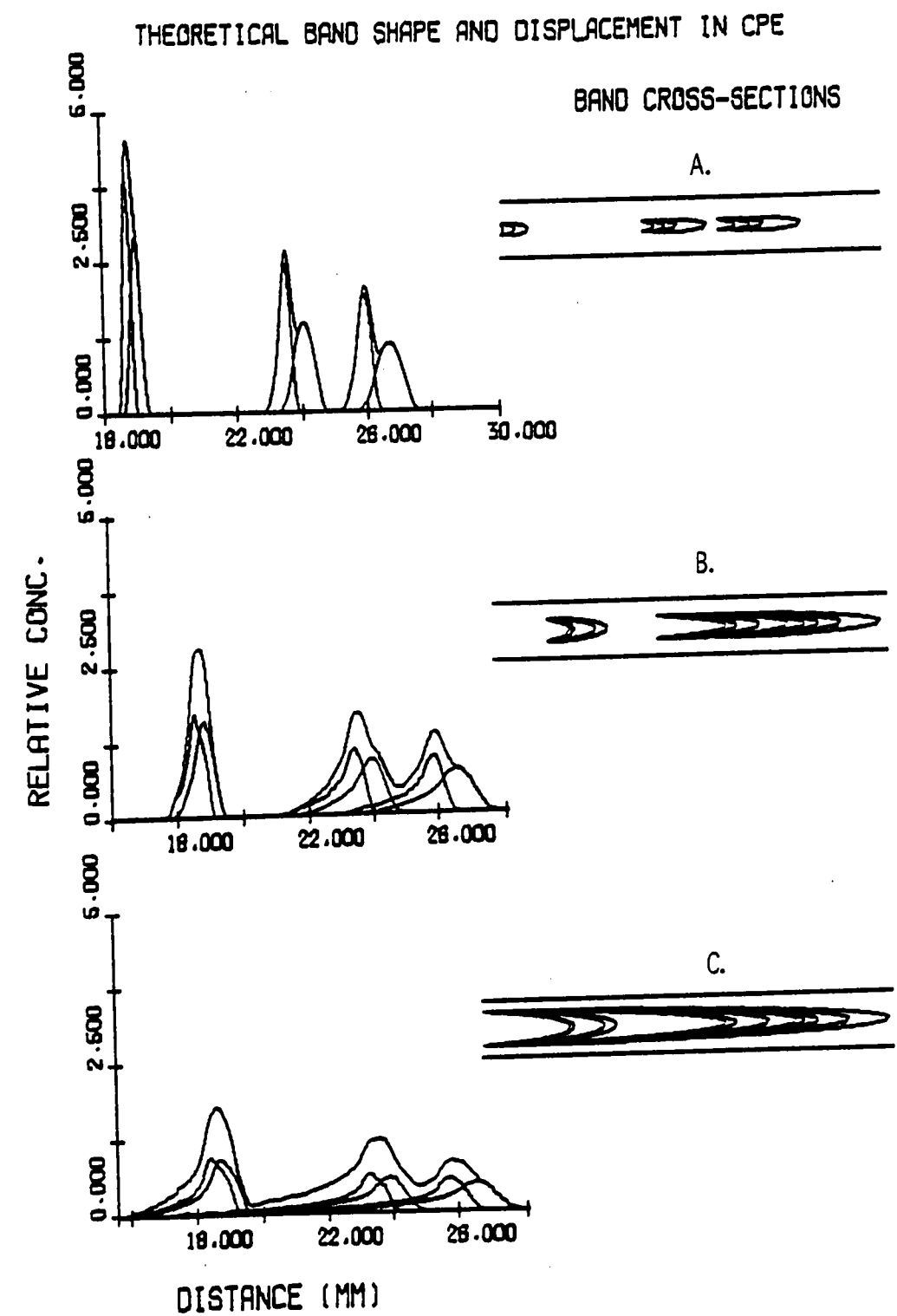


Figure 34. Computed Particle Displacement Showing the Effect of Increasing the Injection Radius with  $U_{os} = -21.37 \text{ } \mu\text{m cm/volt sec.}$ ; A.  $R = 0.2$ , B.  $R = 0.4$ , and C.  $R = 0.6$ .

separation of the sample bands. In Figure 34, there is a pronounced decrease in resolution and all the particle bands are parabolic since the zeta potential at the walls has not been matched to the mean electrophoretic mobility of the particles.

If sample throughput is of interest, it may be desired to change the configuration of the sample injection system from circular to rectangular and determine whether an increase in the sample width ( $R$ ) in the  $Z$ -direction, or the sample thickness ( $\theta$ ) in the  $X$ -direction is most detrimental to a separation. Figure 35 shows the effect of a rectangular cross-sectional injection port. Here one-dimension can be varied to increase the sample volume. From these results it is shown for a system in which the electroosmotic mobility does not equal the electrophoretic mobility of the particles, it is better to increase  $\theta$  rather than  $R$  to achieve best resolution. Krumrine<sup>(2)</sup> has shown for an ideal system, where the electrophoretic mobility has been matched to the electroosmotic mobility, it is better to increase  $R$  rather than  $\theta$  to obtain optimum resolution.

Similarly, as the electroosmosis is increased decreased and the dimensions  $R$  and  $\theta$  varied, it is best to increase  $\theta$  when the electrophoretic and electroosmotic mobilities are not equal, Figure 36, and to increase  $R$  when the zeta potential has been matched to the electrophoretic mobilities of the particles, Reference 10.

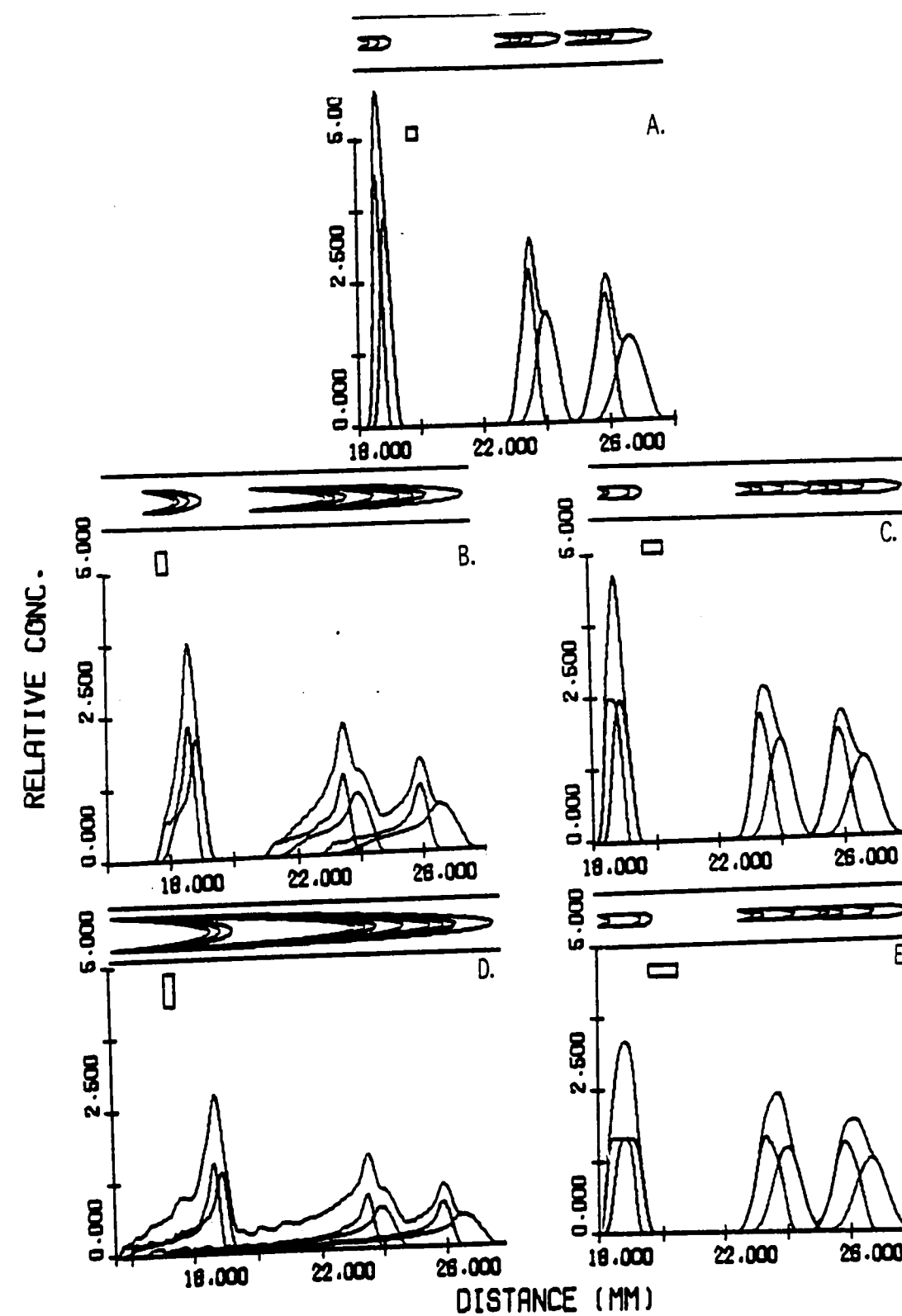


Figure 35. Computed Particle Displacement Showing the Effect of Increasing Band Volume in the R or  $\theta$  Direction with  $U_{os} = -21.37 \text{ } \mu\text{m cm/volt sec.}$ ; A.  $R = 0.2$ ,  $\theta = 0.2$ , B.  $R = 0.4$ ,  $\theta = 0.2$ , C.  $R = 0.2$ ,  $\theta = 0.4$ , D.  $R = 0.6$ ,  $\theta = 0.2$ , and E.  $R = 0.2$ ,  $\theta = 0.6$ .

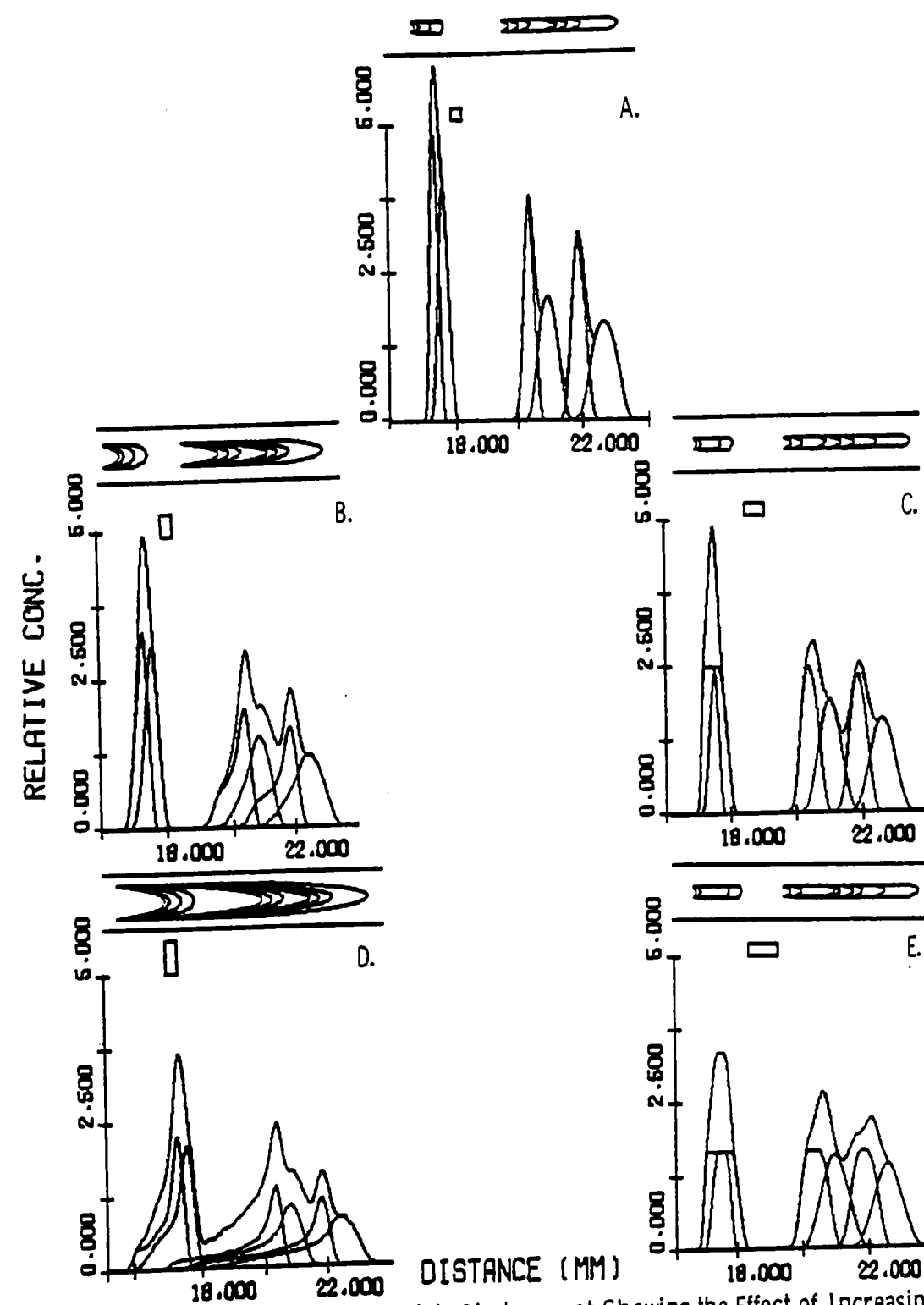


Figure 36.

Computed Particle Displacement Showing the Effect of Increasing Band Volume in the R or  $\theta$  Direction with  $U_{os} = -11.37 \text{ um cm/volt sec.}$ ; A.  $R = 0.2, \theta = 0.2$ , B.  $R = 0.4, \theta = 0.2$ , C.  $R = 0.2, \theta = 0.4$ , D.  $R = 0.6, \theta = 0.2$ , and E.  $R = 0.2, \theta = 0.6$ .

### C. Conclusions

In summary, comparisons of experimental and theoretical separations of latexes ranging in size from 1.10 to 0.109  $\mu\text{m}$ . were found to be in good agreement. This indicates that Krumrine's model works for separated systems where there is little particle-particle interaction and that such a condition can be found for a particular separated system.

Using this computer model as a basis, it is possible to change the different experimental parameters to determine the specific effect of each parameter. The considerations show there is not single method for choosing the optimum separation conditions. The resolution depends upon the value of electroosmosis and may be affected by the geometry and position of the sample injection system, applied voltage, mobility distribution of the particles, or the channel dimensions.

When the radius of the sample injection port is small relative to the separation chamber ( $R \leq 0.2$ ) the effect of electroosmosis is small, and distortion is not important. Therefore, electroosmosis may be increased and the effective separation decreased when distortion is not a factor.

When the effect of electroosmosis is large ( $R > 0.2$ ) then distortion is important and it is necessary to match the values of electroosmosis to the mean electrophoretic mobility of the particles. This increases the resolution by decreasing the extent of distortion. The minimum distortion occurs when the electroosmotic mobility is equal to the electrophoretic mobility, and at other conditions band-broadening occurs.



If sample throughput is important, it is impractical to use small sample volumes. Therefore it is important to match the electrophoretic mobility to the zeta potential of the walls and increase the port width of the injection system.

Thus, even though the conditions cannot be defined for every separation, these results show trends which should be considered in attempting to optimize the resolution.

## CHAPTER 5

### Surface Charge Density and Electrophoretic Mobility

#### A. Experimental Results and Conclusions

An attempt was made to evaluate the relationship between the surface charge density of the latexes studied and their electrophoretic mobilities. In order to achieve this, the latexes underwent an ion-exchange procedure in order to remove any surfactant and adsorbed chemical groups from the surface of the latexes to be analyzed. It was found, see Table 6, that the electrophoretic mobilities of the latex particles appear to decrease as the latexes become more 'clean'. This can be seen by independent comparison between the NBE and BE latexes suspended in  $1 \times 10^{-4}$  BSB, and the NIE and IE latexes suspended in distilled deionized water.

From Table 6, it is seen that the particle electrophoretic mobilities are proportional to their size only after a buffer-exchange procedure. Adsorbed surfactant could account for fluxations in electrophoretic mobilities in the non-buffer-exchanged system, however at this high dilution this possibility is unclear. Measurements taken for latexes suspended in distilled-deionized water gave puzzeling results as the electrophoretic mobility decreased with an increase in particle size. This may be a result of the very extended electrical double layers and/or adsorption of impurities on the surface of the latex. Adsorption of impurities on the surface of the latex resulting in an increase in electrophoresis mobility is supported by data which shows the

TABLE 6

The Effect of Various Degrees of Cleaning Upon the  
Electrophoretic Mobilities of Polystyrene Latexes

Polystyrene Latexes Sizes, $\mu\text{m}$ .	NBE $1 \times 10^{-4}$ BSB	BE $1 \times 10^{-4}$ BSB	NIE DDI	IE DDI
0.109	3.11	2.33	2.46	1.70
0.234	3.33	2.64	2.24	1.78
0.357	3.13	2.80	1.81	1.65
1.100	3.54	3.52	1.47	1.36

where:

DDI = distilled-deionized water

NBE = non-buffer-exchanged latex

BE = buffer-exchanged latex

NIE = non-ion-exchanged latex

IE = ion-exchanged latex

TABLE 7

Comparison of Surface Charge to the Electrophoretic Mobility  
and the Zeta Potential (H<sup>+</sup> counterion)

Polystyrene Latex Size, um.	% Std.Dev.	Surface Charge (uc/cm <sup>2</sup> )			IE-U <sub>E</sub> ( $\frac{\text{um. cm.}}{\text{volt sec.}}$ )	$\zeta$ (MV)
		SO <sub>4</sub> <sup>-</sup>	COO <sup>-</sup>	Total		
0.109	0.0027	2.45	0.887	3.33	1.70	21.85
		1.60***				
0.234	0.0026	2.54*	---	---	1.78	22.87
		2.63**				
		2.00***				
0.357	0.0056	3.32**	---	---	1.65	
					1.41**	21.20
1.100	0.0055	4.99	5.03	10.01	1.36	17.48

where:

IE-U<sub>E</sub> = electrophoretic mobility of the ion-exchanged latex

\* = value determined by Ahmed<sup>(66)</sup>

\*\* = values determined by Wu<sup>(65)</sup>

\*\*\* = values determined by Vanderhoff<sup>(67)</sup>

electrophoretic mobilities of the ion-exchanged latexes increases after they were left to stand (in sealed glass bottles) for several days. This indicates a change in the system, possibly due to leaching of sodium ions from the glass to the solution or to the latex.

In order to compare the overall surface charge to the electrophoretic mobility of the latexes studied, the surface charge of the 0.109 and the 1.10  $\mu\text{m}$ . latexes was determined by conductometric titration, see Appendix D. The electrophoretic mobilities of the latexes were immediately determined in distilled deionized water to avoid aging effects. Table 7 summarizes the result of this study.

According to Wu<sup>(65)</sup> the electrophoretic mobility depends upon the nature of the counterions of the sulfate endgroups, therefore the surface charge based upon the sulfate endgroups was determined. No direct correlation could be made between the surface charge density, based on dissociated sulfate endgroups, and the electrophoretic mobility or the zeta potential. This behavior may be due to experimental limitations. Previously it has been found that this method of determining surface charge density does not represent the effective surface charge and only part of the sulfate groups of the latex are dissociated<sup>(67,68)</sup>. Also, the zeta potential may be a complicated function of the surface charge, or unrelated entirely. Further experimental and theoretical investigations are needed in order to understand this phenomena.

## CHAPTER 6

### Conclusions

The objective of this investigation was to optimize the resolution of separation in continuous particle electrophoresis (CPE). The resolution of separation in the CPE may be reduced by the influence of electroosmosis, or by particle-particle interactions of the electrical double layers surrounding the particles to be separated.

Electroosmosis may be controlled by the development of a stable coating with controlled electrokinetic properties. Several coatings were evaluated using the concept that a combination of at least two different latexes, where at least one of the latexes is a film-former will result in a coating with electrokinetic properties inbetween the electrokinetic properties of the two latexes. For example, combinations of two film-forming latexes, XX210 (polyvinyl acetate) and Acrysol (acrylic copolymer) resulted in electroosmotic mobility values that were a function of their respective concentrations. These coatings appeared stable after a 48-hour dynamic rinse. Future work in this area would allow a more detailed analysis of this concept of coating. The data collected was limited by the confirmation of these results by repeated experimentation.

The resolution of separation in the CPE may also be reduced by particle-particle interactions at high concentrations or at low electrolyte concentrations. The present work studied particle-particle interaction using four monodisperse latexes of similar and different mobility at a low ionic concentration of  $1 \times 10^{-4}$  BSB, where the double layers

around the particles are very extended and the effect of particle-particle interaction is very pronounced. These interactions will be a function of the number of collisions between the particles and will be reflected in the distance between the separated bands of latex particles. It was found that at high particle concentrations the affect of particle-particle interaction is greatest, and at low particle concentration the affect of particle-particle interaction is less defined. The affect of particle-particle interaction in this system was limited by the presence of band-broadening effects and the densitivity of the light source detection system. Band broadening effects may be reduced to a minimum if the zeta potential of the chamber walls is identical to that of the particles to be separated. Experimental limitations were also encountered in determining the peak-to-peak separation distance when one particle was at a high solids content and the second particle was at a low solids content. The light source detection system may not be able to distinguish between the closely separated bands.

The main problem in obtaining maximum resolution of separation is control of electroosmosis. Krumrine was able to develop a computer model to simulate the affect of various operational parameters on electroosmosis, and hence on the separation of model colloids. This study compared Krumrine's theoretical predictions against experimental data obtained from the separation of different latexes in  $1 \times 10^{-4}$  BSB. It was found that Krumrine's model worked for separated systems where there was little particle-particle interaction and the effect of sedimentation was not a problem. Also, this computer program was applied to predict the influence of changes in various operational parameters on the separation

of a real particle system. The results showed a more dramatic reduction in resolution in this system as the affect of electroosmosis is encountered by variance of the geometry and position of the sample injection system, applied voltage, mobility distribution of the latexes, or the channel dimensions. Although no single method was evident for choosing the optimum separation conditions, some important trends can be considered.

When the radius of the sample injection port is small relative to the separation chamber ( $R \leq 0.2$ ) the effect of electroosmosis is small, and distortion is not important. Therefore, electroosmosis may be increased and the effective separation decreased when distortion is not a factor.

When the effect of electroosmosis is large ( $R > 0.2$ ), then distortion is important and it is necessary to match the values of electroosmosis to the mean electrophoretic mobility of the particles. This increases the resolution by decreasing the extent of distortion. The minimum distortion occurs when the electroosmotic mobility is equal to the electrophoretic mobility, and at other conditions band-broadening occurs.

If sample throughput is important, it is impractical to use small sample volumes. Therefore it is important to match the electrophoretic mobility to the zeta potential of the walls and increase the port width of the injection system.

Thus, although conditions cannot be defined for every separation, these results show trends which should be considered in attempting to optimize the resolution of separation in continuous electrophoresis.



The surface charge densities of the latexes of interest were determined as a function of their sulfate end-groups. These values were compared to the electrophoretic mobilities and the zeta potentials of the latexes. No direct relationship could be drawn between the number of sulfate end groups determined by conductometric titration and the zeta potential or the electrophoretic mobility.

Future work would include the development of a computer model to simulate the separation of particles in the CPE which takes into account the effect of sedimentation and the affect of particle-particle interaction. Also, an improved light source detection system and the minimization of distortion due to electroosmosis would allow further, more detailed study of particle-particle interaction using the CPE. These results could then be compared and verified against a theoretical rate of collision model for particles undergoing electrophoretic separation under laminar flow conditions.

## APPENDICES

# APPENDIX A

Table A-1. Composition and Properties of R-1 Buffer <sup>(69)</sup>

## Recipe for R-1 Buffer

Substance	MW	10XR-1	1XR-1	Millimolarity
		g/l	g/l	
Na <sub>2</sub> HPO <sub>4</sub>	141.96	2.50	0.25	1.76
KH <sub>2</sub> PO <sub>4</sub>	136.09	0.50	0.05	0.367
Na <sub>2</sub> EDTA·2H <sub>2</sub> O	372.24	1.251	1.25	0.336

10X R-1 Buffer concentrate properties:

$$K_{25^{\circ}\text{C}} = 3.49 \times 10^{-3} \text{ mho/cm}$$

$$\text{pH } 23^{\circ}\text{C} = 7.21$$

$$\eta_{25^{\circ}\text{C}} = 0.898 \text{ cp}$$

Osmolality = 56.5 milliosmoles/kg (based on measurements of freezing point depression using KCl standards)

## APPENDIX B

Electrokinetic Mobility Results of Coated Glass

Capillaries in DDI and R-1 Buffer

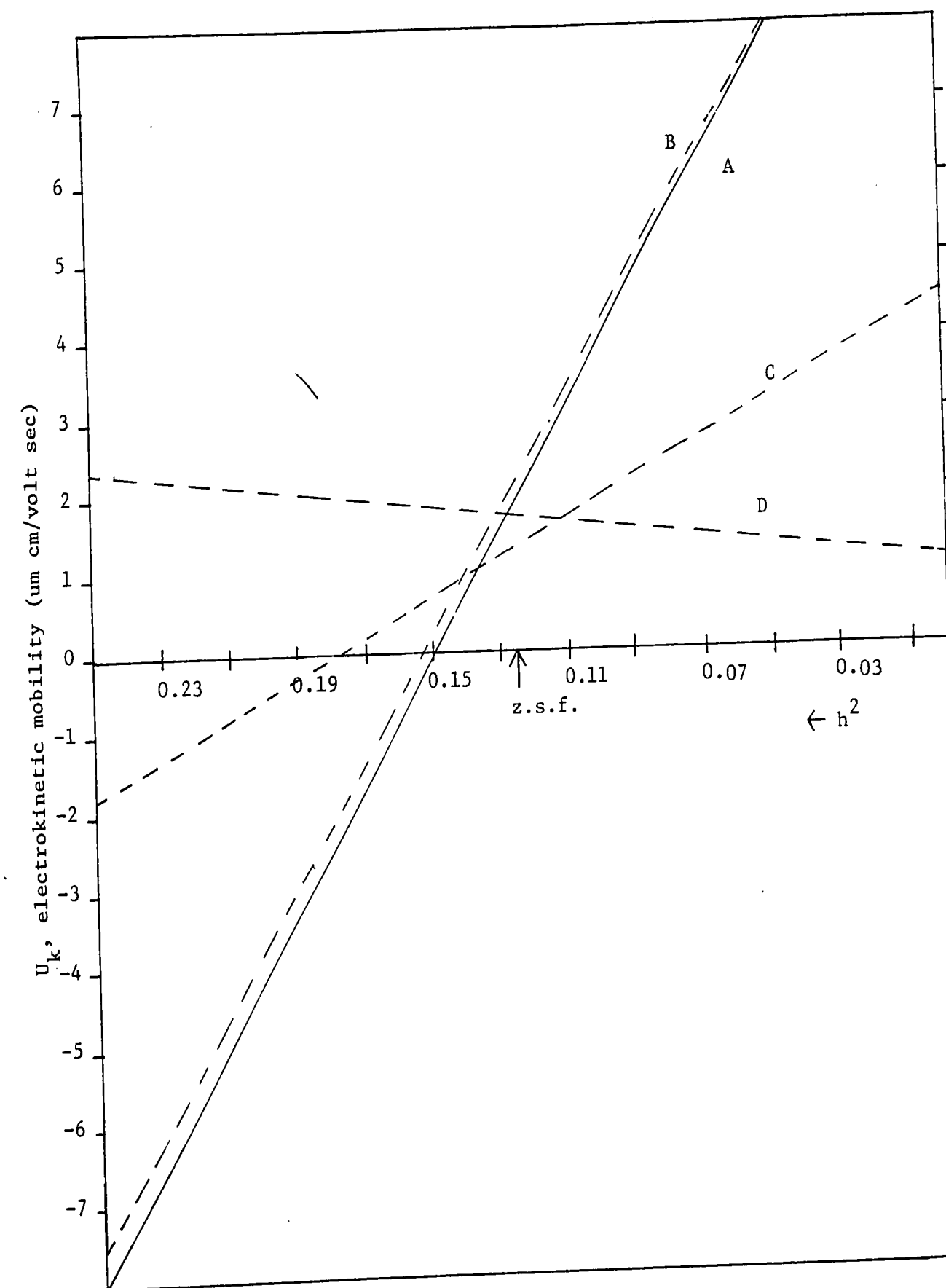


Figure B-1. Comparison of electrokinetic mobilities versus the square of the distance for coated capillaries using distilled-deionized water as the solvent. A. uncoated, B. Acrysol coated, C. XX210 coated, and D. Locron-P coated capillaries.

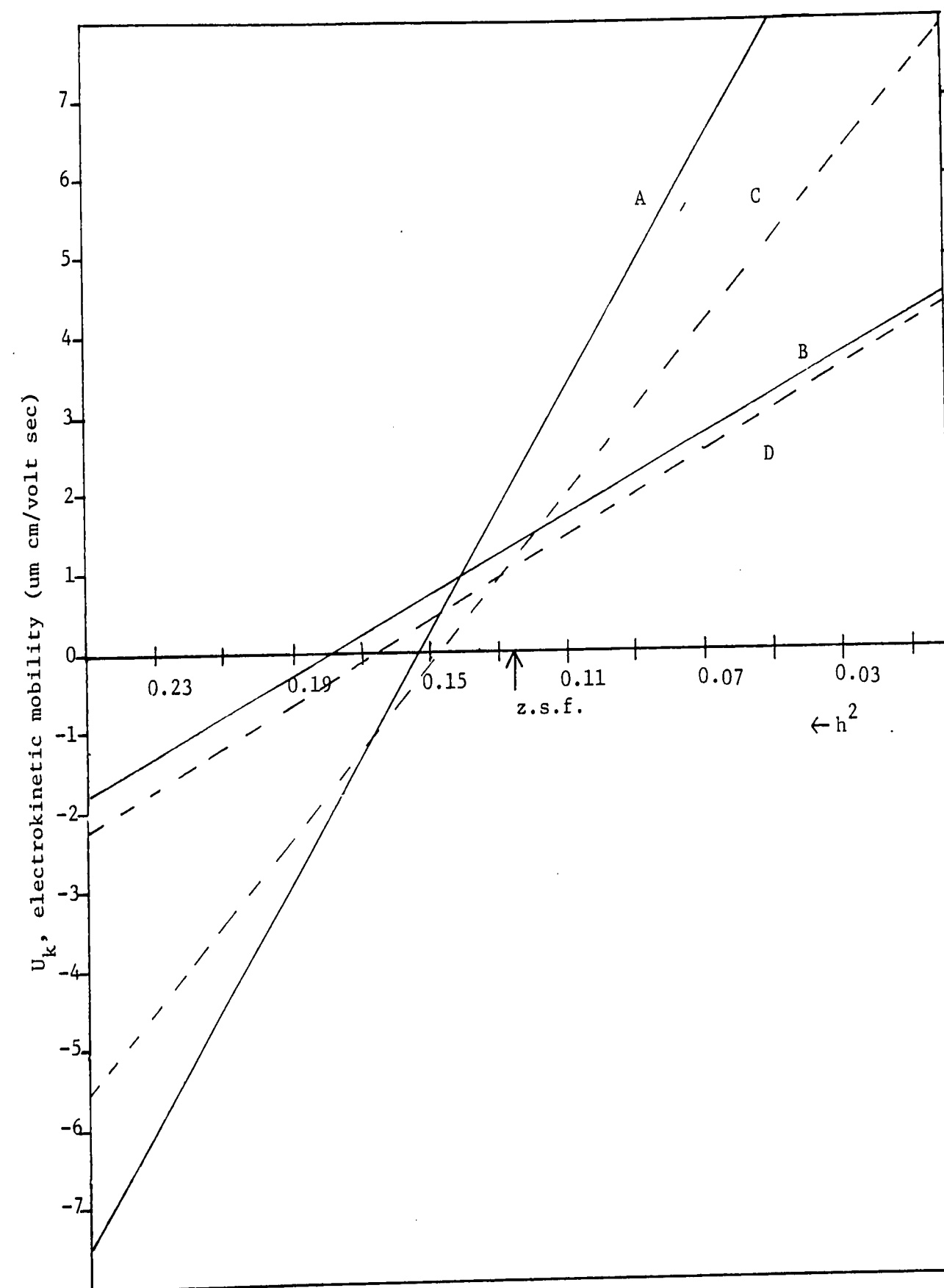


Figure B-2. Comparison of controlled electrokinetic mobilities versus the square of the distance for coated capillaries using distilled-deionized water as the solvent. A. Acrysol coated, B. XX210 coated, C. 50/50 by weight XX210/Acrysol coated, and D. 75/25 by weight XX210/Acrysol coated capillaries.

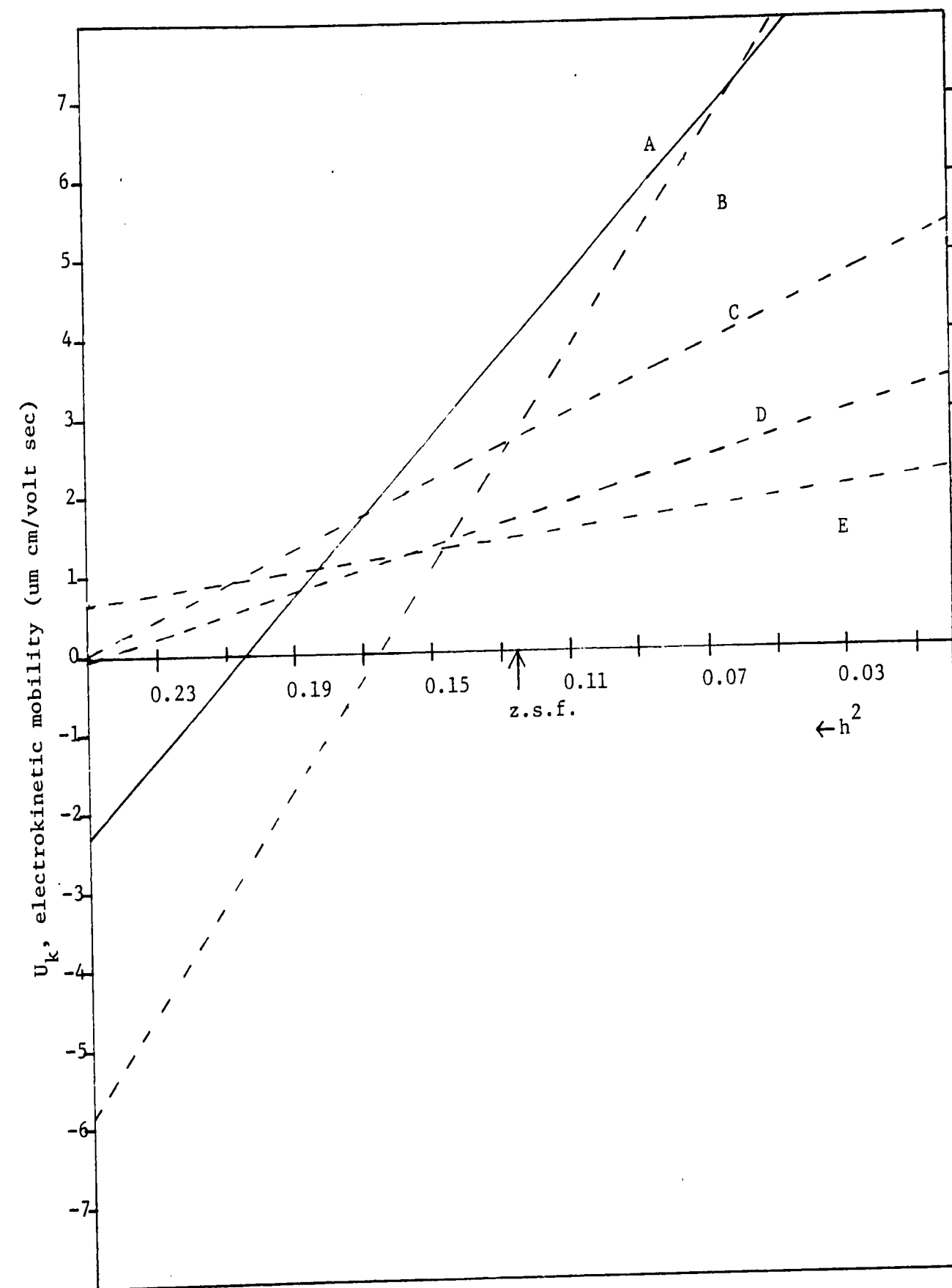


Figure B-3. Comparison of electrokinetic mobilities versus the square of the distance for coated capillaries using R-1 buffer as the solvent. A. uncoated, B. Acrysol coated, C. Locron-P coated, D. polystyrene in toluene, and E. XX210 coated capillaries.

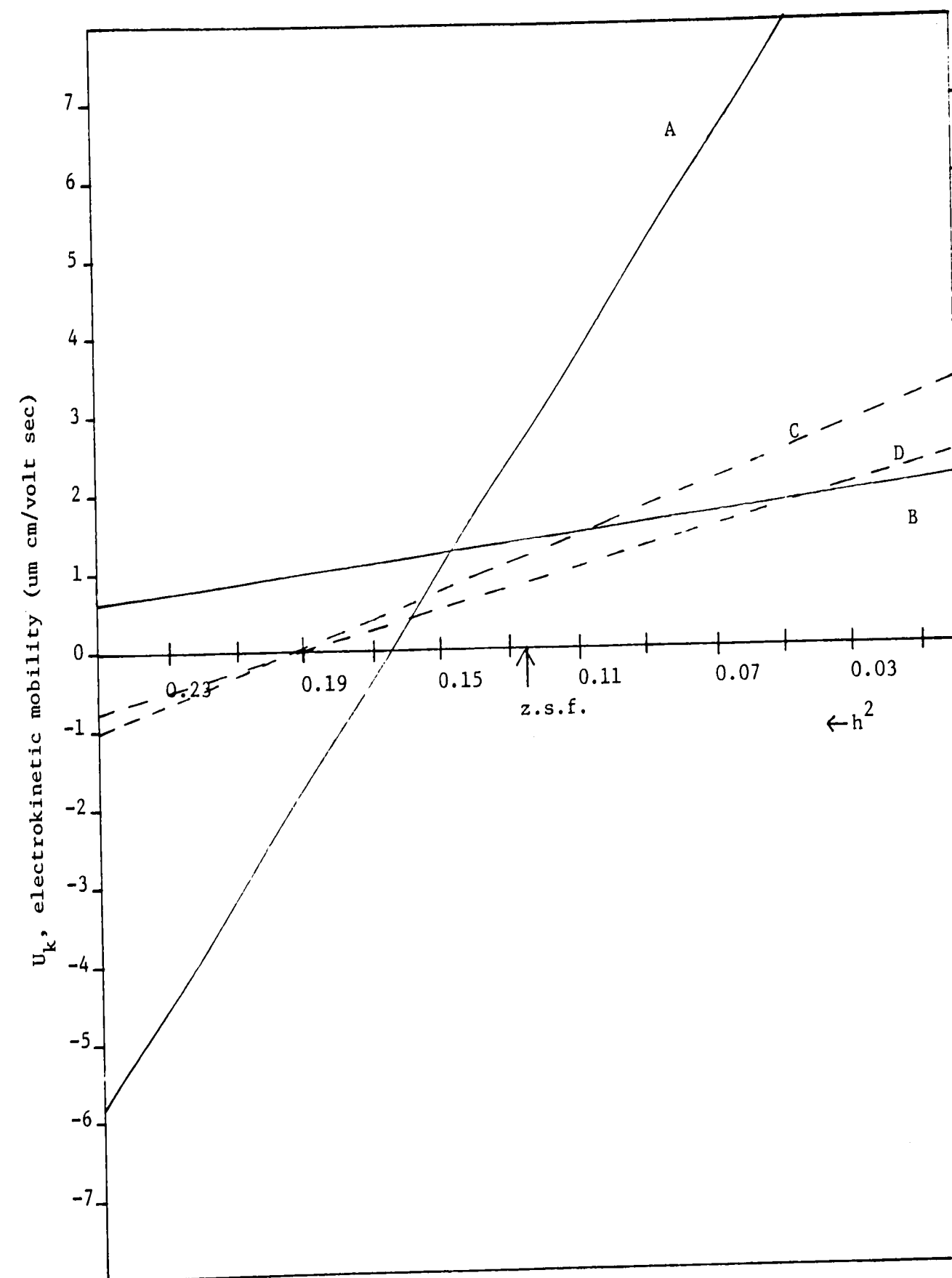


Figure B-4. Comparison of controlled electrokinetic mobilities versus the square of the distance for coated capillaries using R-1 buffer as the solvent. A. Acrysol coated, B. XX210 coated, C. 75/25 by weight XX210/Acrysol coated and D. 50/50 by weight XX210/Acrysol coated capillaries.



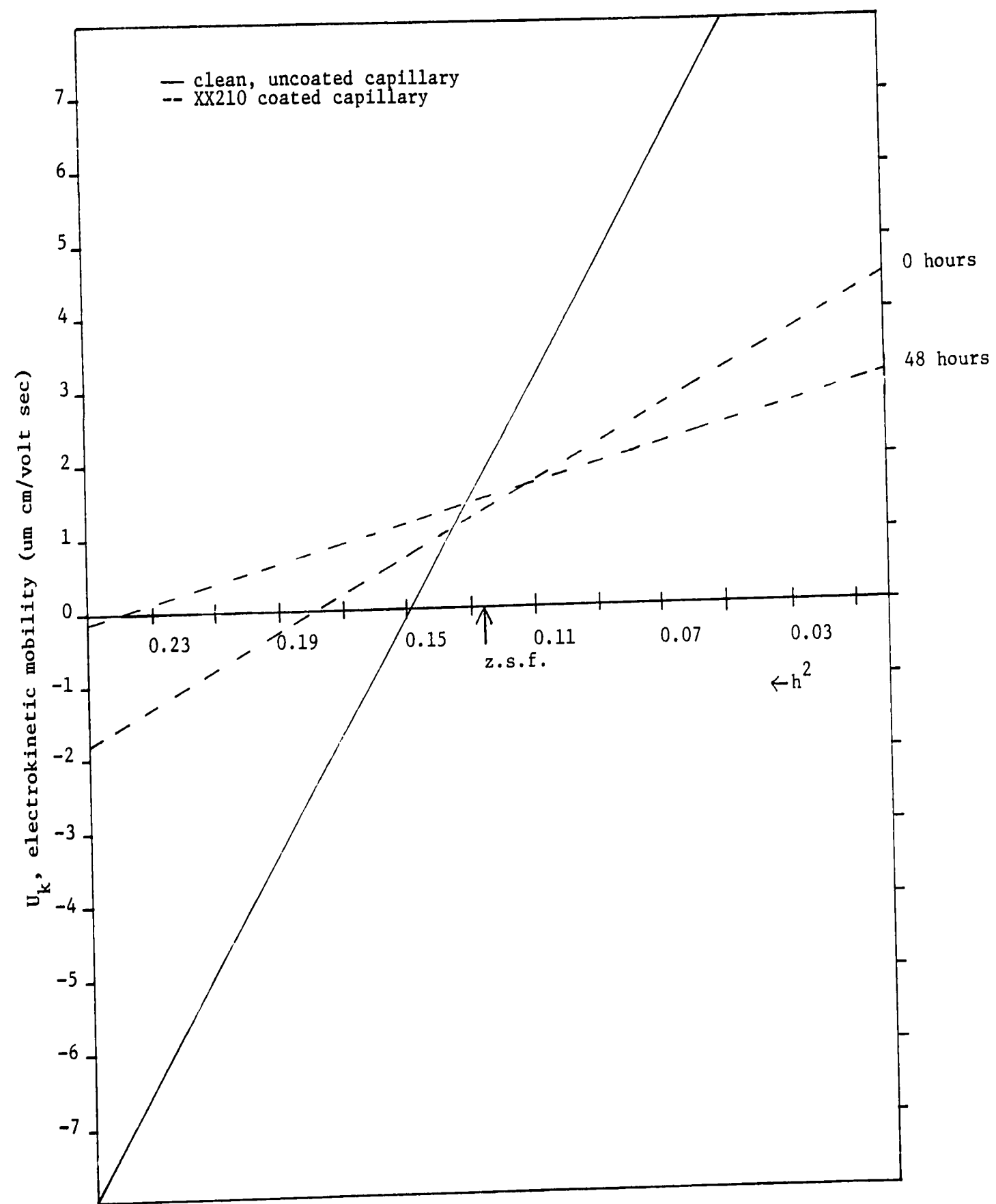


Figure B-5. Effect of dynamic rinsing upon the electrokinetic mobility results of coated glass capillaries in distilled-deionized water.

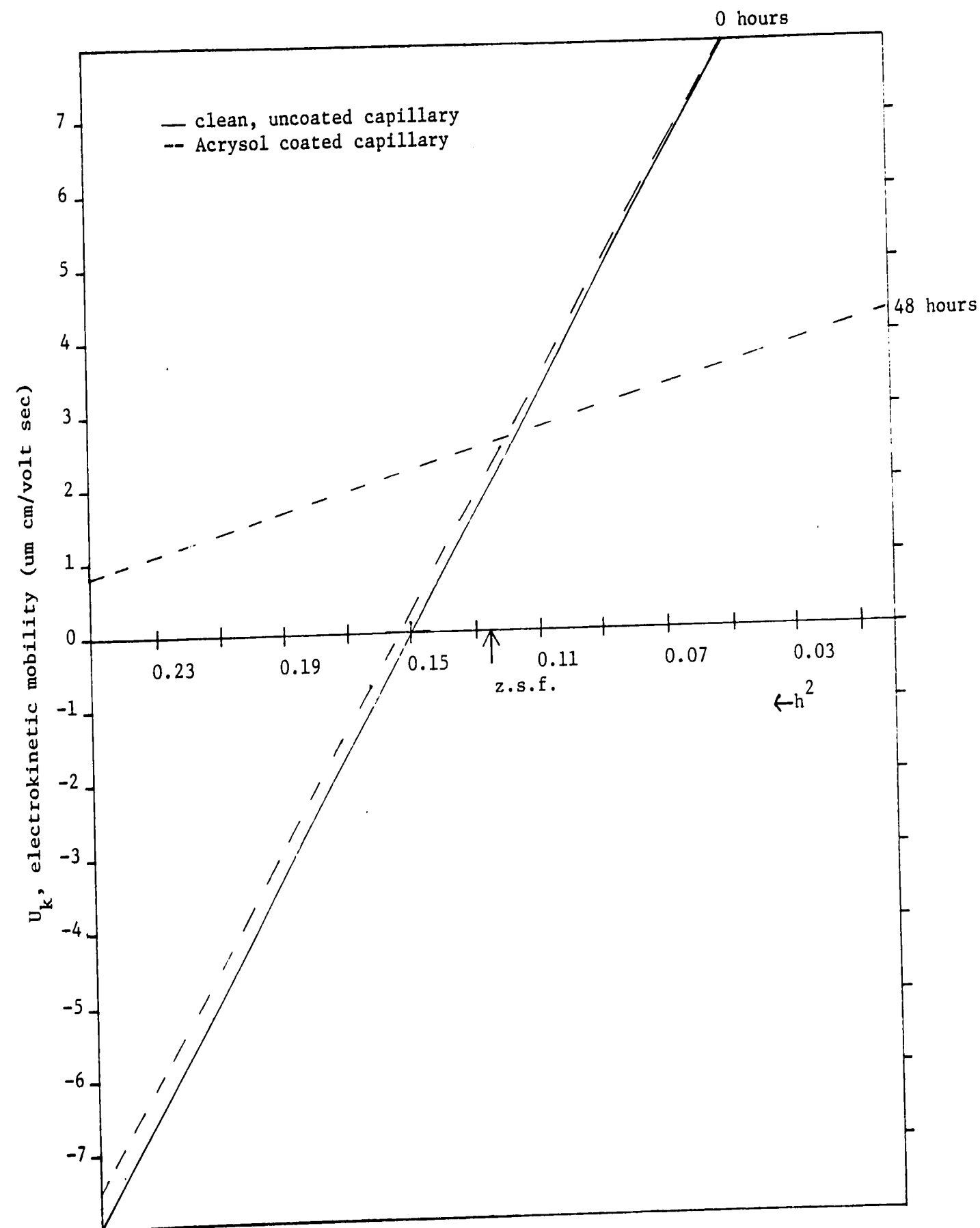


Figure B-6. Effect of dynamic rinsing upon the electrokinetic mobility results of coated glass capillaries in distilled-deionized water.

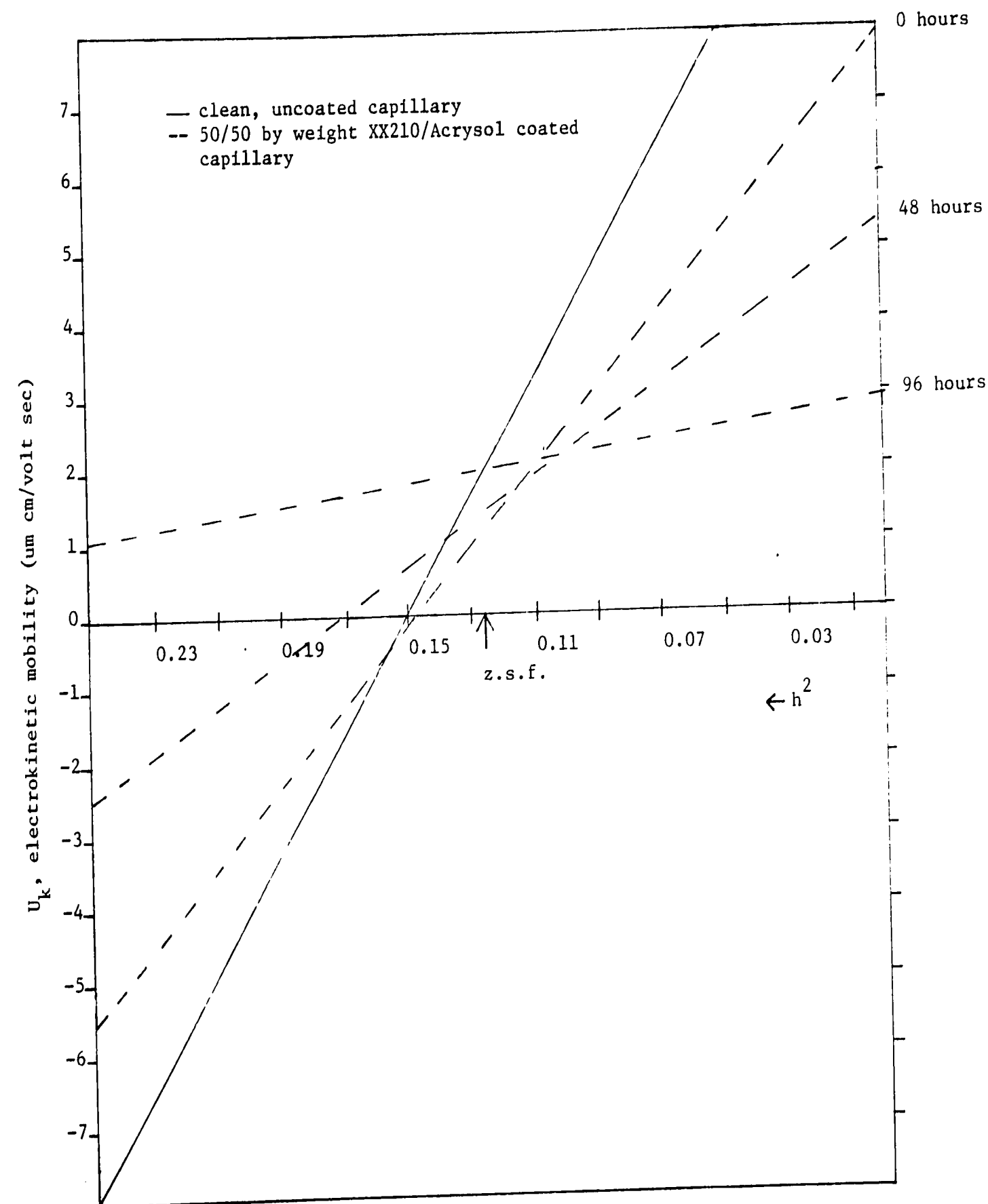


Figure B-7. Effect of dynamic rinsing upon the electrokinetic mobility results of coated glass capillaries in distilled-deionized water.

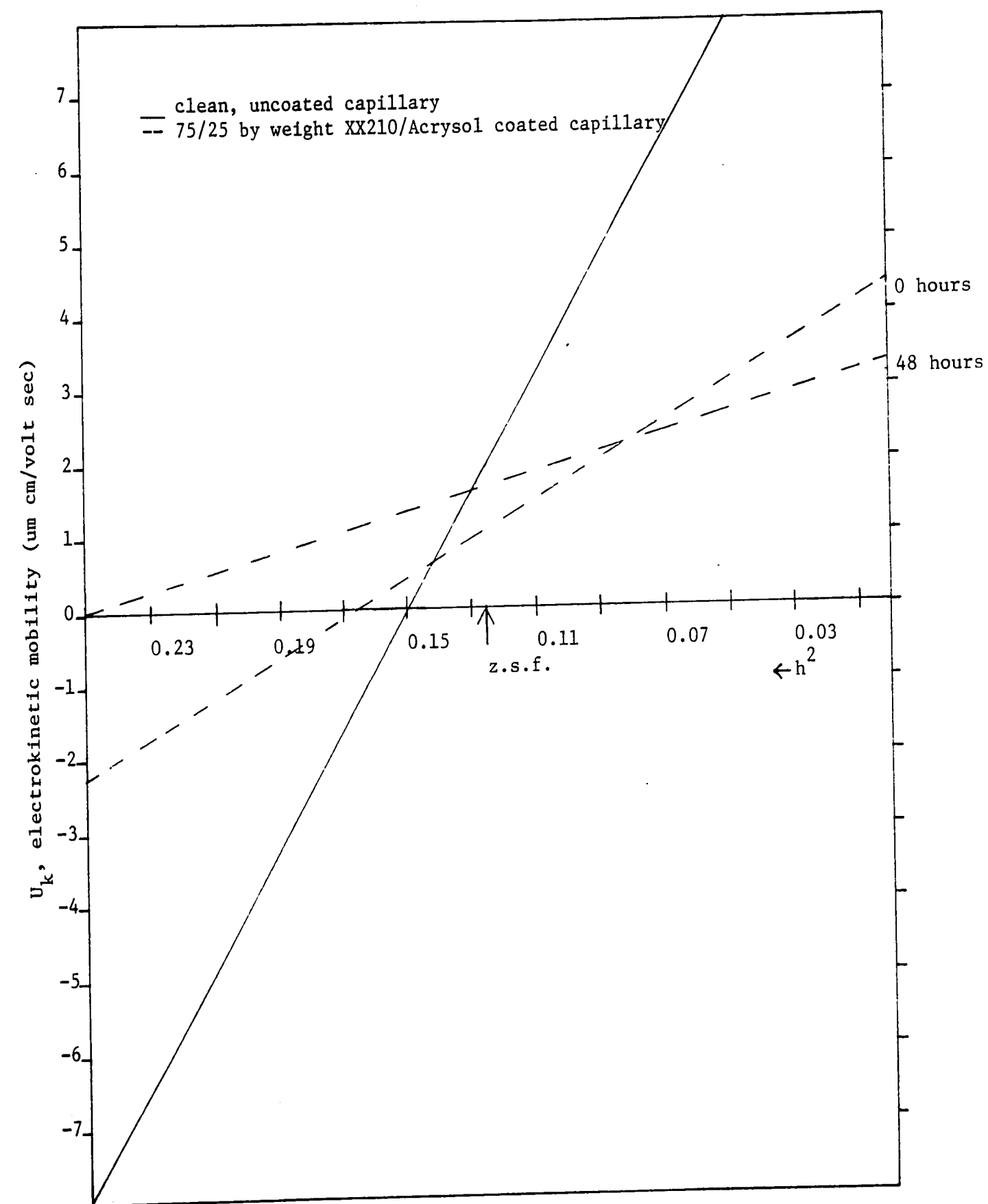


Figure B-8. Effect of dynamic rinsing upon the electrokinetic mobility results of coated glass capillaries in distilled- deionized water.

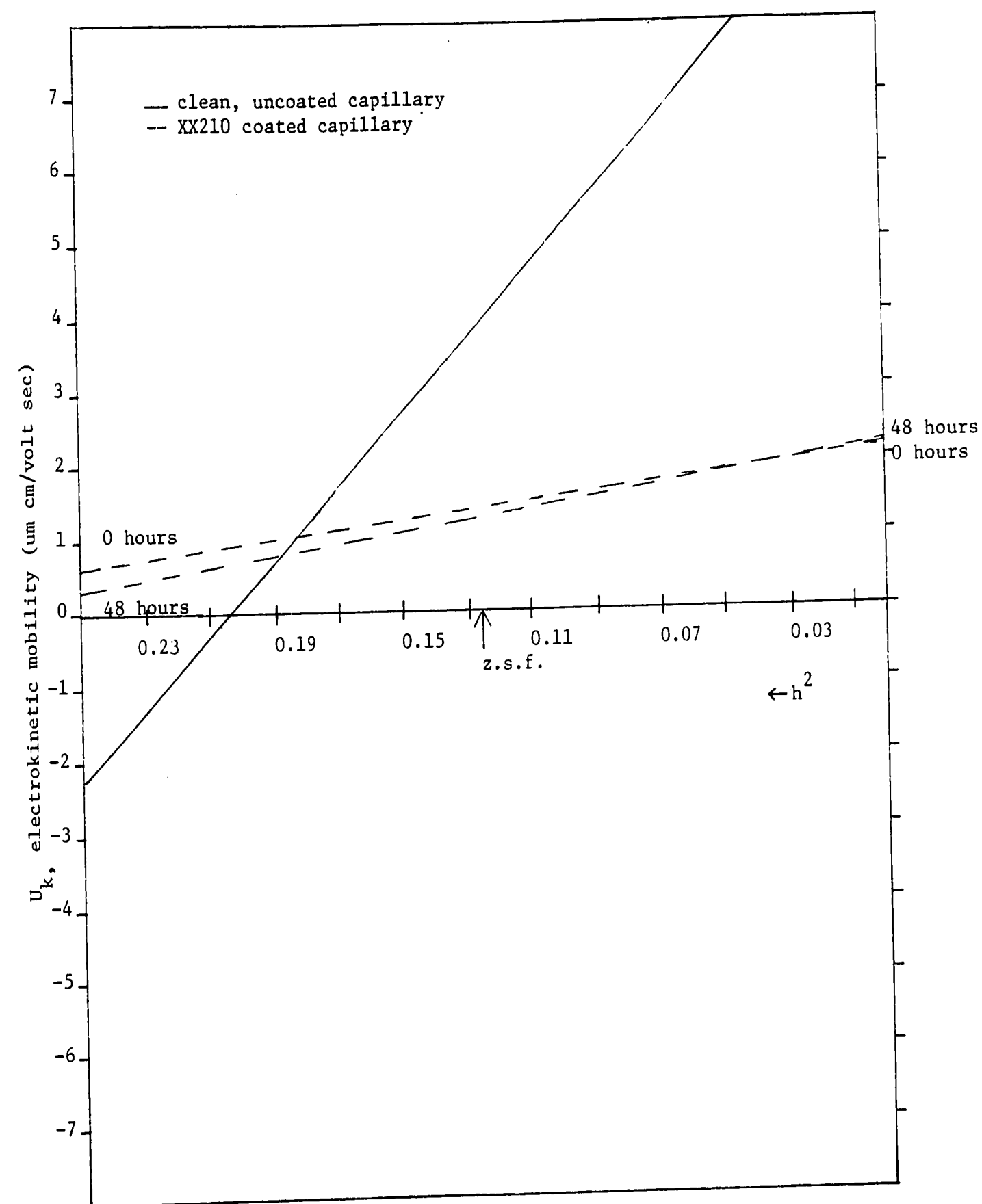


Figure B-9. Effect of dynamic rinsing upon the electrophoretic mobility results of coated glass capillaries in R-1 buffer.

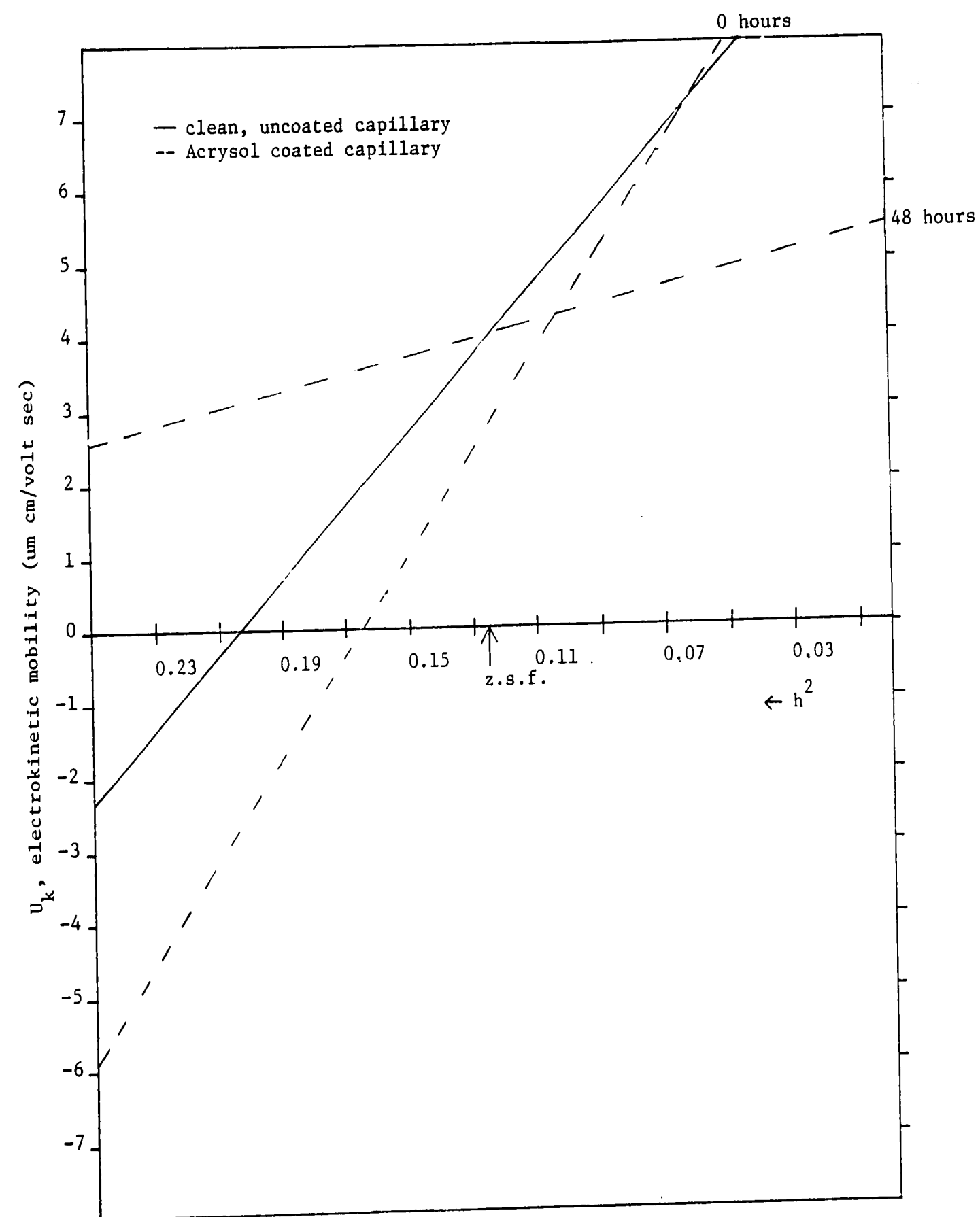


Figure B-10. Effect of dynamic rinsing upon the electrokinetic mobility results of coated glass capillaries in R-1 buffer.

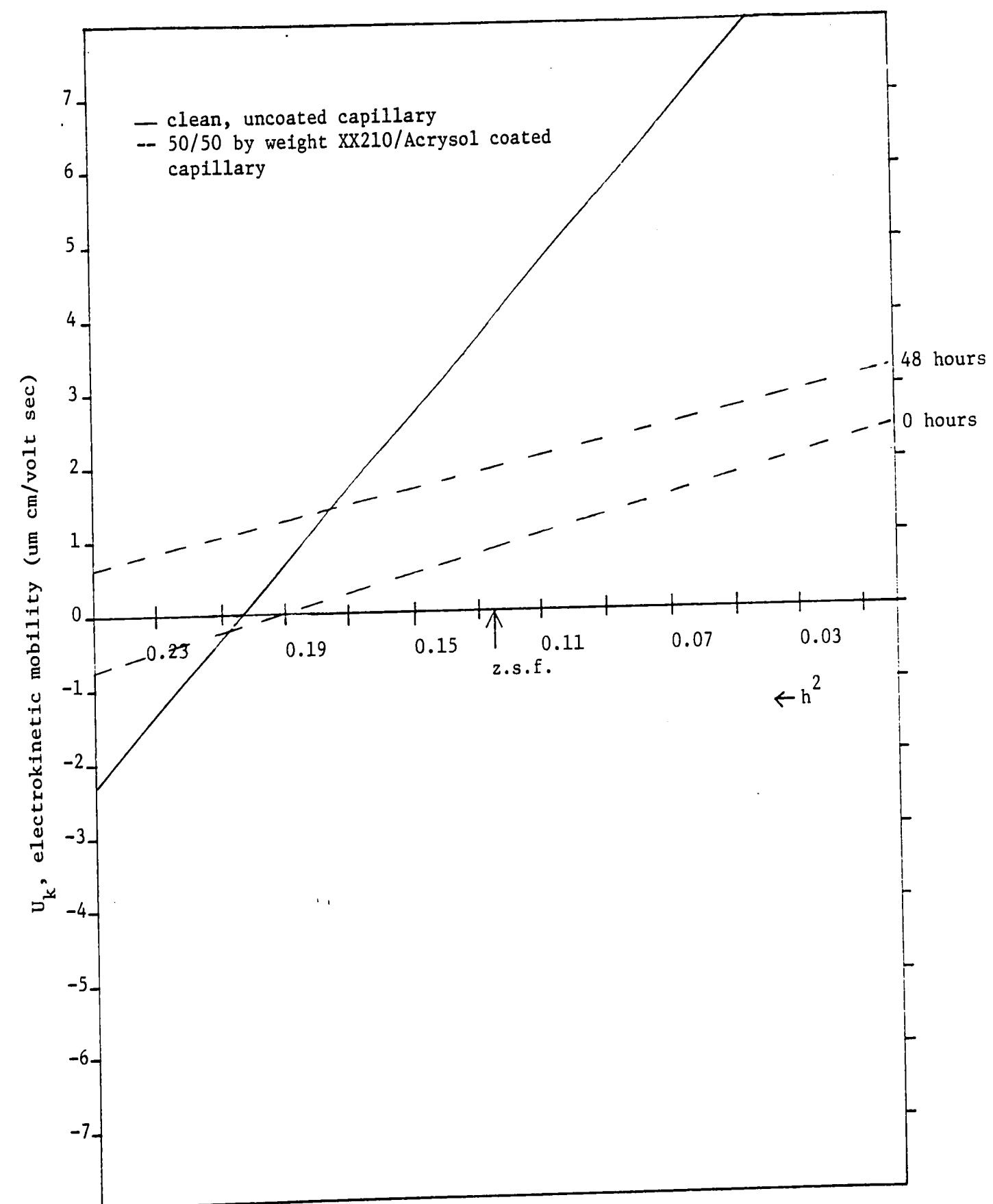


Figure B-11. Effect of dynamic rinsing upon the electrokinetic mobility results of coated glass capillaries in R-1 buffer.

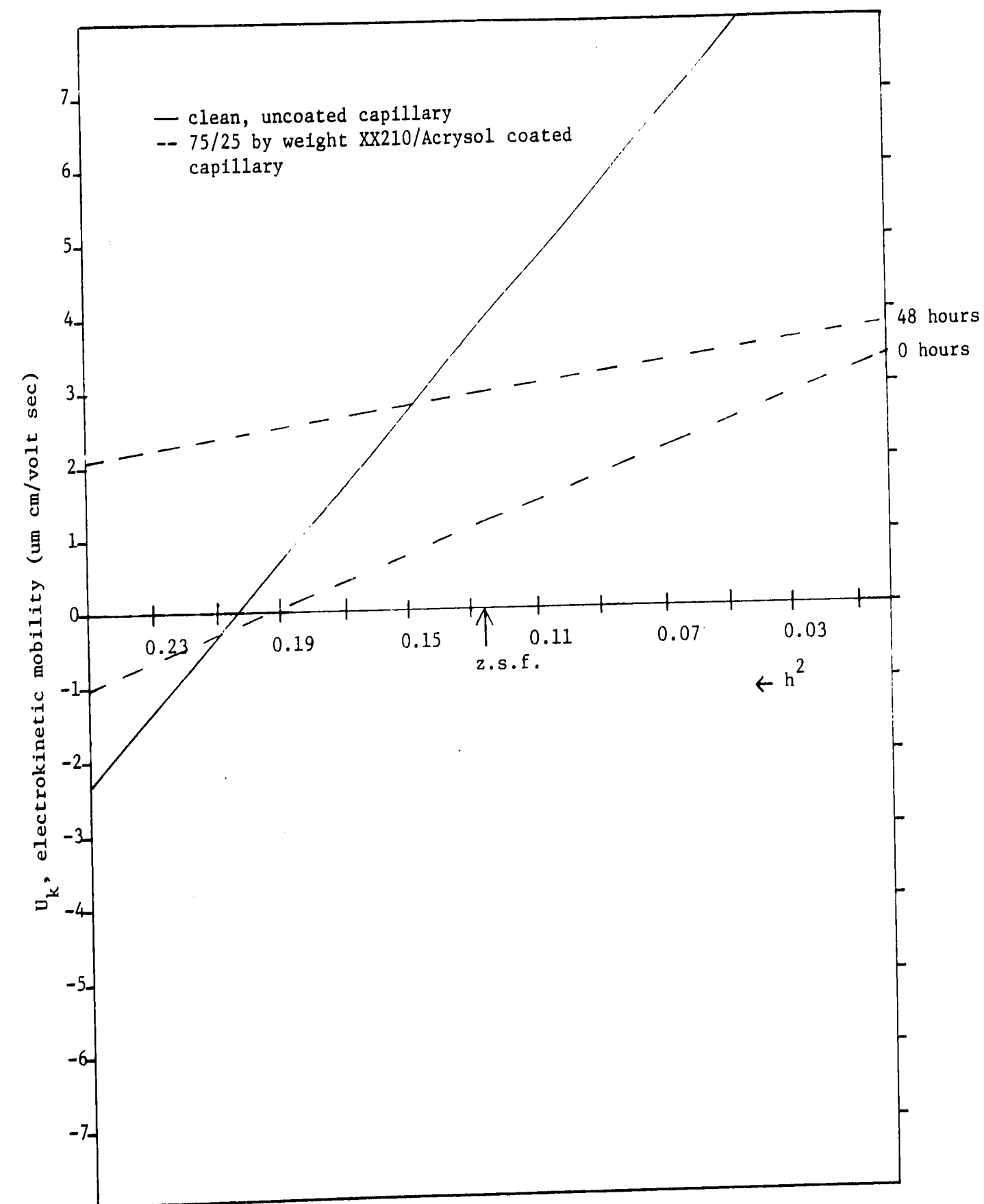


Figure B-12. Effect of dynamic rinsing upon the electrokinetic mobility results of coated glass capillaries in R-1 buffer.



## APPENDIX C

### Guideline to CPE-Optical Computer Program (70)

Note: The values in parentheses are the normal working values for the CPE.

#### Dimensions of CPE

XLU = curtain width (4.50 cm) }  
XWU = curtain thickness (0.15 cm) } cross sectional area  
of CPE

HLEN = length of electrodes { 10.0 cm for SPAR-CPE  
30.0 cm for CPE

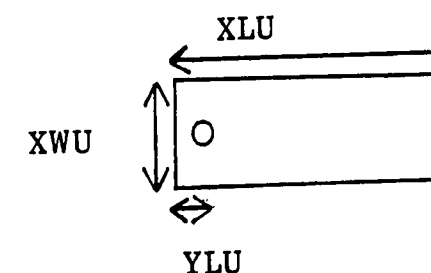
FLOW = curtain flow rate (cm<sup>3</sup>/min.)

#### Band Injection Data

YLU = position of injection (1.5 cm. from left edge)

XLU = position of injection (4.5 cm. from bottom edge)

Example:



RU = fraction of cross-section (XWU) you want shown (0 → 1) (1.0)

Example: at RU = 1.0, all is shown

RA = fraction of cross-section covered by band (0.20), or the ratio  
of injection diameter to thickness (XWU)

CEN = distance from center (0.0 → 1.0) (0.0) where: 0.0 = center

1.0 = wall

WIDTH = parameter for rectangular injection port (0.00); use only if  
INJECT = 2, which means rectangular shapes injection  
(WIDTH = width of sample (cm))

IPRINT = print option

0 no plot

1 1 plot of theoretical band displacement and shape

2 2 plots of comparion between theoretical and experimental

3 3 plots (combination of IPRINT 1 and 2)

INJECT = 1 if cylindrical injection port (CPE)

= 2 if rectangular injection port

#### Parameters

UOSRU = electroosmosis for rear upper wall

UOSFU = electroosmosis for front upper wall

UOSRL = electroosmosis for rear lower wall

UOSFL = electroosmosis for front lower wall

T1 = wall temperature, K

T2 = center temperature, K(CPE-midplane)

} determine using trial

} and error procedure

EL = lower voltage (2nd set of electrodes)

EU = upper voltage (voltage of interest for CPE)

LOVE = number of particles

JAX = number of voltages

LAX = no use in OPTICAL, but in PHORESE equal to the number of  
stages in focusing

XDATA = scaling factor for plots on print-out (0.5 - 1.0); determines  
how particles appear in the column; (use at 1.0)

Example: XDATA=0.5 ; middle - half of CPE; cross-section of flow stream.

Particle data-mobility distribution data:

UMEAN = peak mobility

UVAR = mobility distance of peak, left edge (-)

UVARR = mobility distance of peak, right edge (+)

Example

UVAR = 0.5 to 1.0 for 1.10 um PS	}	greater UVAR
0.3 for 0.357 um PS		
0.2 to 0.3 for 0.20 um PS	}	with larger particles
0.1 for 0.10 um PS		

AB = AREA = particle concentration, area under curve (10 - 100) find  
value using trial and error procedure

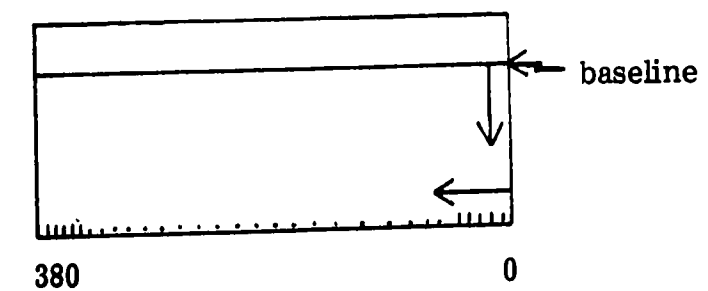
IDIST = shape of curve option

- 1 Gaussion fit
- 2 triangular fit
- 3 parabolic fit
- 4 square fit
- 5 random

Experimental data

NUM = number of data points on one complete scan of CPE (usually  
380); only use if want to compare actual to theoretical  
results (one of print options) from CPE graph

Example:



EU = upper voltage, 1st set of electrodes

NPLT = request plot

0 no plot

1 plot

IFOCUS = not used in OPTICAL, but only PHORESE, reads voltage  
for 2nd set of electrodes

1 no focusing

2 focusing

NOTE: Using CPE-OPTICAL:

1. does not allow optical focusing

2. may get "time" limit for large numbers of particles or if the voltage  
is very high

## APPENDIX D

Conductometric Titration of 0.109  $\mu\text{m}$  and 1.10  $\mu\text{m}$   
Latexes After Cleaning Using the Ion-exchange Technique

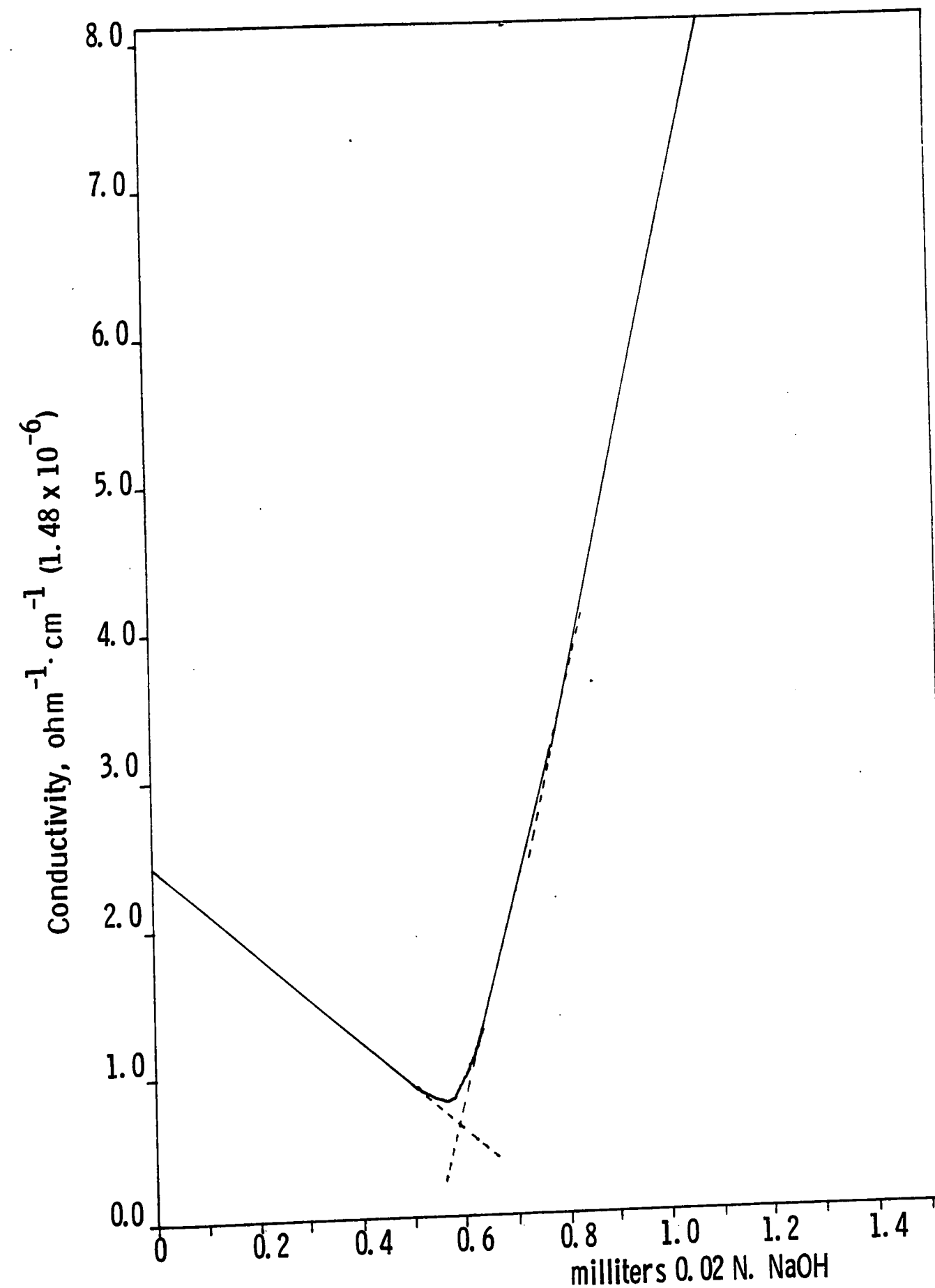


Figure D-1. Conductometric titration of 0.109  $\mu\text{m}$ . PS latex after cleaning three times using the ion-exchange technique.

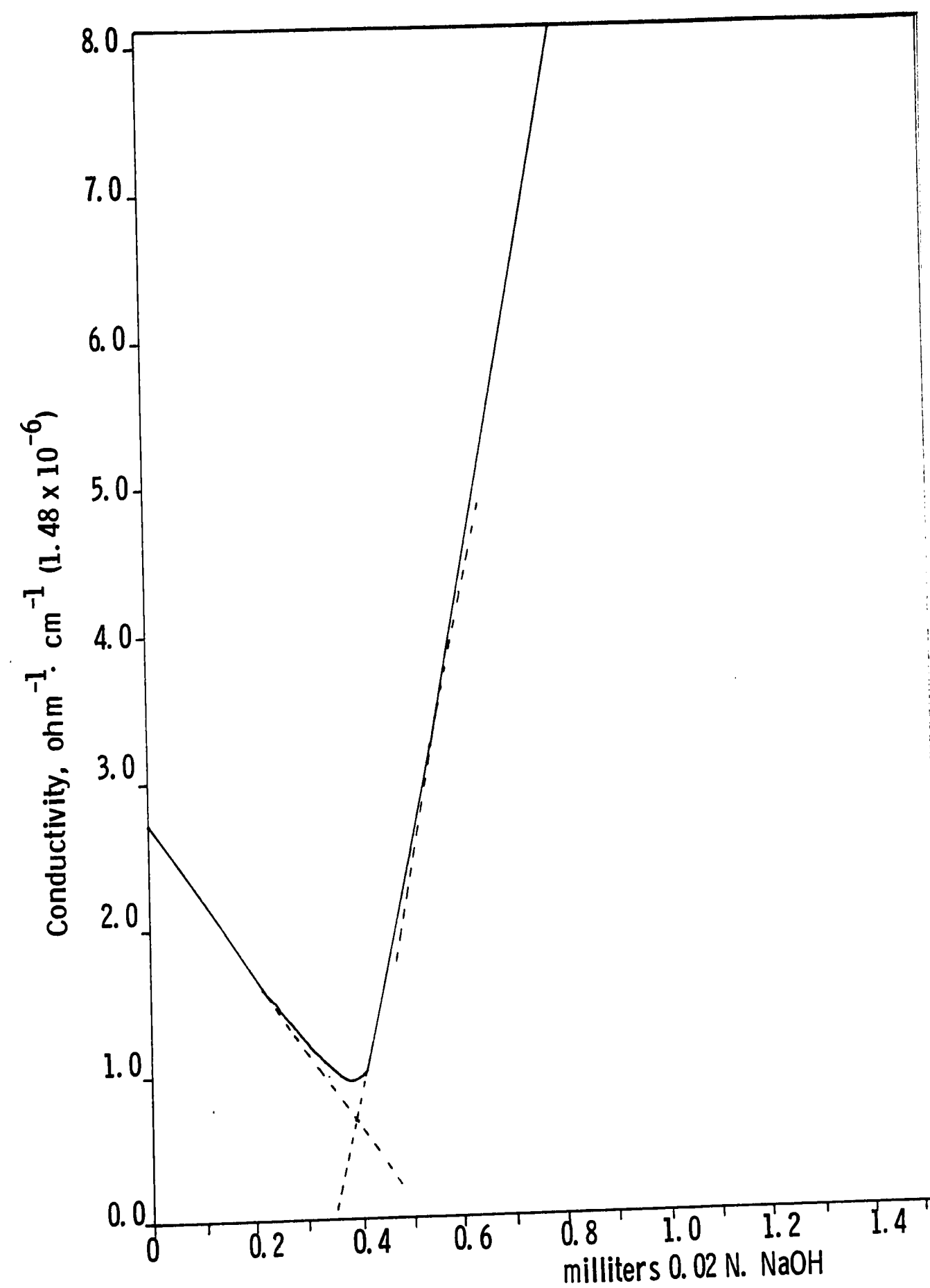


Figure D-2. Conductometric titration of 0.109  $\mu\text{m}$ . PS latex after cleaning four times using the ion-exchange technique.

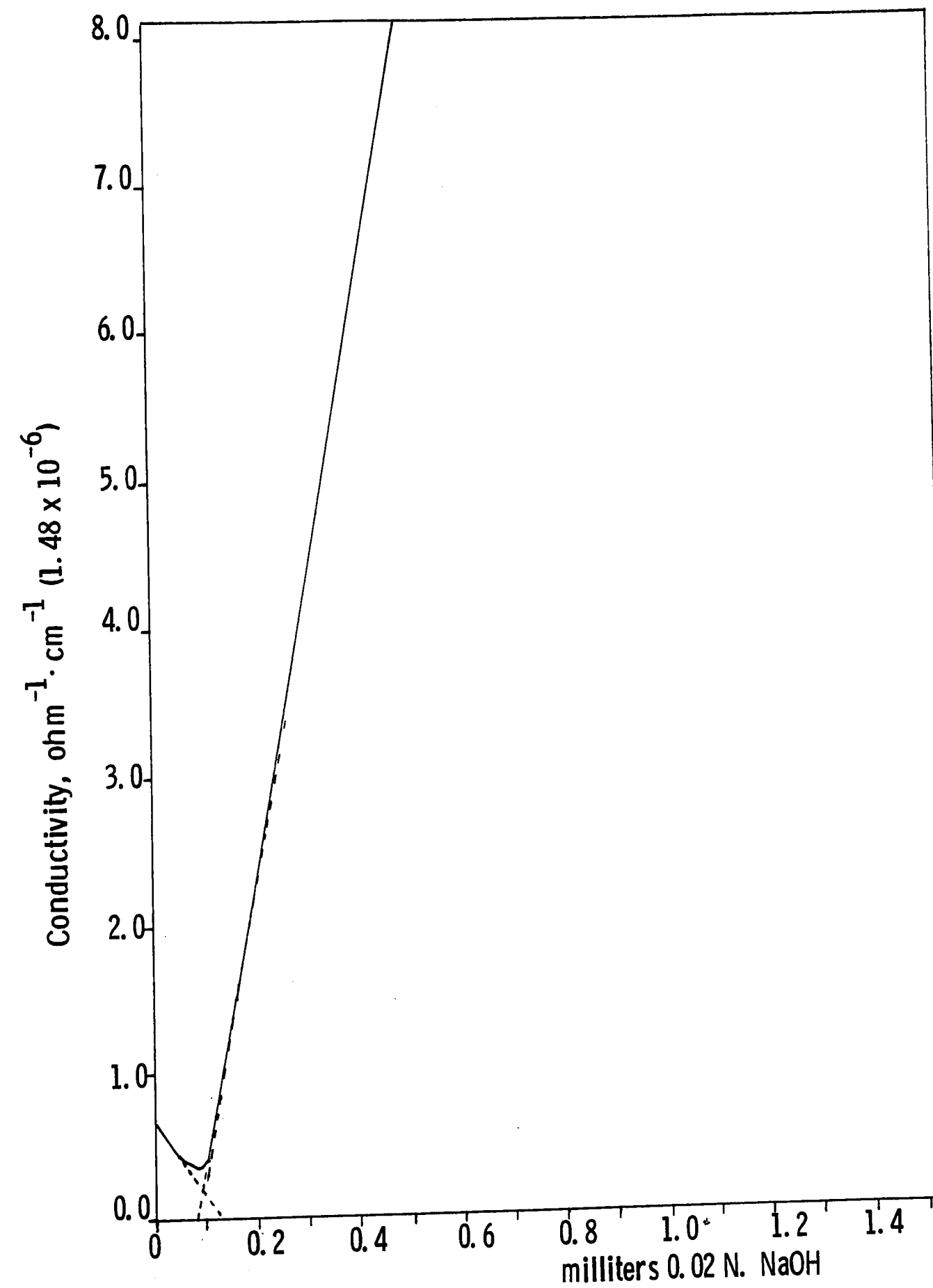


Figure D-3. Conductometric titration of 1.10  $\mu\text{m}$ . PS latex after cleaning three times using the ion-exchange technique.



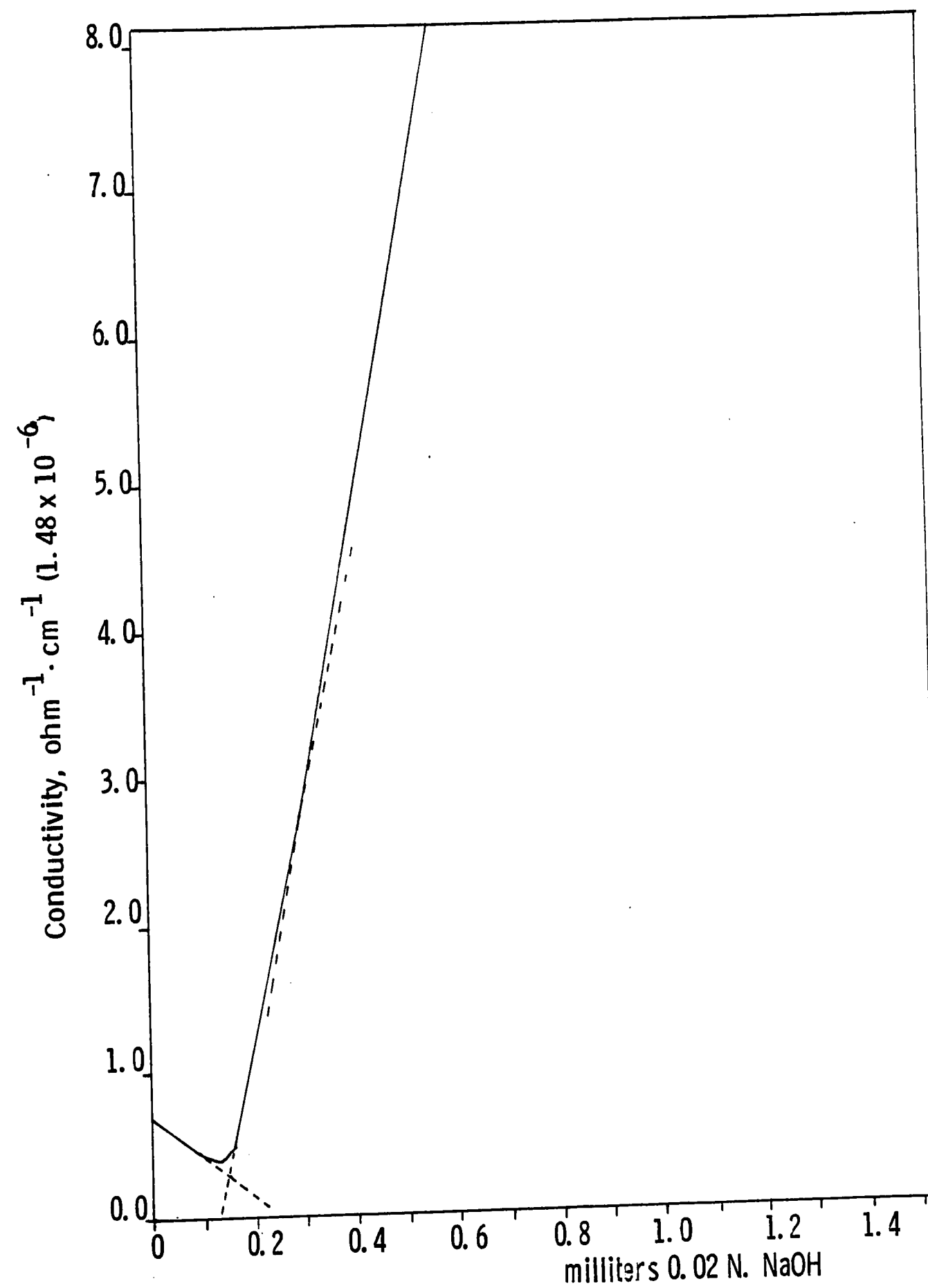


Figure D-4. Conductometric titration of 1.10  $\mu\text{m}$ . latex after cleaning four times using the ion-exchange technique.

## BIBLIOGRAPHY

1. F. M. Everaerts, J. L. Beckers, Th.P.E.M. Verheggen, J.  
Chromat. Lib., Vol. 6, Isotachophoresis: theory, instrumentation  
and application, 1976.
2. P. H. Krumrine, Ph.D. Thesis, Lehigh University, 1978.
3. A. Kolin, J. Chromatog., 26, 180 (1967).
4. A. Strickler, T. Sacks, Ann. N. Y. Acad. Sci., 209, 497, 1973.
5. M. Bier, Electrophoresis: theory, methods and applications, Academic  
Press, Inc., New York, 1959.
6. Operating Instructions and Manual for the Particle Micro-electro-  
phoresis Apparatus-Mark II, Rank Brothers, High Street, Bottisham,  
Cambridge, CB5-9DA, England.
7. C. J. Van Oss, R. M. Fike, R. J. Good, J. M. Reinig, Anal. Biochem,  
60, 242, 1974.
8. P. H. Krumrine, unpublished data.
9. J. W. Vanderhoff, C. J. Van Oss, Electrokinetic Separation Methods,  
Elsevier/North-Holland Biomedical Press, 257, 1979.
10. J. A. V. Butler, Electrical Phenomena at Interfaces in Chemistry,  
Physics and Biology, Methuen and Co., LTD., London, 102, 1951.
11. J. W. Vanderhoff, F. J. Micale, Electrokinetic Separation Methods,  
Elsevier/North-Holland Biomedical Press, 81, 1979.
12. P. H. Krumrine, M. S. Thesis, Lehigh University, 1976.
13. R. S. Snyder, M. Bier, R. N. Griffin, A. J. Johnson, H.  
Leisheiser, Jr., F. J. Micale, S. Ross, C. J. Van Oss, Sep. and

- Purif. Meth., 2 (2), 259, 1973.
14. C. Lerche, Acta. Pathol. Microbiol. Scand. Suppl., 98, 1, 1953.
  15. P. C. Hiemenz, Principles of Colloid and Surface Chemistry, Marcel Dekker, Inc., New York, 453, 1977.
  16. F. J. Micale, J. W. Vanderhoff, R. S. Snyder, Sep. and Purif. Meth., 5 (2), 361, 1976.
  17. J. W. Vanderhoff, F. J. Micale, P. H. Krumrine, Electrophoresis, 78, Elsevier/North Holland, Inc., 405, 1978.
  18. J. W. Vanderhoff, F. J. Micale, P. H. Krumrine, Sep. and Purif. Meth., 6 (1), 61, 1977.
  19. A. Kolin, M. J. Luner, Analyt. Biochem. 30, 111, 1969.
  20. E. C. McKannan, A. C. Krupnick, R. N. Griffin, L. R. McCreight, "Electrophoresis Separation in Space-Apollo 14," NASA Technical Memorandum TMX-64611, 1971.
  21. S. Hjertén, Free Zone Electrophoresis, Almquist and Wiksells Boktryckem AB, Uppsala, 51, 1967.
  22. J. W. Vanderhoff, F. J. Micale, "Electrophoresis Experiment for Space", Final Report, Contract NA S8-28654, April 1976.
  23. D. A. Skoog, D. M. West, Analytical Chemistry, Holt, Rinehart and Winston, Inc., 88, 1965.
  24. H. C. Mel, J. Chem. Phys., 31, 559, 1959.
  25. M. Adolf, W. Pauli, Biochem. Z., 152, 360, 1924.
  26. M. Bier, Science, 145, 1084, 1957.
  27. A. Kolin, Proc. Nat. Acad. Sci., 46, 509, 1960.
  28. W. Grassman, K. Hannig, Continuous Carrier-free Electrophoresis,

- U. S. 3,125,500 (Cl. 204-299), Mar. 17, 1964.
29. K. Hannig, Z. Anal. Chem., 181, 244, 1961.
30. K. Hannig, Clin. Chim. Acta, 3, 10, 1958.
31. A. Karler, Anal. Chem., 31, 848, 1959.
32. R. Dobry, R. K. Finn, Science, 127, 697, 1958.
33. A. Kolín, P. Cox, Proc. Nat. Acad. Sci., 52, 19, 1964.
34. A. Kolín, Proc. Nat. Acad. Sci., 51, 1110, 1964.
35. V. J. Barrolier, E. Watzke, H. Gibian, Z. Naturforsch., 13b, 754, 1958.
36. K. Hannig, Z. Physiol. Chem., 338, 211, 1964.
37. A. Schweiger, K. Hannig, H-S Z. Phys. Chem., 348, 1005, 1967.
38. K. Hannig, K. Zeiller, H-S Z. Phys. Chem., 350, 467, 1969.
39. K. Hannig, R. Stahn, K-P. Maier, H-S Z. Phys. Chem., 350, 784, 1969.
40. A. Strickler, A. Kaplan, E. Vigh, Microchem. J., 10, 529, 1966.
41. V. R. Huebner, R. H. Lawson, Sep. Sci., 3 (3), 265, 1968.
42. A. Strickler, Sep. Sci., 2 (3), 335, 1967.
43. G. D. McCann, J. W. Vanderhoff, A. Strickler, T. Sacks, Sep. and Purif. Meth., 2 (1), 153, 1973.
44. F. J. Micale, P. H. Krumrine, J. W. Vanderhoff, Coll. and Interf. Sci., IV, 247, 1976.
45. J. W. Vanderhoff, F. J. Micale, P. H. Krumrine, Electrokinetic Separation Methods, Elsevier/North Holland Biomedical Press, 121, 1979.
46. A. Strickler, T. Sacks, Ann. N. Y. Acad. Sci., 209, 497, 1973.
47. A. Strickler, T. Sacks, Prep. Bioch., 3 (3), 269, 1973.

48. M. Zaoral, M. Flegel, T. Barth, A. Machová, Coll. Czech. Chem. Comm., 43, 511, 1978.
49. D. G. Streeter, M. P. Gordon, Phytopathol., 56, 419, 1966.
50. S. Sarkar, Z. Naturfo. B., 21, 1202, 1966.
51. S. J. Luner, A. Kolin, Biophy, J. 8, A109, 1968.
52. T. A. Mashburn, Jr., P. Hoffman, Anal. Biochem., 16, 267, 1966.
53. K. Hannig, H-G. Heidrich, K. Spiegel, H. Wirth, J. Clin. Chem., 16 (3), 203, 1978.
54. M. Andreoli, Rass. Fisiop. Cl. Ter. Agosto, Vol. XXXI, No. 8, 779, 1959.
55. W. W. Just, J. O. León-V, G. Werner, Anal. Biochem., 67, 590, 1975.
56. K. Zeiller, R. Loser, G. Pascher, K. Hannig, H-S Z. Phys. Chem., 356, 1225, 1975.
57. J. I. Drever, Amer. Miner., 54, 937, 1969.
58. N. Catsimpoolas, A. L. Griffith, J. M. Williams, A. Chrambach, D. Rodbard, Anal. Biochem, 69, 372, 1975.
59. Z. Prusik, E. Sedlakova, T. Barth, H-S Z. Phys. Chem., 353, 1837, 1972.
60. J. J. Evans, Anal. Biochem., 32, 101, 1969.
61. U. Stosick, F. C. Zimmermann, W. Helmbold, W. Hardegg, Pfl. Arch., 310, 95, 1969.
62. C. K. Bartell, M. Fingerman, Biol. Bull., 137, 390, 1969.
63. S. Sulkowski, M. Laskowski, Anal. Biochem., 20, 94, 1967.
64. R. P. Müller, Anal. Chem., 39 (14), 103A, 1967.
65. W. C. Wu, Ph. D. Thesis, Lehigh University, 1977.

66. S. M. Ahmed, Ph. D. Thesis, Lehigh University, 1979.
67. J. W. Vanderhoff, H. J. Vander Hul, R. J. M. Tausk, J. Th. G. Overbeek, Clean Surfaces: Their Preparation and Characterization for Interfacial Studies, G. Goldfinger, Marcel Dekker, N. Y., 15, 1970.
68. J. W. Vanderhoff, F. J. Micale, M. S. El-Aasser, W. C. Wu, Polymer Preprints, 16 (1), 125, 1975.
69. G. V. F. Seaman, University of Oregon Health Sciences Center, personal correspondence, July 1977.
70. P. H. Krumrine, personal correspondence, 1979.

## VITA

Tina Jean Vital was born on December 22, 1953 in Atlantic City, New Jersey. She attended the Los Angeles County School System in Los Angeles, California until September of 1969 when she entered and graduated from Johnstown High School in Johnstown, Pennsylvania in 1971, majoring in mathematics and science. In 1976, she graduated from the University of Pittsburgh in Pittsburgh, Pennsylvania, with majors in biochemistry and biology, and minors in chemistry, physics and mathematics. In the fall of 1977, she entered Lehigh University majoring in chemical engineering. In October of 1979, Ms. Vital received the Master of Science Degree in Chemical Engineering.

From this investigation, one paper has been written and presented entitled "Experimental Parameters Involved in the Separation of Colloidal Particles by Continuous Electrophoresis" (in press).